**Title**
The Effects of Environmental Variation on the Persistence of Freshwater Invertebrates in California Streams



**Author**
King, Emily

**Publication Date**
2021

Peer reviewed|Thesis/dissertation

# The Effects of Environmental Variation on the Persistence of Freshwater Invertebrates in California Streams

By

Emily E. King

A dissertation submitted in partial satisfaction of the

requirements for the degree of

Doctor of Philosophy

in

Integrative Biology

in the

Graduate Division

of the

University of California, Berkeley

Committee in charge:

Professor Caroline Williams, Co-Chair
Professor Jonathon Stillman, Co-Chair
Professor Wayne Sousa
Professor Stephanie Carlson

Spring 2021

Abstract

The Effects of Environmental Variation on the Persistence of Freshwater Invertebrates in California Streams

by

Emily E. King

Doctor of Philosophy in Integrative Biology

University of California, Berkeley

Professor Caroline M. Williams, Co-Chair
Professor Jonathon H. Stillman, Co-Chair

Freshwater streams are incredibly variable habitats where abiotic conditions change daily and seasonally. The species that inhabit streams must have the physiological capacity to deal with that variation. Variation that extends outside of the limits of an organism's tolerance thresholds can cause sub-lethal or lethal stress and dictate which habitats are suitable to the organism. In addition to variation in abiotic conditions, organisms must fit into the ecological interaction web of their habitat and handle variation in biotic conditions. In my dissertation, I focus on two pathways for organisms to encounter new sources of environmental variation: invasion of novel habitats and climate change. Understanding how organisms deal with environmental variation is critical to predicting where they can live now and in the future.

In Chapter 1, I aimed to identify the temperature and oxygen conditions that limit respiration and locomotion in the highly invasive New Zealand mud snail, *Potamopyrgus antipodarum*. To accomplish this, I generated thermal performance curves for resting respiration rate and voluntary locomotor behaviors under normoxia and hypoxia to find the conditions that limited each performance. I found that extremely high and low temperatures limited respiration and activity, but respiration rate was more sensitive to changes in oxygen at low temperatures. Hypoxia did not significantly decrease activity. Under hypoxic conditions, activity was less thermally sensitive, increased under high temperatures, and may be fueled by anaerobic metabolism. Relying on anaerobic energy is a time-limited survival strategy, so further warming and deoxygenation of freshwater systems may limit the spread of this invasive species.

In Chapter 2, I focused on finding the abiotic and biotic conditions that explain variation in *Potamopyrgus antipodarum* population density in San Francisco Bay Area streams. *P. antipodarum* is a prolific invader of freshwater streams in California and worldwide, with the ability to form extremely dense populations that dominate the invaded habitat. To strengthen our ability to predict where this species can thrive, it is critical to understand which abiotic and biotic conditions explain variation in population density. I approached this need by measuring 25 conditions over one year in three streams with varying densities of *P. antipodarum* populations. The different streams could be distinguished by their water chemistry profiles. Conductivity and

filamentous green algae cover were the factors most correlated to population density, but there was only marginal linear statistical support for the response to algae. Overall, *P. antipodarum* is robust to considerable variation in many ecological factors, and each factor may have a small effect in controlling their population sizes.

In Chapter 3, I focused on the effect that past environmental variation, specifically thermal history, had on the response to different warming regimes in the larval caddisfly *Dicosmoecus gilvipes*. To accomplish this, I tested the molecular physiology responses of three populations of field-acclimatized *D. gilvipes* from different eco-regions (mountain, valley, coast) to current and future warming scenarios. I hypothesized that distinct thermal histories could differentiate populations at baseline levels of gene expression and gene expression changes in response to daily warming and heat shock. Population-specific responses were apparent under the control and daily warming conditions, while responses to heat shock were similar across populations. In addition, underlying gene expression patterns in the daily warming and heat shock treatments were different. These results highlight the importance and limitations of measuring the stress response of wild-caught organisms in their natural environment.

## TABLE OF CONTENTS

**Acknowledgments**

The journey to finishing a dissertation has been long and challenging, but I've been supported by so many people, personally and professionally. As a first-generation scientist, it took quite a network to help me figure it all out. There is no way to convey all the ways I am deeply grateful for your support.

Thanks to my PhD advisors: To Jonathon Stillman, thank you for inviting me into your lab six years ago and training me to be an integrative aquatic physiologist in the field and at the bench. Thanks for letting me be the third PhD student to study mollusks rather than crustaceans. And to Caroline Williams, thank you for taking a chance and choosing to co-advise me after I asked you to be my advisor *during* the interview and for letting me bring mollusks into an insect lab. I feel incredibly lucky to have had twice as many amazing and supportive advisors as most students. You both made me a much better scientist and informed my mentorship practice. I am honored to pay those things forward to other budding researchers.

My family deserves the most thanks of all. Thank you for supporting my drive to be a scientist since I was a child obsessed with whales, through the otter, fish, crab, and finally, snail phases. Thank you for supporting me emotionally and financially as we figured out how the university worked and where to go from there. Thanks Dad, for recording my talks with your iPad, even though I thought it was embarrassing. Thanks Mom, for cheering for my accomplishments even before you knew what they meant. Thanks Nana, for always being there to lean on and play Rummy with. I also want to thank my youngest siblings, Ryan, Reese and Mariah, for going with me to find my first New Zealand mud snails. I have to especially thank Mariah for recording the data in the early days and learning how to replace temperature loggers. Also, thank you Natalie, for being my concert buddy for all these years.

Thank you, Tyler McClellan, for being exactly who you are and coming back into my life. Thank you for all the late-night and weekend drives to the lab and your patience as I finished "just this one little thing" before closing my computer at night. I'm also incredibly fortunate that you would give up every other weekend for a year through fires, floods, and a pandemic to help me finish collecting the data presented here.

The list of friends I've made in graduate school is long, and I owe much of my well-being over the years to their friendship. I'm grateful to Stillman and Williams lab members, past and present but especially: Richelle Tanner, Emily Lam, Eric Armstrong, Kevin Roberts, Lisa Treidel, André Szejner Sigal, and Ana Lyons. I'm also thankful to the undergraduate students I have worked with: Ben Liu, Hossein Moein Taghavi, and all my BSP researchers.

I want to thank all the people who helped build my skills and confidence, helped me find my passion for research as an undergraduate, and helped me get started in graduate school: Don Mautner, the Undergraduate Research Opportunities Center, Bill Head, Heather Haeger, Bridgette Clarkston, Natasha Oehlman, Cheryl Logan, and Lauren Brooks (the best randomly assigned roommate in history).

I’m also grateful to the following groups for their funding support in completing this work: the UC Berkeley Graduate Division, the Department of Integrative Biology, the Biology Scholars Program, Berkeley Connect, and Save Mount Diablo.

And last but not least, thank you to the snails, not for the invasion stuff but for captivating my curiosity for five years.

**Hypoxia decreases thermal sensitivity and increases thermal breadth of locomotion in the invasive freshwater snail, *Potamopyrgus antipodarum***

## Introduction

Invasive species can greatly alter natural communities and ecosystems in their introduced range and cause ecological harm with annual economic impacts estimated at $120 billion and €20 billion in the United States and in the European Union, respectively (Pimentel et al. 2005; Kettunen et al. 2008). The impacts of invasive species can be mitigated by preventing their establishment and predicting and preventing their spread. Succeeding at the latter requires understanding key aspects of the life history, ecological niche, and environmental sensitivity of the invasive species.

Invasive species must pass through a series of three environmental filters before establishing viable populations in a new environment: biogeographic, abiotic, and biotic (Rahel 2002). To invade, dispersal into a new location by a species cannot be blocked by landscape features (e.g., mountains, rivers, human infrastructure), it must have the physiological capacity to live under the new location's abiotic conditions, and it must be able to persist within the new location's biotic interaction web (e.g., find prey, avoid predation, avoid competitive exclusion). Commonly, invasive species circumvent biogeographic barriers by being transported (intentionally or unintentionally) by humans and only need to pass the latter two filters (Rahel 2002; Hulme 2009). Physiological barriers to establishment become the first challenge a potentially invasive species faces in the new environment, thus highlighting the importance of understanding the species' abiotic niche (Lennox et al. 2015).

The New Zealand mud snail, *Potamopyrgus antipodarum* (Gray, 1853), is an invasive organism for which the environmental filters regulating its continued spread are not yet understood. *P. antipodarum* are small operculate prosobranch snails native to fresh and brackish water in New Zealand where they have both sexual and asexual lineages (Winterbourn 1970; Neiman et al. 2005). Invasive populations, comprised of parthenogenetically reproducing viviparous females, exist globally and are widespread in the western U.S. and Great Lakes region (Dybdahl and Drown 2011; Alonso and Castro-Díez 2012a). In the non-native range, *P. antipodarum* are found in diverse environments, including snowmelt-fed rivers, brackish estuaries, and polluted canals, demonstrating their broad physiological tolerances (Hall et al. 2003; Alonso and Castro-Díez 2012a).

The abiotic variables that might be physiological filters for *P. antipodarum* in its aquatic environment include temperature, oxygen availability, substrate type, and salinity, which all change over time and space (Brown et al. 1998; Giller and Malmqvist 1998). The effects of different physical stressors are both dynamic and interactive in nature, necessitating study of the interplay of multiple factors together in order to draw ecologically relevant inferences. In aquatic ectotherms specifically, it is critical to understand the physiological responses to simultaneous shifts in oxygen availability and water temperature. Changes in temperature directly affect oxygen availability in water by changing its solubility and diffusion properties (Verberk et al. 2011). Oxygen is more soluble in cold water. However, oxygen is more readily diffused across respiratory membranes when it is warm due to increased molecular energy. In addition to the physical relationship between temperature and oxygen, there is a metabolic relationship for ectotherms. As the temperature increases, metabolic oxygen demand also increases (Gillooly et al. 2001; Clarke and Fraser 2004). The oxygen solubility index (OSI) is a

function of solubility, diffusion, and partial pressure to estimate how much oxygen is actually available to the organism at a given temperature (Verberk et al. 2011). Using this function, oxygen supply increases as temperature increases, but the point at which the organism's oxygen demand outpaces supply depends on the thermal sensitivity of its metabolic rate. Understanding the conditions where oxygen supply is less than the oxygen demand of a resting snail and an active snail is essential to defining the niche requirements of this invasive species.

While many researchers have addressed the abiotic filter of temperature tolerance in *P. antipodarum*, many studies fail to acknowledge the corresponding changes in oxygen availability and demand (Winterbourn 1969; Hylleberg and Siegismund 1987; Siegismund and Hylleberg 1987; Zaranko et al. 1997; Richards et al. 2004; Alonso and Castro-Díez 2012b; Sardiña et al. 2015; Koopman et al. 2016). The effects of hypoxia on *P. antipodarum* physiology have been much less studied than the effects of temperature in U.S. populations. The majority of what we know is inferred because *P. antipodarum* often spread on fishing and wading gear, boat trailers, and even inside the guts of fish and birds, where access to oxygen is limited (ANS Task Force 2007; Alonso and Castro-Diez 2008). We hypothesize that *P. antipodarum* are very tolerant to hypoxia in nature because *P. antipodarum* have been collected in regions of Lake Erie that become hypoxic in the summer (Levri et al. 2007). However, prosobranch mollusks are considered to be poor oxygen regulators (i.e., oxyconformers) and thus not be able to maintain high respiration as environmental oxygen declines (Brown et al. 1998; Alexander Jr and McMahon 2004). As oxygen consumption decreases, activities relying on aerobic metabolism beyond basic maintenance will be compromised and thus limit the ability of this species to spread under hypoxic conditions.

This study aimed to identify the temperature and oxygen conditions that limit resting respiration rate and voluntary locomotor behaviors. It is important to understand at what point the environment can restrict basic survival and when it restricts fitness-associated aerobic activities like foraging in *P. antipodarum*, which we approximated by measuring respiration and locomotion, respectively. We compared the responses across the temperature range in a thermal performance curve framework (Angilletta 2006) and compared the thermal optima ($T_{opt}$, temperature at maximum performance) and thermal breadth ($T_{br}$, temperature range above 85% of maximum performance). We also examined changes in the thermal performance curve properties between normoxia and hypoxia. We hypothesized that: 1) performance of resting respiration and voluntary locomotion would be limited at the high and low temperature extremes, 2) that hypoxia would exacerbate the temperature effects resulting in decreased performance at the $T_{opt}$ and reduced $T_{br}$. We tested these hypotheses by measuring resting respiration rate through a progressive hypoxia challenge and comparing climbing activity under normoxia and hypoxia.

## Methods

### *Snail Collection and Maintenance*

New Zealand mud snails (*Potamopyrgus antipodarum*) were collected from the same location in Mt. Diablo Creek in California, U.S.A. (37.943958 N,-121.937397 W) on 10/7/18 and 9/2/19. Snails from this location are extremely likely to be the "U.S. 1" clonal type that is the most widespread across the western United States (Dybdahl and Drown 2011). They were transported to aquaria in Berkeley, CA where they were held for at least two weeks before experimentation. Snails were maintained in 20-gallon benchtop aquaria equipped with an air

stone, a Fluval Aqua Clear 20 Power Filter (Rolf C. Hagen Corp. Mansfield, MA) with 3-part filtration (mechanical, chemical, and biological components), and a heater to maintain the water at 15° C (±1°C), reflecting the mean annual temperature at the collection site in Mt. Diablo Creek. Aquaria were filled with artificial freshwater created by mixing deionized water with Equilibrium™ (Seachem, Madison, GA) per the manufacturer's instructions. Deionized water was added three times weekly to account for evaporation.

Snails were housed differently for the hypoxia and activity experiments. Before respirometry, 100 snails were housed in each of three 500mL beakers covered with window screen and placed in the aquaria. Powdered *Spirulina* (0.1g, Earthrise, CA) was added to each beaker weekly (Bankers et al. 2017). Before the activity experiment, 500 snails per aquarium were allowed to roam in the entire aquarium without beakers. In that case, 0.3 g of *Spirulina* was added to the entire aquarium weekly. In both cases, dead snails were removed from the beakers or aquarium every other day.

*Snail Morphometrics*

Prior to the experiments, each snail was blotted dry on a Kimwipe before weighing the whole wet mass, including the shell, on a Mettler Toledo XP6 microbalance balance (Sharbrough et al. 2017) (Figure S1). After the experiments, the shell length was measured from digital photographs with ImageJ (Schneider, C.A., Rasband, W.S., Eliceiri 2012) or Nikon NIS-Elements software (Tokyo, Japan)( Figure S2).

*Experimental and Field Conditions*

The range of experimental conditions, 7-35°C and 100%-20% oxygen saturation, was selected from benchmarks in the literature that spans the likely physiological breadth of *P. antipodarum* (Hylleberg and Siegismund 1987; Richards et al. 2004; A.N.S. Task Force 2007; Levri et al. 2007; Alonso and Castro-Diez 2008; Koopman et al. 2016). We compared these conditions to those experienced by snails in the study population in the wild between September 2019 – September 2020. Both stream temperature and dissolved oxygen were recorded in Mt. Diablo Creek, the same site of snail collection. Stream temperature was recorded every 30 minutes between 9/8/19-9/22/20 using a HOBO UA-001-64 temperature logger (Onset Computer Corporation, Bourne, MA). Dissolved oxygen saturation was measured every 30 minutes for two weeks out of every six weeks (17 weeks total) between 9/8/19-8/23/20 with a MiniDOT logger (Precision Measurement Engineering, Vista, CA).

*Progressive Hypoxia Respirometry*

Respirometry was performed in a glass microplate containing 24 individually capped 750µL wells, each equipped with an oxygen optode sensor spot (Loligo Systems, Viborg, Denmark). Each well is a closed system. The capped microplate was held in a custom acrylic water jacket connected to an Isotemp 4100 circulating water bath (Fisher Scientific, Hampton, NH) for temperature control. The oxygen saturation of each well was measured by a PreSens Sensor reader dish (SDR-421) under the water jacket and monitored in real-time with the accompanying software (SDR_v38, PreSens, Regensburg, Germany). The water bath and treatment water were allowed to equilibrate at the test temperature before snails were added to the wells. The treatment water was prepared the same way as the artificial freshwater described above. The test temperatures were 7, 11, 15, 18, 22, 25, 28, 31, and 35 ±0.1 °C.

Oxygen consumption was measured through progressive hypoxia from ~100% air saturation until the individual snails stopped respiring. We measured oxygen consumption in two replicate blocks consisting of 10 unique snails per temperature (total N=20 individuals/temperature). After all individuals were sealed in the plate, the instrument recorded the dissolved oxygen in each well every minute until the snails stopped respiring. Snails typically experienced air saturations between 100% and 20% at each temperature. The assay duration depended on the temperature sensitivity of respiration rates; assays ranged from 12.2 to 262.5 hours. At the end of each assay, the snails were removed from the plate to be photographed and frozen.

*Progressive Hypoxia Analysis*

To address inadequate mixing in the chamber causing periods of oxygen increase, we trimmed and smoothed the raw data. The raw oxygen consumption data for each individual were trimmed to only include values under 100% air saturation. The trimmed data set was used to estimate a smooth exponential decay function ("SSasymp" in the *stats* package in R statistical program v.3.5.1). The smoothed data were used in subsequent respiration rate analyses.

The smoothed curves were used to calculate the respiration rate (via oxygen consumption) in normoxia (85-100% air saturation) and hypoxia (<35% air saturation) using the linear slope of the data in between the specified air saturation values. The slope was converted from percent saturation change/min to μmol/L/hr using ideal gas law conversions. We tested for differences in the respiration rates between temperatures and oxygen levels with a mixed-effects 2- way ANOVA, with temperature and oxygen level as fixed factors, mass as a covariate, and individual nested within temperature and block as random factors (*nlme* package).

To determine whether these snails are oxygen conformers or regulators, the respiration rate was also calculated for each 5% increment in oxygen saturation (Alexander Jr and McMahon 2004; Wood 2018). We fit a linear model to the smoothed data in 5% increments using a sliding window, without any overlap between increments (i.e., 100-95%, 94.9-90%, etc.). Each rate was then scaled to a percentage of the maximum rate for that individual at that temperature.

The regulation value, R, was assessed for each individual by calculating the integral of the curve produced by plotting the percentage of the maximum respiration rates as described above and represented as a percentage of the value for a perfect oxygen regulator (Alexander Jr and McMahon 2004). A perfect oxygen regulator would have an R value of 100%, and a perfect conformer would have a value of 50%. Individuals with an R value between 50%-100% show some degree of oxygen regulation, and those with values below 50% are sensitive to decreases in oxygen availability. R values across the measured temperatures were compared with a linear mixed-effects model, with temperature as a fixed factor and individual nested within temperature and block as random factors (*nlme* package R v3.1-137).

*Climbing Activity under Differing Oxygen Conditions*

The climbing assay was designed following the Rapid Iterative Negative Geotaxis (RING) assay developed for *Drosophila melanogaster* (Gargano et al. 2005). Climbing was measured in gas-tight borosilicate glass tubes (13m; 16x125mm). Climbing assays were run at two oxygen saturations, "100%" (92.0±4.74% air saturation) and "20%" (17.22±3.54% air saturation), at the nine temperatures used for respirometry (7, 11, 15, 18, 22, 25, 28, 31, 35 °C) for 18 total treatments. One liter of test water was prepared by heating water on a hot plate or

cooling in an ice bath and mixing with a magnetic stir bar. When the water reached the appropriate test temperature, oxygen conditions were achieved by bubbling test water with air or nitrogen gas and confirming the dissolved oxygen with a temperature compensating dip probe (Vernier Optical D.O. probe and LabQuest2 reader, Beaverton, OR). Snails were added to empty climbing chambers that were immediately filled using a small tube drawing water from the bottom of the 1L flask until there was a positive meniscus and then capped to exclude air bubbles. Oxygen conditions in the tube were confirmed with oxygen optode spots (PreSens) glued to the wall of the chambers as previously described in Miller et al. (2014) and Paganini et al. (2014). Ten chambers, each containing one snail, were assayed as one block then replicated with a second block of 10 new individuals (n=20 snails total per temperature x oxygen treatment).

For the duration of the experiment, all chambers were held in a water bath at the appropriate temperature (±1°C). All chambers were incubated in the water bath for 60 minutes prior to the climbing assay to allow the snails to acclimate to the test temperature before activity measurements began. One additional chamber (blank) was filled with test water but no snail to measure background oxygen uptake and compare with test chambers. Negligible differences in oxygen saturation were recorded in the first or second hour in blank and test vials. At the end of the incubation period, the climbing assay was initiated by tapping all snails to the bottom of the chamber. Each snail's position at the mid-body was marked with paint on the outside of the tube every 10 minutes for 60 minutes (6 unique positions recorded). At the end of the assay, snails were removed from the chambers and photographed as described above.

We calculated the total body lengths climbed for each individual by summing the distances between the six sequential markings, then dividing by shell length (Fig. S2, available online). We compared the total distance climbed between temperatures for both oxygen treatments. The resulting thermal performance curves, one for each oxygen condition, were modeled with nonlinear functions in the R package *rTPC* (Padfield et al. 2020), and the best fitting model was chosen by AIC. The normoxia curve was best modeled with a gaussian function, and a Weibull function best modeled the hypoxia curve. The $T_{opt}$ and $T_{br}$ were extracted from the best models for comparison.

**Results**

*Field Conditions*

*Potamopyrgus antipodarum* in Mt. Diablo Creek experience a range of conditions that were included within the range of experimental conditions chosen for this study. During the study period, stream temperatures fluctuated from 8.08°- 23.96°C (Fig. 1a). The lowest temperatures occurred during and after cold winter storms that brought snow to the upper watershed. The highest temperatures occurred during a prolonged, late summer heatwave. Mt. Diablo Creek does not exhibit the highest temperatures this species was exposed to in this study (25-35°C).

Dissolved oxygen fluctuated from supersaturation (104.04%) to anoxia (1.30% saturation) (Fig. 1b). Oxygen conditions exhibited strong diel patterns with maximum oxygen conditions occurring in the mid-afternoon and minimum conditions often occurring in the middle of the night. There was not a clear seasonal trend in oxygen saturation. However, the lowest oxygen saturation period overlapped with the winter storm creating the lowest temperature conditions.

*Respiration*

Thermal performance curves for respiration rate showed significant differences in oxygen consumption between temperatures ($F_{8,8}$= 19.1147, $p<0.001$) and oxygen conditions ($F_{1,143}$= 498.0376, $p<.0001$)(Fig. 2a). Respiration rates under normoxia were between 13.7-31.1 times greater than under hypoxia. There was also significant covariation between snail mass and respiration rate, with larger snails respiring more ($F_{1,156}$=5.0389 $p=0.0262$). Temperature and oxygen level interacted to determine the respiration rate ($F_{8,143}$=34.9471, $p<0.0001$). However, the $T_{opt}$ was consistently at 28°C despite experimental block or oxygen conditions (Fig S3, available online).

During progressive hypoxia, the respiration rate decreased linearly with decreasing oxygen availability (Fig. 2b). Respiration rates were higher at high temperatures than at cool temperatures. The respiration rates converged on zero below 30% air saturation at most temperatures.

*P. antipodarum* were sensitive to changes in oxygen at all temperatures, demonstrated by R values that were less than 50% (33.15-39.71; Fig. 3a). Hypoxia sensitivity of respiration had a negative relationship with temperature (ANOVA, $F_{8,157}$= 4.28, $p<0.05$).

The experiments ended when snails stopped respiring. Using the raw respiration data, without smoothing, we saw that snails at warmer temperatures stopped respiring with less oxygen remaining than snails at cooler temperatures (ANOVA, $F_{8,162}$= 15.5659, $p<0.001$; Fig. 3b). Below 20°C, snails stopped respiring near 30% air saturation (123.44 - 92.12 μmol/L), but above 20°C they stopped respiring closer to 22% air saturation (61.78 - 48.88 μmol/L).

*Activity*

Regardless of oxygen level, snails climbed the least at the extreme hot (minimum 0 body lengths were climbed by an individual) and cold temperatures and most at the intermediate temperatures (15-28°C; maximum 90 body lengths climbed by an individual ). The thermal performance curve under hypoxia was shifted to the right of the normoxic curve, with the $T_{opt}$ at 24.3°C ±0.55 and 18.6°C ±0.40 for hypoxia and normoxia, respectively (Fig. 4). Snails experiencing hypoxia had a wider $T_{br}$ as well, 6.7°C as opposed to 3.7°C for their normoxic counterparts.

To compare the thermal performance curves resulting from both the respiration and activity experiments, we transformed each data point to a percentage of the maximum value under that oxygen condition. Hypoxia affected the activity curve more than the respiration curve (Fig. 5). Peak activity occurred at a lower temperature than peak respiration regardless of oxygen conditions, but the optimal temperatures for both traits were more alike under hypoxic than normoxic conditions (4°C vs. 10°C difference).

We expressed oxygen consumption relative to the distance traveled, using the means of each trait at each temperature, to provide an index comparing relative changes in respiration and locomotor activity. Respiration was higher relative to activity in normoxia compared to hypoxia, and this difference widened as temperature increased (Fig. 6). In normoxia, respiration increased abruptly relative to activity at temperatures above 22°C, an increase that did not occur under hypoxia.

**Discussion**

The New Zealand mud snail (*Potamopyrgus antipodarum*) is a worldwide invader of freshwater habitats. To understand the characteristics of its abiotic niche, it is critical to

understand the physiological responses to simultaneous shifts in oxygen availability and water temperature due to the physical and biological effects of each factor and their interactions. We tested these responses by measuring resting respiration rate through a progressive hypoxia challenge and comparing climbing activity under normoxia and hypoxia. We found that extremely high and low temperatures limited respiration and activity, but that respiration rate was more sensitive to changes in oxygen at low temperatures. Hypoxia did not significantly decrease activity but instead shifted peak activity to warmer temperatures.

*Thermal performance curves are mismatched between traits*

As we hypothesized, extreme high and low temperatures limited metabolism and activity in *Potamopyrgus antipodarum*. The shape of the respiratory thermal performance curve created in this study broadly matched the shape of the curve created for *P. antipodarum* from 4 different habitats in the native range (Hudson 1975), with oxygen consumption increasing toward the $T_{opt}$ at 28°C then sharply declining above that temperature. Koopman et al. (2016) showed that the critical thermal maximum for foot muscle function is 28°C in snails that invaded the Netherlands, suggesting 28°C is a critical threshold for multiple traits. It is likely that above 28°C while at rest, snails rely on anaerobic metabolism to avoid organ failure caused by disruptions in oxygen transport at the mitochondria, decreasing ATP supply, electron leakage, and increased oxidative damage (Abele et al. 2002; Abele et al. 2007; Pörtner et al. 2017; Macmillan 2019). At 30°C, *P. antipodarum* from the native range in New Zealand showed a negative relationship between electron flux and oxygen consumption, suggesting that electron leak plays a role in the respiratory damage that occurs at high temperatures in this species (Sharbrough et al. 2017).

Maximum climbing performance under normoxia was observed between 15-22°C, a thermal range that overlaps with the highest population growth and survival measured in other studies of *P. antipodarum* (Dybdahl and Kane 2005; Bennett et al. 2014). These results suggest that locomotion is an adequate indicator of the temperatures that maximize organismal fitness. This species has few or no predators and no parasites in the invasive range, so reproduction and foraging (a locomotion-based trait) are the main fitness components (Gérard et al. 2003; Vinson and Baker 2008; Alonso and Castro-Díez 2012a; Levri et al. 2020). Due to the multi-year timescales required to observe variation in reproductive fitness (1-2 generations/year in the lab (ANS Task Force 2007; Levri et al. 2020)), locomotor performance is a tractable alternative fitness measure that represents the distance these snails will travel in search of food under different conditions. *P. antipodarum* is notoriously voracious, consuming up to 75% of the available primary productivity in the densest populations (Hall et al. 2003), and thus locomotion is a trait that is very ecologically relevant. The individuals in the current study were not motivated by a food reward so these patterns reflect only voluntary activity, driven by negative geotaxis (Levri et al. 2017, E. King, pers. obs.), and not necessarily total capacity for movement.

In our study, thermal performance curve features ($T_{opt}$, $T_{br}$) varied across levels of biological organization (Schulte et al. 2011; Rezende and Bozinovic 2019). The $T_{opt}$ for respiration occurred 10°C higher than the $T_{opt}$ for activity under normoxia (Fig. 5). The $T_{br}$ of respiration was narrower than the $T_{br}$ for activity, 1.8° and 3.7°C, respectively. This suggests that either the thermal optima of the traits are mismatched ecologically (Marshall et al. 2011), or that a high resting respiration rate does not indicate optimal performance of the whole organism. Resting respiration rate, as a proxy for metabolic rate, estimates the ATP cost of living for an organism at that moment (Clarke and Fraser 2004), so high ATP demand may indicate increased

maintenance costs (e.g., a stress response) or investment in life-history traits such as growth, reproduction or locomotion. For *P. antipodarum* above 22°C under normoxia, increased respiration did not coincide with increased movement, suggesting that increased ATP demand was balancing increased costs for mounting a stress response.

*Snails rely on hypoxia tolerance rather than oxyregulation*

We hypothesized that decreases in oxygen availability would lower respiration and activity and decrease the thermal breadth of both traits. However, this hypothesis was only supported for respiration rate. Respiration rates under hypoxia were less than 10% of those measured under normoxia, signaling considerable metabolic suppression under hypoxia. The snails were sensitive to declining oxygen levels, especially at cooler temperatures (Fig. 3a). Oxygen is likely less available to the snails at cool temperatures because the diffusion rate is greatly decreased and is not overcome by the increased solubility of oxygen in cold water (Verberk et al. 2011). Our results fit well with other evidence that gastropods (especially gilled snails) are oxyconformers (Brown et al. 1998). Marsden and colleagues (2012) found that none of the 32 British gastropods studied under progressive hypoxia are oxyregulators across the oxygen saturation gradient. Some researchers have hypothesized that gastropods lack the compensatory mechanisms (e.g., changing ventilation capacity, heart rate, or extraction efficiency) that other mollusks, such as bivalves, use to maintain high oxygen consumption rates in the face of declining environmental oxygen availability (Alexander Jr and McMahon 2004; Marsden et al. 2012). Early sensitivity to deoxygenation leading to metabolic depression may allow the snails to conserve energy and extend their survival time under hypoxia (Hochachka and Somero 2002).

The ability to respire or move under very low oxygen conditions is likely more important for *P. antipodarum* than the ability to maintain high performance across the oxygen gradient. At the end of the respirometry experiments, there was more oxygen left in the chambers at low temperatures when the snails stopped respiring, suggesting there was no conserved lower limit for respiration to occur (Fig. 2B). Snails above 22°C respired past the common threshold for sublethal hypoxia effects (2mg/L of oxygen) that was established for predicting the collapse of marine fisheries (Renaud 1983), though some investigators suggest that this threshold should be closer to 4.5 mg/L (Vaquer-Sunyer and Duarte 2008; Saari et al. 2018). *P. antipodarum* are not only respiring for many hours under the higher threshold at all temperatures and under the lower threshold above 22°C, but they can still locomote, suggesting that 4.5 mg/L of oxygen is not adequate to observe acute sublethal effects of hypoxia.

*Effects of temperature and oxygen interact to create tradeoffs*

Changes to snail activity under hypoxia highlighted the interactive effects of oxygen and temperature and did not fully support our original hypotheses. We expected to see decreased overall performance and a narrower thermal performance curve due to increases in oxygen demand at warm temperatures not being met by the environment and an inability to extract oxygen out of cool, dense water (Verberk et al. 2011) on top of the 80% reduction in the oxygen supply in the chamber. Snail activity was reduced at cool temperatures under hypoxic conditions compared to normoxic conditions, and no activity was recorded at the highest temperature as we hypothesized. However, we observed a wider $T_{br}$ and an increased $T_{opt}$ for activity under hypoxia (Fig. 4). At moderately warm temperatures (22-28°C), climbing activity was significantly higher under hypoxic than normoxic conditions. The increase in activity may relate to increased

motivation to move under stress. Aquatic taxa commonly respond to hypoxia first by altering their behavior; highly mobile species (e.g., fish) flee the area and less mobile organisms (e.g., snails) climb available substrates (Diaz and Rosenberg 1995; Riedel et al. 2014). However, prior studies rarely address how temperature might interact with these patterns, as increased oxygen is required at high temperatures for basic maintenance and movement to suitable oxygen refugia.

The shift toward activity in warm, hypoxic water may indicate an escape response to interacting temperature and oxygen stresses fueled by anaerobic metabolism. The large increases in movement under hypoxia at high temperatures did not correspond with increases in aerobic metabolism (Fig. 6), so the snails may be using anaerobic pathways to generate ATP for movement. The need for anaerobic metabolism increases to augment or replace energy obtained through aerobic metabolism as temperatures rise and oxygen levels fall (Pörtner 2010; Ern 2019). Anaerobic metabolism is better studied in other gastropods (Houlihan and Innes 1982; Storey 1993; Pörtner 2001; Sokolova 2003), but Paolucci and Thuesen (2020) found that *P. antipodarum* use alanopine dehydrogenase over other -opine enzymes for anaerobic metabolism. The ability to power movement or other performance traits through fermentation for significant periods might expand the niche of this species past our current expectations.

Interactions between temperature and oxygen introduce tradeoffs between energy conservation and escaping suboptimal conditions. When oxygen is plentiful at temperature extremes, the snails may prioritize energy conservation, demonstrated by low activity levels. But under the added stress of hypoxia at warm temperatures, it may be most beneficial to rely on limited anaerobic metabolism to find an oxygen-rich and/or preferred temperature refuge until conditions improve, as demonstrated by increased activity in our study. The timescale of oxygen and temperature stress may also influence the tradeoff. Short bouts of stressful conditions may favor the movement reduction response, while longer episodes of stressful conditions may favor escape. The length and magnitude of stressful temperature and oxygen conditions must be considered to predict population spread under various microhabitat conditions.

*Effects of temperature and oxygen in nature*

A model relying on climate data predicts that *P. antipodarum* could invade most waterways in North America (Loo et al. 2007). However, this model does not include oxygen level, which plays an important role in the survival of aquatic species and is expected to be impacted by continued nutrient inputs in waterways and climate change leading to deoxygenated freshwater systems (Saari et al. 2018). Understanding the interactive effects of oxygen and temperature experienced by *P. antipodarum* gives us a deeper understanding of what level of performance might be possible in microclimates not represented in current models.

Our study highlights that low temperatures limit both respiration and activity regardless of oxygen saturation. *Potamopyrgus antipodarum* are not freeze tolerant so there is a clear lower temperature limit for their survival (Hylleberg and Siegismund 1987; Siegismund and Hylleberg 1987; Richards et al. 2004). Long low temperature periods (less than 7°C) might push the limits of this snail's energy storage capabilities such that food must be obtained, but cool temperatures make movement unlikely or impossible. However, where autumn and winter temperatures are less than 15°C, low metabolic demand and food scarcity might co-occur, allowing snails to "sit and wait" with no negative metabolic consequences.

The sit and wait strategy will likely have negative consequences in warm water. Extreme warm temperatures (greater than 25°C) are likely to limit population movement even when oxygen levels are high. Resting respiration rates are highest under those conditions as well.

Anaerobic metabolism might fuel some escape behavior but is still a time-limited solution. If heatwaves intensify in magnitude or frequency as climate models suggest (Perkins-Kirkpatrick and Lewis 2020), snails may not be able to move and will be effectively trapped and requiring large amounts of oxygen for survival. This situation is most likely to occur in disconnected water bodies (e.g., small ponds, puddles, intermittent streams) where the water can quickly become hot and hypoxic.

Streams with *P. antipodarum* populations demonstrate both prolonged hypoxia (up to a week at less than 50% air saturation) and periodic bouts of hypoxia and reoxygenation on a diel cycle. Due to this species' continued presence in these streams, we must conclude that they can withstand these conditions, especially because we observed low oxygen conditions coupled with high temperatures at this stream site during a heatwave (23°C and 45% oxygen saturation). The spread of this species worldwide is supported by its ability to survive harsh, low oxygen conditions in transport (A.N.S. Task Force 2007; Alonso and Castro-Diez 2008). Snails in transport without water close their opercula to avoid desiccation, thus cutting off oxygen supply to the gills (Richards et al. 2004). Dependence on anaerobiosis could greatly facilitate current and future spread. However, with the data we have now, we do not know which processes rely on the ability to produce aerobic energy and which can be sustained by anaerobic processes. Prolonged hypoxia and the respiratory suppression that follows may still have unknown effects on reproduction, immune function, and other vital processes.

Our study investigated the limits that temperature and oxygen place on respiration and activity in *Potamopyrgus antipodarum*. We found that extreme temperatures limit both respiration and activity but that hypoxia alters the thermal sensitivity of activity, which may be fueled by anaerobic metabolism under stress. The establishment of this species depends on the interacting temperature and oxygen conditions in the new microhabitat. The combination of high-quality environmental data, population sizes over time, and what we have learned from their physiology in this study will be necessary to understand if the conditions necessary to limit the individual and population growth of *P. antipodarum* exist now or in the future natural systems of North America.

**Acknowledgments**

Our work was partially supported by a Summer Research Award from the Department of Integrative Biology, UC Berkeley, and the Mary Bowerman Science and Research grant from Save Mount Diablo, both to E.E.K. Animal work was permitted by CDFW permits SC-13772 and S-182910001-18291-001. We have no competing interests that might have influenced the work described in this manuscript. E.E.K., J.H.S., and C.M.W. conceived and designed the experiments. E.E.K. performed the experiments and analyzed the data. E.E.K., J.H.S., and C.M.W. prepared the manuscript.

**Figures**

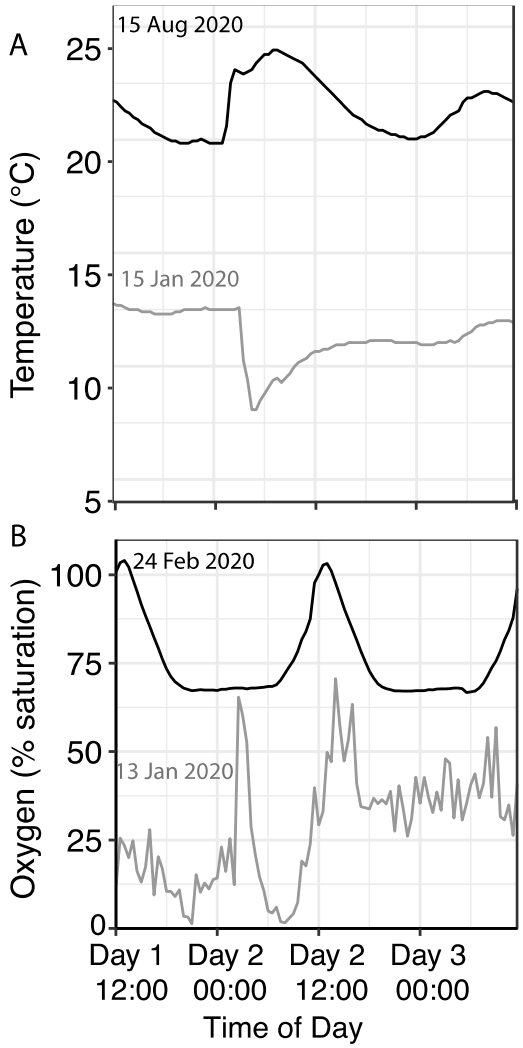


**Figure 1. Most extreme field temperature and oxygen conditions in Mt. Diablo Creek**. The most extreme 48-hour periods (noon-noon) of temperature and oxygen saturation were recorded at Mt. Diablo Creek in Clayton, California, U.S.A. (37.943958 N,-121.937397 W). **A)** High temperatures recorded on 8/15/2020-8/17/2020 (black line) and low temperatures recorded 1/15/2020-1/17/2020 (gray line) **B)** High oxygen saturation recorded on 1/13/2020-1/15/2020 (black line) and low oxygen saturations recorded on 2/24/2020-2/26/2020 (gray line).

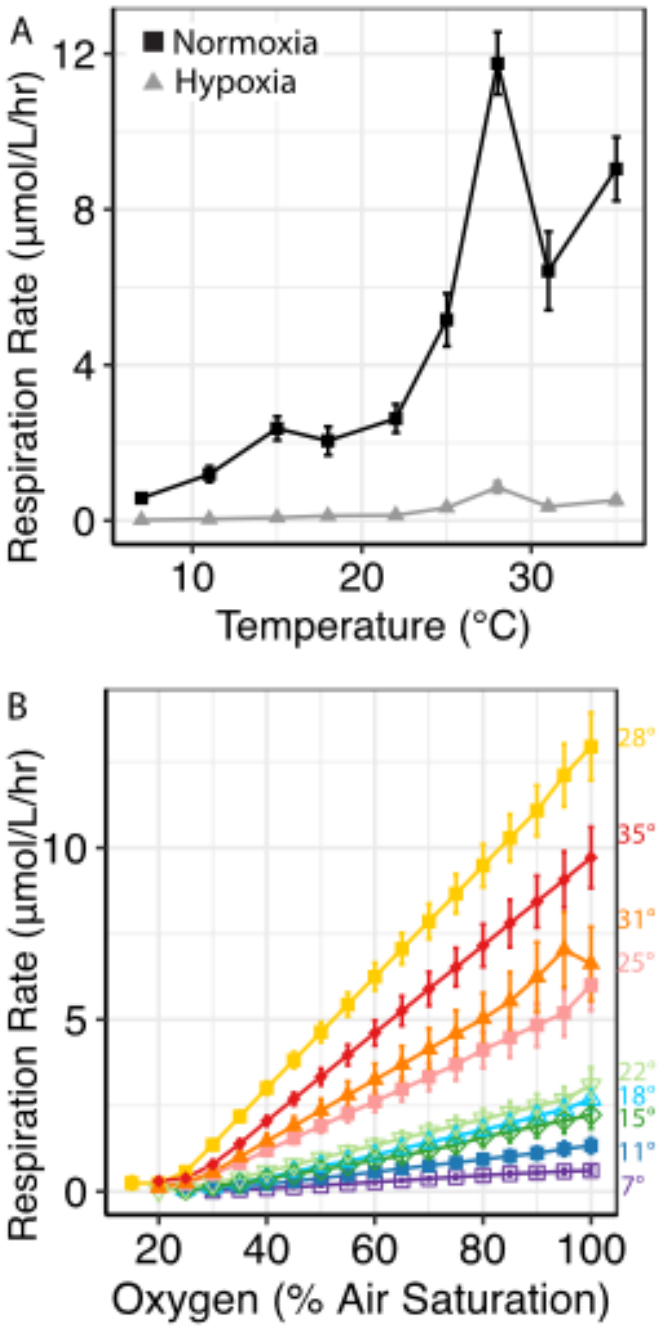


**Figure 2. Temperature and oxygen sensitivity of respiration rate. A)** Respiration rates across temperatures in normoxia(100-85%) and hypoxia (<35%). Black squares represent normoxia and gray triangle represent hypoxia. **B)** Respiration rate through progressive hypoxia (100% air saturation until no oxygen uptake) for *Potamopyrgus antipodarum* at 9 temperatures. Temperatures are denoted by color and point shape. Points are means ± standard error.

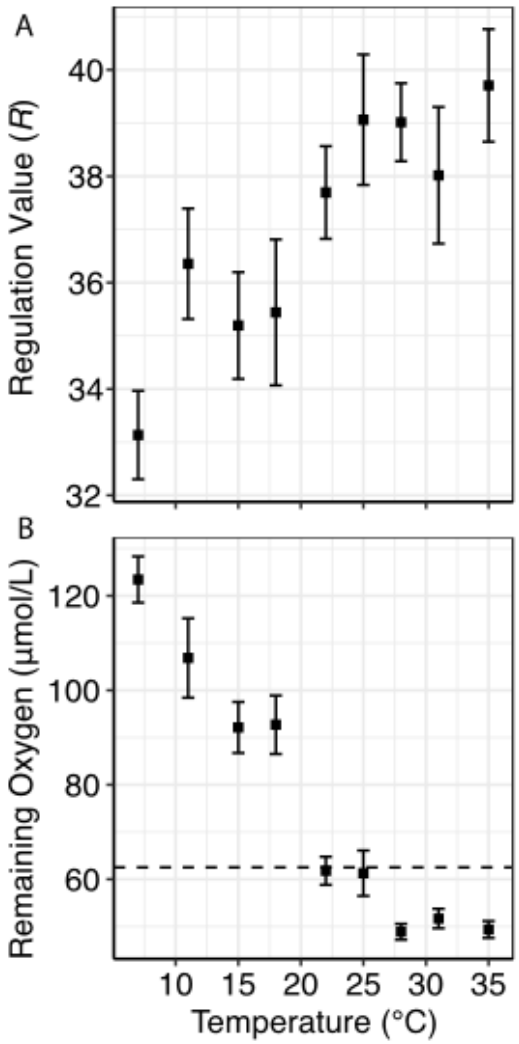


**Figure 3. Oxygen sensitivity of respiration rate. A)** Regulation values, R, were calculated across temperatures for *Potamopyrgus antipodarum* respiration during progressive hypoxia. Lower values indicate that respiration rate is more sensitive to decreasing oxygen.(N= 19 or 20 snails per temperature) **B)** Oxygen left remaining in the respirometry chamber at the end of the progressive hypoxia experiment. Dashed line denotes 2 mg/L threshold. All points are below the 4.5 mg/L (140.6 µmol/L). All points are means ± standard error. N=20 snails per temperature.

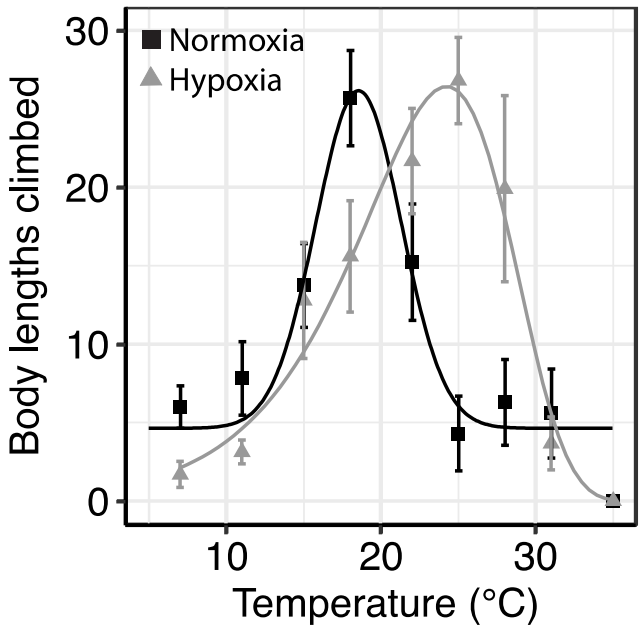


**Figure 4. Climbing activity under across temperatures and oxygen conditions.** Thermal performance curves for *Potamopyrgus antipodarum* were generated under 9 temperatures at normoxia (100%, N=20) and hypoxia (20%, N=20). Normoxia curve best fits a Gaussian model and the hypoxia curve best fits a Weibull model. Points are means ± standard error. Black squares represent normoxia and gray triangles represent hypoxia.

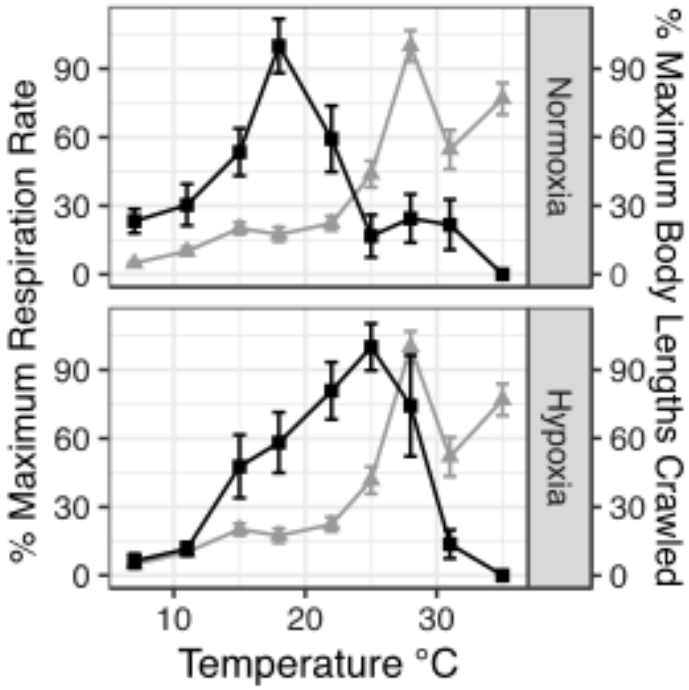


**Figure 5. Comparison of thermal performance curves.** Thermal performance curves are compared for respiration (gray triangles) and activity (black squares) under normoxia (top panel) and hypoxia (bottom panel) in Potamopyrgus antipodarum. Each response is scaled to a percentage of the maximum value under that oxygen condition. Points represent means with standard error bars.

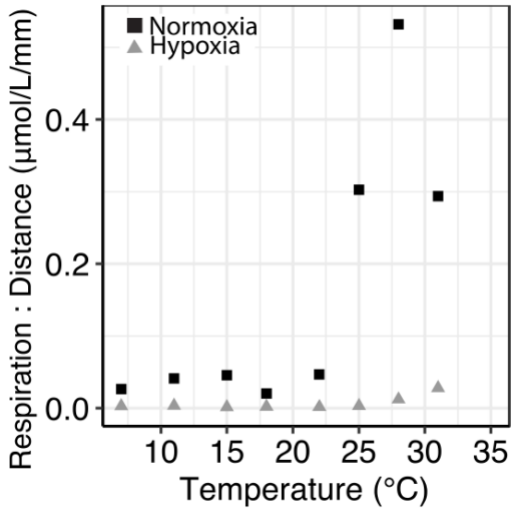


**Figure 6. Ratio of respiration to distance traveled in *Potamopyrgus antipodarum* under different temperature conditions.** Points are the ratio of mean oxygen respired to mean distance climbed at each temperature under normoxic and hypoxic conditions. Black squares represent normoxia and gray triangles represent hypoxia.

**Supplemental Materials**

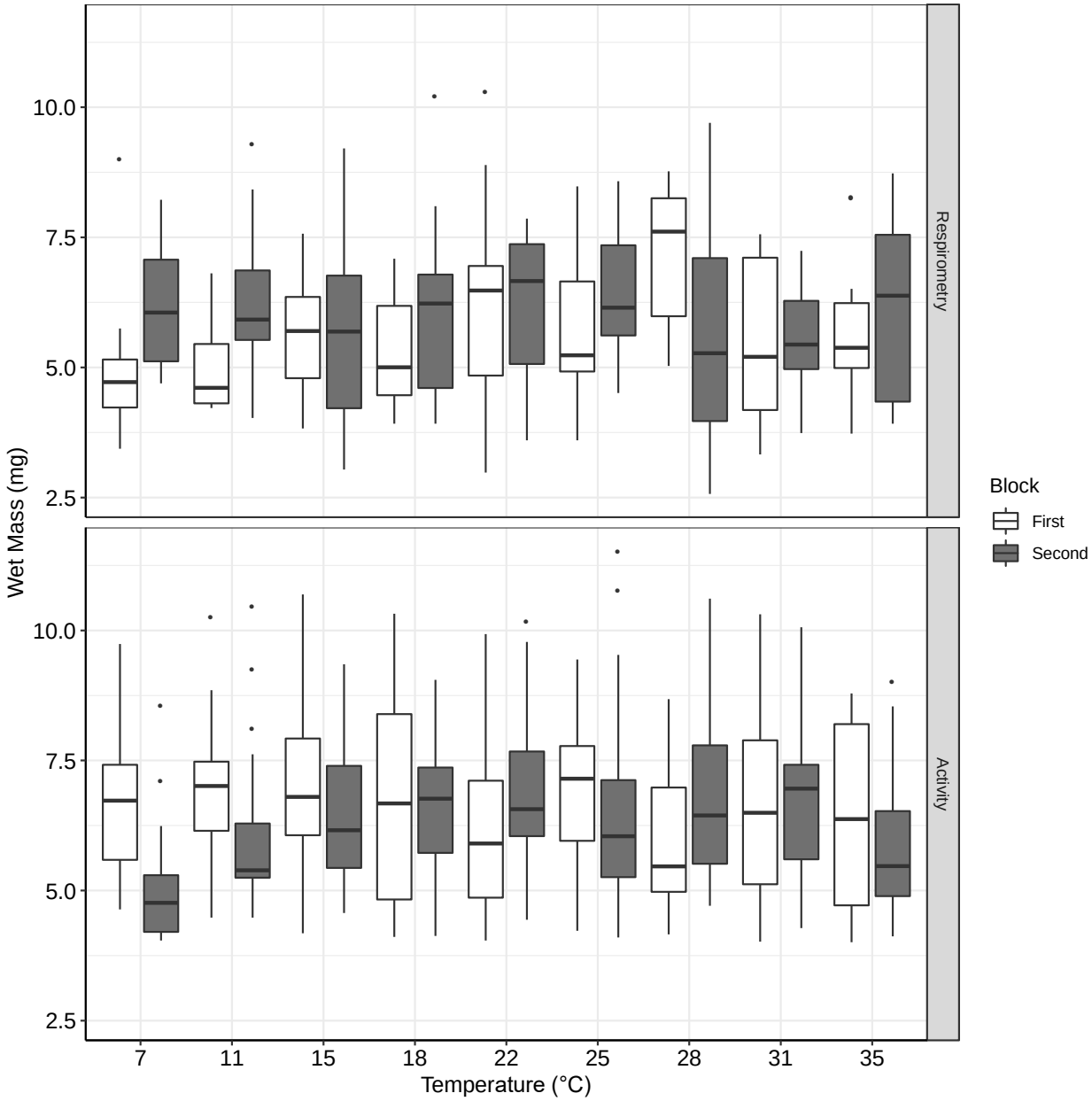


**Figure S1.** Wet masses of *Potamopyrgus antipodarum* from the respirometry and activity experiments.

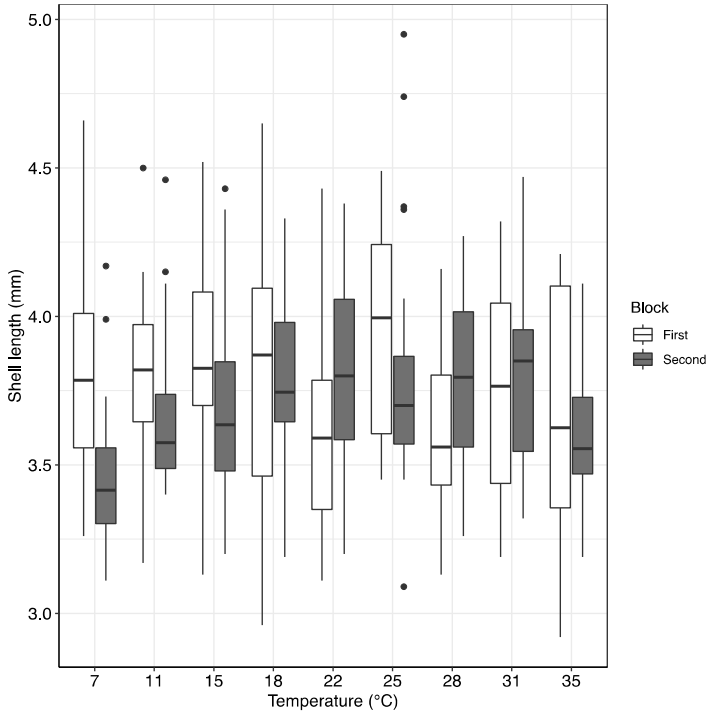


**Figure S2.** Shell lengths of *Potamopyrgus antipodarum* from the activity experiments.

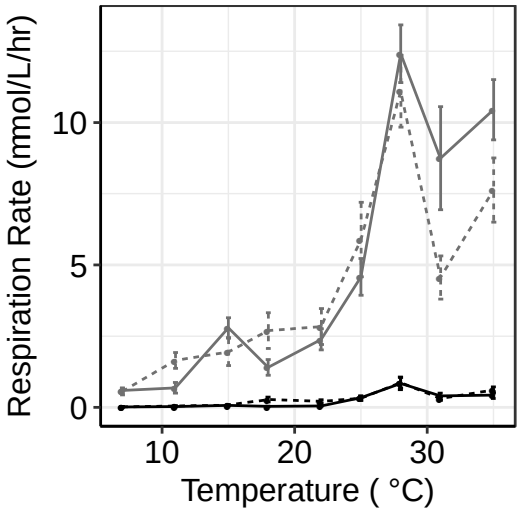


**Figure S3.** Respiration rates across temperatures in normoxia(100-85%) and hypoxia (<35%). Black lines represent hypoxia, gray lines represent normoxia. The solid lines were generated from the first experimental block, the dashed lines were generated from the second experimental block.

**Literature Cited**

Abele D, Heise K, Pörtner HO, Puntarulo S. 2002. Temperature-dependence of mitochondrial function and production of reactive oxygen species in the intertidal mud clam *Mya arenaria*. J Exp Biol 205:1831–1841. doi:10.1006/fsim.1997.0094.

Abele D, Philipp E, Gonzalez PM, Puntarulo S. 2007. Marine invertebrate mitochondria and oxidative stress. Front Biosci 12:933–946.

Alexander Jr JE, McMahon RF. 2004. Respiratory response to temperature and hypoxia in the zebra mussel *Dreissena polymorpha*. Comp Biochem Physiol Part A Mol Integr Physiol 137:425–434. doi:10.1016/j.cbpb.2003.11.003.

Alonso A, Castro-Diez P. 2008. What explains the invading success of the aquatic mud snail *Potamopyrgus antipodarum* (Hydrobiidae, Mollusca)? In: Hydrobiologia. Vol. 614. p. 107–116.

Alonso Á, Castro-Díez P. 2012a. The exotic aquatic mud snail *Potamopyrgus antipodarum* (Hydrobiidae, Mollusca): State of the art of a worldwide invasion. Aquat Sci 74:375–383. doi:10.1007/s00027-012-0254-7.

Alonso Á, Castro-Díez P. 2012b. Tolerance to air exposure of the New Zealand mudsnail *Potamopyrgus antipodarum* (Hydrobiidae, Mollusca) as a prerequisite to survival in overland translocations. NeoBiota 14:67–74. doi:10.3897/neobiota.14.3140.

Angilletta MJ. 2006. Estimating and comparing thermal performance curves. J Therm Biol 31:541–545. doi:10.1016/j.jtherbio.2006.06.002.

A.N.S. Task Force. 2007. National management and control plan for the New Zealand mudsnail (*Potamopyrgus antipodarum*) prepared for the Aquatic Nuisance Species Task Force by the New Zealand mudsnail management and control plan working group.

Bankers L, Fields P, McElroy KE, Boore J, Logsdon JM, Neiman M. 2017. Genomic evidence for population-specific responses to coevolving parasites in a New Zealand freshwater snail. Mol Ecol:1–13. doi:10.1111/mec.14146.

Bennett DM, Dudley TL, Cooper SD, Sweet SS. 2014. Ecology of the invasive New Zealand mud snail, *Potamopyrgus antipodarum* (Hydrobiidae), in a Mediterranean-climate stream system. Hydrobiologia 746:375–399. doi:10.1007/s10750-014-2136-6.

Brown KM, Alexander JE, Thorp JH. 1998. Differences in the ecology and distribution of lotic pulmonate and prosobranch gastropods. Am Malacol Bull 14:91–101.

Clarke A, Fraser KPP. 2004. Why does metabolism scale with temperature? Funct Ecol 18:243–251. doi:10.1111/j.0269-8463.2004.00841.x.

Diaz RJ, Rosenberg R. 1995. Marine benthic hypoxia: a review of its ecological effects and the behavioural responses of benthic macrofauna. Oceanogr Mar Biol an Annu Rev Vol 33:245–303.

Dybdahl MF, Drown DM. 2011. The absence of genotypic diversity in a successful

parthenogenetic invader. Biol Invasions 13:1663–1672. doi:10.1007/s10530-010-9923-4.

Dybdahl MF, Kane SL. 2005. Adaptation vs. phenotypic plasticity in the success of a clonal invader. Ecology 86:1592–1601. doi:10.1890/04-0898.

Ern R. 2019. A mechanistic oxygen- And temperature-limited metabolic niche framework. Philos Trans R Soc B Biol Sci 374:6–10. doi:10.1098/rstb.2018.0540.

Gargano JW, Martin I, Bhandari P, Grotewiel MS. 2005. Rapid iterative negative geotaxis (RING): A new method for assessing age-related locomotor decline in *Drosophila*. Exp Gerontol 40:386–395. doi:10.1016/j.exger.2005.02.005.

Gérard C, Blanc A, Costil K. 2003. *Potamopyrgus antipodarum* (Mollusca:Hydrobiidae) in continental aquatic gastropod communities: Impact of salinity and trematode parasitism. Hydrobiologia 493:167–172. doi:10.1023/A:1025443910836.

Giller PS, Malmqvist B. 1998. The biology of streams and rivers. Crawley M, Little C, Southwood T, Ulfstrand S, editors. Oxford: Oxford University Press.

Gillooly JF, Brown JH, West GB, Savage VM, Charnov EL. 2001. Effects of size and temperature on metabolic rate. Science (80- ) 293:2248–2251. doi:10.1126/science.1061967.

Hall RO, Tank JL, Dybdahl MF. 2003. Exotic snails dominate nitrogen and carbon cycling in a highly productive stream. Front Ecol Environ 1:407–411. doi:10.1890/1540-9295(2003)001[0407:ESDNAC]2.0.CO;2.

Hochachka PW, Somero GN. 2002. Biochemical adaptation : mechanism and process in physiological evolution. Oxford University Press.

Houlihan DF, Innes AJ. 1982. Oxygen consumption, crawling speeds, and cost of transport in four mediterranean intertidal gastropods. J Comp Physiol B 147:113–121. doi:10.1007/BF00689299.

Hudson JL. 1975. Oxygen consumption of the mollusc *Potamopyrgus antipodarum* in relation to habitat. Mauri Ora 3:63–75.

Hulme PE. 2009. Trade, transport and trouble: managing invasive species pathways in an era of globalization. J Appl Ecol 46:10–18. doi:10.1111/j.1365-2664.2008.01600.x.

Hylleberg J, Siegismund H. 1987. Niche overlap in mud snails (Hydrobiidae): freezing tolerance. Mar Biol 94:403–407.

Kettunen M, Genovesi P, Gollasch S, Pagad S, Starfinger U, ten Brink P, Shine C. 2008. Technical support to E.U. strategy on invasive species (I.A.S.) - assessment of the impacts of I.A.S. in Europe and the E.U.

Koopman KR, Collas FPL, van der Velde G, Verberk WC. 2016. Oxygen can limit heat tolerance in freshwater gastropods: differences between gill and lung breathers. Hydrobiologia 763:301–312. doi:10.1007/s10750-015-2386-y.

Lennox R, Choi K, Harrison PM, Paterson JE, Peat TB, Ward TD, Cooke SJ. 2015. Improving science-based invasive species management with physiological knowledge, concepts, and tools. Biol Invasions 17:2213–2227. doi:10.1007/s10530-015-0884-5.

Levri EP, Berkheimer C, Wilson K, Xu J, Woods T, Hutchinson S, Yoder K, Zhang X, Li X. 2020. The cost of predator avoidance behaviors in an invasive freshwater snail. Freshw Sci 39. doi:10.1086/710107.

Levri EP, Kelly AA, Love E. 2007. The invasive New Zealand mud snail (*Potamopyrgus antipodarum*) in Lake Erie. J Great Lakes Res 33:1–6.

Levri EP, Landis S, Smith B, Colledge E, Metz E, Li X. 2017. Variation in predator-induced behavioral changes in introduced and native populations of the invasive New Zealand mud snail (*Potamopyrgus antipodarum* Gray, 1843). Aquat Invasions 12:499–508. doi:10.3391/ai.2017.12.4.07.

Loo SE, Mac Nally R, Lake P.S. 2007. Forecasting New Zealand mudsnail invasion range: model comparisons using native and invaded ranges. Ecol Appl 17:181–189. doi:10.1890/1051-0761(2007)017[0181:FNZMIR]2.0.CO;2.

Macmillan HA. 2019. Dissecting cause from consequence: a systematic approach to thermal limits. doi:10.1242/jeb.191593.

Marsden ID, Shumway SE, Padilla DK. 2012. Does size matter? the effects of body size and declining oxygen tension on oxygen uptake in gastropods. J Mar Biol Assoc United Kingdom 92:1603–1617. doi:10.1017/S0025315411001512.

Marshall DJ, Dong YW, McQuaid CD, Williams GA. 2011. Thermal adaptation in the intertidal snail *Echinolittorina malaccana* contradicts current theory by revealing the crucial roles of resting metabolism. J Exp Biol 214:3649–3657. doi:10.1242/jeb.059899.

Miller NA, Chen X, Stillman JH. 2014. Metabolic physiology of the invasive clam, *Potamocorbula amurensis*: the interactive role of temperature, salinity, and food availability. PLoS One 9:3–9. doi:10.1371/journal.pone.0091064.

Neiman M, Jokela J, Lively CM. 2005. Variation in asexual lineage age in *Potamopyrgus antipodarum*, a New Zealand snail. Evolution 59:1945–1952. doi:10.1111/j.0014-3820.2005.tb01064.x.

Padfield D, O'sullivan H, Pawar S. 2020. rTPC and nls.multstart: a new pipeline to fit thermal performance curves in R. bioRxiv:2020.12.16.423089.

Paganini AW, Miller NA, Stillman JH. 2014. Temperature and acidification variability reduce physiological performance in the intertidal zone porcelain crab *Petrolisthes cinctipes*. J Exp Biol 217:3974–3980. doi:10.1242/jeb.109801.

Paolucci EM, Thuesen E V. 2020. Effects of osmotic and thermal shock on the invasive aquatic mudsnail *Potamopyrgus antipodarum*: Mortality and physiology under stressful conditions. NeoBiota 54:1–22. doi:10.3897/neobiota.54.39465.

Perkins-Kirkpatrick SE, Lewis SC. 2020. Increasing trends in regional heatwaves. Nat Commun 11:1–8. doi:10.1038/s41467-020-16970-7.

Pimentel D, Zuniga R, Morrison D. 2005. Update on the environmental and economic costs associated with alien-invasive species in the United States. Ecol Econ 52:273–288. doi:10.1016/j.ecolecon.2004.10.002.

Pörtner H-O. 2010. Oxygen- and capacity-limitation of thermal tolerance: a matrix for integrating climate-related stressor effects in marine ecosystems. J Exp Biol 213:881–893. doi:10.1242/jeb.037523.

Pörtner H-O, Bock C, Mark FC. 2017. Oxygen- and capacity-limited thermal tolerance: bridging ecology and physiology. J Exp Biol 220:2685–2696. doi:10.1242/jeb.134585.

Pörtner H. 2001. Climate change and temperature-dependent biogeography: Oxygen limitation of thermal tolerance in animals. Naturwissenschaften 88:137–146. doi:10.1007/s001140100216.

Rahel FJ. 2002. Homogenization of freshwater faunas. Annu Rev Ecol Syst 33:291–315. doi:10.1146/annurev.ecolsys.33.010802.150429.

Renaud ML. 1983. Hypoxia in Louisiana coastal waters during 1983: implications for fisheries. Fish Bull 84:19–26.

Rezende EL, Bozinovic F. 2019. Thermal performance across levels of biological organization. Philos Trans R Soc B Biol Sci 374. doi:10.1098/rstb.2018.0549.

Richards DC, O'Connell P, Cazier Shinn D. 2004. Simple control method to limit the spread of the New Zealand mudsnail *Potamopyrgus antipodarum*. North Am J Fish Manag 24:114–117. doi:10.1577/M02-133.

Riedel B, Pados T, Pretterebner K, Schiemer L, Steckbauer A, Haselmair A, Zuschin M, Stachowitsch M. 2014. Effect of hypoxia and anoxia on invertebrate behaviour: ecological perspectives from species to community level. Biogeosciences 11:1491–1518. doi:10.5194/bg-11-1491-2014.

Saari GN, Wang Z, Brooks BW. 2018. Revisiting inland hypoxia: diverse exceedances of dissolved oxygen thresholds for freshwater aquatic life. Environ Sci Pollut Res 25:3139–3150. doi:10.1007/s11356-017-8908-6.

Sardiña P, Beringer J, Roche D, Thompson RM. 2015. Temperature influences species interactions between a native and a globally invasive freshwater snail. Freshw Sci 34:933–941. doi:10.1086/681639.

Schneider, C.A., Rasband, W.S., Eliceiri KW. 2012. N.I.H. Image to ImageJ: 25 years of image analysis. Nat Methods 9:671–675.

Schulte PM, Healy TM, Fangue NA. 2011. Thermal performance curves, phenotypic plasticity, and the time scales of temperature exposure. Integr Comp Biol 51:691–702. doi:10.1093/icb/icr097.

Sharbrough J, Cruise JL, Beetch M, Enright NM, Neiman M, Pecon-Slattery J. 2017. Genetic variation for mitochondrial function in the New Zealand freshwater snail *Potamopyrgus antipodarum*. J Hered 108:759–768. doi:10.1093/jhered/esx041.

Siegismund HR, Hylleberg J. 1987. Dispersal-mediated coexistence of mud snails (Hydrobiidae) in an estuary. Mar Biol 94:395–402. doi:10.1007/BF00428245.

Sokolova IM. 2003. Metabolic plasticity and critical temperatures for aerobic scope in a eurythermal marine invertebrate (*Littorina saxatilis*, Gastropoda: Littorinidae) from different latitudes. J Exp Biol 206:195–207. doi:10.1242/jeb.00054.

Storey K. 1993. Molecular mechanisms of metabolic arrest in mollusks. In: Hochachka; PW, L LP, J ST, Rosenthal M, editors. Surviving Hypoxia: Mechanisms of Control and Adaptation. Ann Arbor: C.R.C. Press. p. 253–270.

Vaquer-Sunyer R, Duarte CM. 2008. Thresholds of hypoxia for marine biodiversity. Proc Natl Acad Sci 105:15452–15457. doi:10.1073/pnas.0803833105.

Verberk WC, Bilton DT, Calosi P, Spicer JI. 2011. Oxygen supply in aquatic ectotherms: partial pressure and solubility together explain biodiversity and size patterns. Ecology 92:1565–1572.

Vinson MR, Baker MA. 2008. Poor growth of rainbow trout fed New Zealand mud snails *Potamopyrgus antipodarum*. North Am J Fish Manag 28:701–709. doi:10.1577/m06-039.1.

Winterbourn MJ. 1969. Water temperature as a factor limiting the distribution of *Potamopyrgus antipodum* (Gastropoda-Prosobranchia) in the New Zealand thermal region. New Zeal J Mar Freshw Res 3:453–458. doi:10.1080/00288330.1969.9515310.

Winterbourn MJ. 1970. The New Zealand species of *Potamopyrgus* (Gastropoda: Hydrobiidae). Malacologia 10:283–321.

Wood CM. 2018. The fallacy of the Pcrit - Are there more useful alternatives? J Exp Biol 221. doi:10.1242/jeb.163717.

Zaranko DT, Farara DG, Thompson FG. 1997. Another exotic mollusc in the Laurentian Great Lakes: the New Zealand native *Potamopyrgus antipodarum* (Gray 1843) (Gastropoda, Hydrobiidae). Can J Fish Aquat Sci 54:809–814. doi:10.1139/cjfas-54-4-809.

**Invasive *Potamopyrgus antipodarum* are robust to most environmental variation in San Francisco Bay streams, but high algae cover explains most variation in population density**

## Introduction

Predicting and preventing the establishment of invasive species can mitigate their environmental and economic impacts, but doing so requires understanding key aspects of their life history, physiology and ecological niche (Lennox et al. 2015). To successfully establish in a new environment, invasive species must pass through three environmental filters: biogeographical, abiotic, and biotic (Rahel 2002; Cadotte and Tucker 2017). Biogeographical filter are landscape features that block dispersal between habitats (e.g. mountains, rivers, human infrastructure). However, intentional or unintentional transport by humans often allows invasive organisms to circumvent biogeographical filters (Rahel 2002; Hulme 2009). Once a non-native species have successfully recruited to a new region, it faces abiotic and biotic filters that often exert an interactive influence on survival, growth, and reproduction (Cadotte and Tucker 2017). To pass the abiotic filter, the organism must have the physiological capacity to live and reproduce in the new habitat's environmental conditions. Lastly, to pass through the biotic filter, the organism must be able to persist in the biotic interaction web of the new environment (e.g. acquire nutrients or food, and persist in the face of predation, parasitism, and competition)). The interaction between abiotic and biotic filters is also critical to establishment as the strength of biotic interactions can be influenced by abiotic conditions (e.g. feeding rates differ by thermal regimes, some species have competitive advantage under certain conditions).

*Potamopyrgus antipodarum* (Gray, 1853) is a small operculate snail native to fresh and brackish waters in New Zealand (Winterbourn 1970). Invasive populations exist worldwide and are particularly widespread in the western US and Great lakes regions, across which they have spread since being introduced in the late 1980s (Figure 1) (Dybdahl and Drown 2011; Alonso and Castro-Díez 2012). Invasive populations of *P. antipodarum* are made up of parthenogenetically reproducing viviparous females and can become as dense as 500,000 individuals/$m^2$, though they have demonstrated boom and bust cycles in some areas (Hall et al. 2003; Moore et al. 2012). Sustained high density populations shift nutrient cycling, negatively impact native invertebrates by grazing all available periphyton, and are indigestible to many predatory fish (Kerans et al. 2005; Vinson and Baker 2008; Moore et al. 2012). Like other invasive species, invasive snail populations are less constrained by their natural enemies. In New Zealand, populations are controlled by closely co-evolved trematode parasites (Bankers et al. 2017). Crayfish are the main predators that invasive populations face because they have the ability to crush thick *P. antipodarum* shells, but generalist predators are considered to have minimal impacts on *P. antipodarum* populations (Alonso and Castro-Díez 2012; Bennett et al. 2014). Given that *P. antipodarum* seems free from many ecological controls, it becomes even more important to be able to predict the filters that will block their establishment in new areas.

In the non-native range, mud snails are found in diverse environments, including snowmelt fed rivers and brackish estuaries, demonstrating their broad habitat tolerances (Hall et al. 2003; Alonso and Castro-Diez 2008; Alonso and Castro-Díez 2012). A model relying only on climate data suggests that *P. antipodarum* will be able to survive in most U.S. watersheds (Loo et al. 2007), but there are regions of the U.S., such as the Midwest and the South, that lack *P. antipodarum* (Figure 1). There are two disadvantages to considering only climate variables on the continental scale. First, this framework completely ignores the role of biotic interactions in

shaping the range. Second, the scale is likely too large identify patchiness in non-climate abiotic factors (e.g., substrate type, water flow, etc.). Focusing on individual streams with known introductions and continuous habitats helps avoid this problem. Individual streams are extremely likely to have had snails introduced everywhere downstream of the original introduction site because *P. antipodarum* commonly drift downstream, are able to crawl upstream and are easily transported by human and animal vectors (Ribi 1986; ANS Task Force 2007; Sepulveda and Marczak 2012). Given the likelihood of spread within a stream, it is reasonable to assume that the area downstream of the original introduction has experienced snail introduction and population density depends on the presence of abiotic and/or biotic filters.

In this study, I aimed to identify the abiotic and biotic factors that explain variation in *P. antipodarum* population density in creeks in the San Francisco Bay Area. I hypothesized that population size can be explained using a multivariate combination of abiotic and biotic variables. To test this hypothesis, I measured snail population density and 25 abiotic and biotic factors for one year on three creeks to capture the variation in characteristics that drive snail abundance. Understanding how environmental processes influence population density may provide insight into the conditions under which this species will remain at low levels rather than dominating the ecosystem, and where they can invade in the future.

## Methods

### *Stream Sites*

I studied three small creeks around the San Francisco Bay Area region that hosted *P. antipodarum* between 6 September 2019 and 8 September 2020 (Table S1). I measured population density and environmental parameters at an upstream and a downstream site along the mainstem of each creek (Figure 1, Table 1). Upstream sites are closer to the creek's headwaters and farther from the San Francisco Bay. The average distance between upstream and downstream sites was 2.24 km. Sites were chosen in the spring of 2019 because they hosted *P. antipodarum* and were publicly accessible at parks or adjacent to public trails. These creeks had first records of mud snail presence between 2014-2016 in the USGS Nonindigenous Aquatic Species database (U.S. Geological Survey 2021). Snails from these location are extremely likely to be the "US 1" clonal type that is the most widespread across the western United States (Dybdahl and Drown 2011). The site at Brazil Quarry (Mt. Diablo Creek) was excluded from most analyses because water, and thus *P. antipodarum*, was absent from this portion of the stream for the duration of the study. This site has intermittent flow and was wet when the site was chosen but water did not return for measurable periods of time in the study period.

### *Measurements of Abiotic Factors*

*High-resolution, continuous data*

I. Temperature

Ambient stream temperature was measured at the substrate by stationary HOBO UA-001-64 loggers (Onset Computer Corporation, Bourne, MA) for the duration of the study at each site (Figure S1). Due to the dry stream conditions and the possibility of logger damage and theft at the Brazil Quarry site (Mt. Diablo Creek), an iButton data logger (accuracy ±0.5°C, DS1921G, Dallas Semiconductor) was deployed instead. The logger was placed in a waterproof brass casing affixed to the underside of a large rock with Z-spar marine epoxy (Gunderson et al. 2019). Both logger types recorded temperature every 30 minutes with ±0.5°C accuracy. There is a gap in the

record for the Clayton site (Mt. Diablo Creek) (7/3/2020-8/14/2020) and the Brazil site (Mt. Diablo Creek) (12/17/19-2/23/20, 4/6-4/18/2020, 7/14-8/9/2020) due to logger damage. Both damaged loggers were subsequently replaced with a duplicate of the same model.

II. Dissolved Oxygen

Ambient dissolved oxygen saturation was measured from a stationary position every 30 minutes for with a temperature compensated MiniDOT logger (Precision Measurement Engineering, Vista, CA)(Figure S2). Oxygen loggers were installed in each creek (1 per site) on the day population density sampling day and left for 2 weeks before being rotated to the next stream. At each site, dissolved oxygen saturation was recorded for two weeks out of every six weeks. Dissolved oxygen was measured simultaneously for upstream and downstream sites on the same creek, then moved to another creek after two weeks. Intermittent water conditions and logger theft prevented dissolved oxygen measurements from being made at the Brazil Quarry (Mt. Diablo Creek) site. The MiniDOT logger was fitted with a copper plate around the sensing mechanism to prevent biofouling.

For both temperature and oxygen, the continuous logging data was summarized in periods that lined up with the population sampling schedule (Table S1). The average mean, maximum and minimum values were calculated for temperature data in six-week intervals and for oxygen in two-week intervals at each site.

*Low resolution measurements*

I. Flow

Water flow was measured on each sampling date with an impeller type flow meter on a wading rod measuring flow from 4cm above the stream bottom (meters/second; Geopacks, Hatherleigh, Devon, UK). Average streamflow was calculated by averaging 3 readings at different positions laterally across the stream. Maximum streamflow was recorded after taking measurements at various positions, especially in riffles downstream of large rocks or other stream features. During spring and summer low-flow periods, there are missing flow data when the water was too shallow for the impeller to rotate.

II. Precipitation

Daily precipitation records for the duration of the study were obtained from the NOAA National Centers for Environmental Information Climate Data Online tool (NCEI 2021). Data for each stream were obtained from the weather station nearest to the stream (Table 1).

III. Water Chemistry

The concentration of calcium, magnesium, and total hardness of stream water was measured periodically with a titration based-test kit, (Model HAC-DT, Hach Company, Loveland, CO). Water samples were taken from all sites at the end of the rainy season (April 2020) and at the end of the study (September 2020). Total hardness and the concentration of calcium were measured via separate titrations. The concentration of magnesium was calculated by subtracting the concentration of calcium from total hardness.

Water pH was measured on sampling dates in the latter period of the study (March - September 2020) with an Ecosense PH100 temperature calibrated meter (YSI Incorporated, Yellow Springs, OH).

IV. Substrate and Canopy Cover

Substrate and canopy cover were measured concurrently on one day at each site in July 2020 (Table 2). Presence or absence of various substrate cover types (rocks, gravel, mud, and plant material) was recorded every meter along the 20m transects described above and across the stream with a 500cm$^2$ PVC quadrat. Percent substrate cover was calculated as the percentage of quadrats containing that cover type.

To measure canopy cover, a digital photograph of the sky was taken from the researcher's waist height (~1m) directly above each quadrat along and across the 20m transect. Photographs were analyzed with ImageJ software (Schneider, C.A., Rasband, W.S., Eliceiri 2012). In the software, each photograph was converted to a binary format that colored the plant material in black and the background sky in white. The percent area of black plant material in each photo was calculated using built in area measurement tools. The total percent canopy cover of each stream is an average of the value for each photo.

***Measurements of Biotic Factors***

*Population Density*

Snail density estimates were made at each stream site every six weeks. Sites along the same stream re sampled on the same day at each time point. At each site, there was an established 20m long study transect. A 12m study transect was used at Ohlone Park (Refugio Creek) this was the longest accessible section before the creek is channeled underground. On each sampling day, a Hess sampler (Hess 1941; Canton and Chadwick 1984) was placed along the study reach at a location determined by a random number generator. The Hess sampler is a stainless-steel cylinder with an 855.3 cm$^2$ footprint and 500 um Nitex mesh facing both up and downstream. The downstream mesh is fashioned into a funnel that leads to a collection bottle to trap benthic invertebrates. The upstream facing mesh prevents debris from entering the funnel. Snails were removed from the substrate inside the sampler by hand and placed into a separate container or washed into the net and then added to the container.

After all of the snails were placed in the container, they were laid out on clean waterproof paper and photographed alongside a metric ruler for scale. The photos were subsequently analyzed with ImageJ software (Schneider, C.A., Rasband, W.S., Eliceiri 2012) to count the number of snails present in each sample. The scale was set to 1 cm using the ruler, then a line was drawn from the apex to the aperture or opening of the snail shell to measure the length of each snail. Prior to analysis, measurements less than 0.9mm were filtered from the data table as it was difficult to identify snails that small in the field, and photographed objects less than 0.9mm were most likely debris.

*Filamentous Green Algae*

Filamentous green algae percent cover was measured every 2 meters along the established 20m transects at each site, with the exception of the Ohlone (Refugio Creek) site, where algae was measured every meter along the 12m transect at the. At each 2m or 1m mark, a 15cmx15cm quadrat was placed along the line and the percent cover of filamentous green algae was estimated by eye.

*Epiphytic algae*

Periphytic microalgae were collected every 6 weeks on the sampling date from 12cmx12cm concrete blocks placed on the stream bed to approximate the abundance of food

sources for *P. antipodarum*, a generalist benthic grazer. The first periphyton sample was taken 6 weeks from the beginning of the study (time point 1, Table S1). A slurry of periphyton and other solids (e.g. mud, sand) was removed from the entire upper surface of the block by scrubbing with a rough plastic brush and using a squirt bottle filled with stream water to rinse the algae into a container for transport to the lab. We scrubbed and rinsed the block until the rinsing water ran clear, removing the vast majority of periphyton. In the lab, periphyton and other solids were filtered out of the slurry using vacuum filtration through a paper filter (Whatman cat. No. 1001 125). Filters were then frozen at -80°C in 15mL plastic tubes wrapped in foil until all samples had been collected. Several early samples were excluded because of improper storage in solvents before freezing. Later samples were frozen while dry.

Algae abundance was estimated using chlorophyll *a* concentration. Chlorophyll *a* was extracted from one quarter of the original filter with 10mL of acetone with a protocol modified from Mandalakis et al (2017). Fluorescence was used to calculate chlorophyll *a* concentration from a standard curve generated with known concentrations from 40-2,000 pg/µL (Sigma-Aldrich; cat. no. C6144) in acetone. All samples, in triplicate, from a site were measured on a single microplate, each containing the standard curve and a blank, in a Synergy H1 fluorometer (BioTek, Winooski, VT). The plate reader protocol was to measure the fluorescence of each well with a 435nm excitation filter, 676nm emission filter, 200ms settling time between wells at 25°C (Mandalakis et al. 2017) The concentration of chlorophyll *a* was calculated by determining the linear slope and intercept of the standard curve on each plate.04

***Data Analysis***

I used a three-stage analytical framework to identify the environmental variables that drive differences in populations and distinguish creeks. All analyses were done in R (v3.5.1, Team 2018). First, random forest modeling, a machine learning technique, was used to select potential drivers of importance on our dependent variables (snail density and creek) from our list of 25 variables described above (Breiman 2001; Roland and Matter 2016). I used random forest analysis to winnow down the list of variables and avoid the researcher bias for finding the significant individual factors through stepwise deletion from a very long list of possible fixed factors and interactions (Harrison et al. 2018; Tredennick et al. 2021). This was accomplished with the "randomForest" package (v4.6-14, Liaw and Wiener 2002). This method generates regression trees with different combinations of explanatory variables and compares them to the "forest" of 499 other trees to determine the percent increase in mean square variance and increase in node purity if that variable is included. However, it does not return a single optimal tree, so only the highest-ranking variables were used in the next step.

The variables with the highest importance scores were the only variables fed into the recursive partitioning regression tree analysis to generate the optimal tree with the "rpart" package (v4.1-15, Therneau and Atkinson 2019). The optimal tree uses one or more of the most important variables to partition the levels of the response variable. Finally, linear mixed effects models were fitted with the subset of variables in the optimal regression tree using "nlme" (v3.1-137, Pinheiro and Bates 2000). The global models included all fixed effects and interactions and the random factor site nested within creek. The best model was chosen by mixed model averaging using function 'model.avg' in "MuMIn" (v1.43.17, Barton 2016) unless there was only one meaningful model ($\Delta$AICc< 2 from best model) in the set simpler than the global model as identified with 'dredge' also in "MuMIn".

## Results

### *Characterizing the Creeks*

*Environmental variation within and between creeks*

Stream conditions varied on both seasonal and daily timescales (Figure 3). Mean water temperature followed a seasonal pattern with mild autumn temperatures that cooled through the winter and increased again in the spring (Figure 3A). Clayton (Mt. Diablo)was generally warmer than the other sites through the year (annual $T_{max}$: 24.0°C, $T_{min}$: 8.0°C). It was only surpassed by John Muir (Refugio) in the late spring and summer (annual $T_{max}$: 26.2°C, $T_{min}$: 7.6°C). The three remaining sites stayed cooler all year but especially through the summer: Ohlone (Refugio, annual $T_{max}$: 20.0°C, $T_{min}$: 7.5°C), DeAnza (San Mateo, annual $T_{max}$: 21.7°C, $T_{min}$: 7.9°C), Gateway (San Mateo, annual $T_{max}$: 22.8°C, $T_{min}$: 8.2°C). The daily temperature range was similar between all sites through the year except at the John Muir site, which was varying more than 5°C in a day (Figure 3B).

Dissolved oxygen generally increased through the winter and was lower in summer and autumn (Figure 3C). However, one time period at Clayton had very low oxygen saturation of 40% average saturation over two weeks, but with high variation (Figure 3D). The San Mateo Creek sites (DeAnza and Gateway) generally had very high and very stable dissolved oxygen profiles. Refugio Creek (Ohlone and John Muir) had the most extreme oxygen profile, oscillating between high oxygen saturation in the day and low saturation at night.

Variables that described the water chemistry of the stream, conductivity (Figure 3E), hardness (Figure 3F), calcium (Figure 3G), and magnesium (Figure 3H) were distinct between streams, but pH (Figure 3I) was variable. Refugio Creek had the highest values regardless of seasonal patterns and San Mateo Creek had low and stable readings through the year. Lower conductivity measurements in Refugio Creek coincided with the rainy season in the region. Measurements at Clayton (Mt. Diablo Creek) were generally in between the other two creeks. Conductivity at Clayton was clearly affected by precipitation; the two lowest measurements were taken on days that it was actively raining (Figure 4). Clayton had distinctly low pH through the study while the other sites were in a similar range (Figure 3F).

Chlorophyll *a*, as a proxy for periphyton abundance, had creek specific patterns throughout the study (Figure 3G). Chlorophyll levels at Clayton (Mt. Diablo Creek) stayed fairly constant except at a time point where periphyton was gathered during a storm. In Refugio Creek, chlorophyll concentration increased through the spring and then stayed high. At Gateway on San Mateo Creek, there was a consistent increasing trend though the spring and summer. Conversely at DeAnza on San Mateo Creek, chlorophyll levels were high in the spring and then sharply decreased until mid-summer before recovering slightly.

Filamentous algae cover was low in San Mateo Creek but more common at other sites (Figure 3H). At Ohlone, algae was low in the winter and increased through the spring and summer. Algae was the dominant substrate (100% cover) at John Muir at the last two sampling time points. Algae cover at Clayton and John Muir decreased during and after storms and high flows (Figures 3&4).

There were three major rain events that impacted the entire region during the study period (Figure 4A). Those rain events caused higher average and maximum flow measurements during sampling dates closest to the storms (Figure 4B). However, rain did not explain changes in flow at DeAnza between March and September 2020. There were no major storms but flow increased

steadily through that period at DeAnza but changed very little at the downstream site, Gateway, on San Mateo Creek.

*Canopy and Substrate Cover*

Canopy cover was similar between Clayton (Mt. Diablo), DeAnza (San Mateo), Gateway (San Mateo) and Ohlone (Refugio Creek) (51-67%) but the riparian zone had very few large plants at the John Muir site (Refugio Creek) (8%)(Table 2). The streambed at the John Muir site was mud dominated with some aquatic plants. Upstream at Ohlone, mud and plants were equally dominant, with rocks and gravel present in less than half of the quadrats. Clayton was dominated by rocks and gravel. DeAnza was mostly gravel and rocks with no mud. Conversely, downstream at Gateway, mud and plant matter dominated the substrate.

*Classifying the creeks by abiotic and biotic conditions*

Random forest modeling identified three variables of importance to classifying the creeks, with the rank order of variables identical when considering both overall accuracy and node purity (Figure 5A). Conductivity was the top variable, followed by total hardness and calcium concentration. Classification tree modeling selected calcium concentration as the only variable required for separating the creeks (Figure 5B). The first node separates San Mateo Creek because it has very little calcium, less than or equal to 47 mg/L. The next node separates the two remaining creeks by which creek has less than 370 mg/L. Mt. Diablo Creek had a lower calcium concentration than Refugio Creek. Calcium concentration is significantly different between all three creeks ($p<0.001$ for all comparisons) (Table 5).

***Snail Population Density Through Time***

*Potamopyrgus antipodarum* density varied between creeks (Figure 6). Snails were rare in San Mateo Creek while being much more common in Mt. Diablo and Refugio Creeks (ANOVA, $p<0.01$, Table 3). There was no strong seasonal pattern in population density across sites and creeks. At the Clayton site and the sites on Refugio Creek (Ohlone and John Muir), population density increased and decreased throughout the year but did not follow a seasonal pattern. There was an increasing trend of snail density at DeAnza (San Mateo Creek) through the spring and summer of 2020 but this trend was not repeated downstream at the Gateway site.

***Potential Drivers of Snail Population Density***

Random forest modeling identified 11 potentially important variables (Figure 7A) to be included in the next step based on the union of mean square error and node purity criteria. Filamentous green algae had the largest explanatory power (8% increase in mean square error of the model when removed), followed by plant cover, conductivity, average mean dissolved oxygen, magnesium concentration, canopy cover, hardness, rock cover, and calcium concentration (5.5-6.25%). Two variables, average daily temperature range and pH, had smaller effects on mean square error but large effects on node purity if included in the trees.

Regression tree modeling determined that the optimal tree for determining population density included cover of filamentous algae and conductivity (Figure 7B). The first node in the tree uses algae cover over 25% to determine the highest snail densities (mean of data in this category is 2,790 snails/$m^2$). If algae cover is less than 25%, low water conductivity (<311 μS) determines small populations (mean = 83.7 snails/$m^2$) and conductivity greater than 311μS determines medium populations (mean = 1290 snails/$m^2$).

The global linear mixed model for snail population density included filamentous algae cover, conductivity, and the interaction between algae cover and conductivity as fixed effects; with a random effect of site nested in creek. There was no significant effect of autocorrelation in these data, so no additional variance structures were included (Figure S3). The optimal model was selected as the only model with a ΔAICc <2 from the five models in the model selection table returned in the 'dredge' step that represent all possible combinations of fixed effects from the global model (Table S2). The optimal model only included the fixed effect of algae cover and the intercept ($R^2_{\text{fixed effects}}$=0.15, $R^2_{\text{fixed + random}}$=0.63). Snail population density increased with increasing algae cover overall (Table 4A, $p<0.05$), but the slope of the relationship differed between creeks. Algae cover was associated with high snail population density only in Refugio Creek (Figure 8A). The positive relationship between algae and snails in Refugio Creek was strongly influenced by one point from the John Muir site. Without this point, there was no relationship between filamentous algae cover and snail abundance in any creek (Table 4B, Figure 8B).

## Discussion

The New Zealand mud snail (*Potamopyrgus antipodarum*) is a prolific invader of freshwater streams in California and worldwide, with the ability to form extremely dense populations that dominate the invaded habitat. To strengthen our ability to predict where this species can thrive, it is critical to understand which abiotic and biotic conditions explain variation in population density. I approached this need by measuring 25 conditions over one year in streams in the San Francisco Bay Area that contain varying densities of *P. antipodarum* populations. The different streams could be distinguished by their water chemistry profiles, specifically calcium concentration. Conductivity and filamentous green algae cover were the factors most correlated to population density, but there was only marginal linear statistical support for the response to algae.

*Biological support for model results*

The three creeks in our study could be distinguished by their population densities, and even more clearly, by their concentration of dissolved calcium. The smallest population occurs in San Mateo Creek, a watershed that has drastically less dissolved calcium than the other two in this study. The average calcium concentration in San Mateo Creek was near 35 mg/L. Peak brood size of *P. antipodarum* in Boulder Creek, CO correlated with the highest total hardness (recorded as concentration of $CaCO_3$) through an eighteen-month field study (McKenzie et al. 2013), suggesting that calcium content may act as a filter and limit snail populations in the US. Adequate available calcium is critical to shell building in gastropods. Many North American species that inhabit soft waters have thin shells making them more vulnerable to predators (Thorp and Rogers 2011). Among freshwater streams in Tennessee, a hotspot for freshwater gastropod diversity, only 10% of streams with less than 20mg/L of calcium hosted snails (Shoup 1943; Herbst et al. 2008). While still above this threshold during a dry water year (CA Dept Water Resources 2020), a wet year could dilution calcium to a level below this threshold. Conductivity at Clayton was reduced to less than half it's typical value when measured while it was raining. A similar decrease in San Mateo Creek could have large impacts on population persistence.

Conductivity may be more limiting to the population in San Mateo Creek than dissolved calcium. Several researchers in the USA and Europe have concluded that *P. antipodarum* tolerates high mineral and high salinity estuary conditions (Jacobsen and Forbes 1997; Drown et al. 2011; Hoy et al. 2012; Paolucci and Thuesen 2020), but low mineral content is likely to be a barrier in our study of freshwater creeks. It is energetically costly for freshwater snails to maintain their status as hyperosmotic regulators and deposit calcium for their shells, especially if ionic content is low (McMahon 1983). Herbst et al. (2008) found that *P. antipodarum* growth and survival decreased in water less than 200uS/cm. The smallest populations in our study, both sites on San Mateo Creek, are on the margin of this threshold with conductivity measurements between 185-255uS/cm through the year. Combined low conductivity and lower calcium don't completely exclude New Zealand mud snail, but may reduce population density. Soft water may exert sublethal effects such as increased energy expenditure for ion pumping, that when coupled with biotic factors limit population density.

*Potamopyrgus antipodarum* is commonly associated with filamentous algae because it provides food and shelter (Suren 2005; Bennett et al. 2014). In our model, large snail populations were best explained by high filamentous algae cover, but the relationship between population density and algae cover was not robust to outliers (Fig. 8A) and across creeks. Despite the lack of strong support for relationship in this study, there is strong support in the literature for the relationship between *P. antipodarum* and filamentous green algae. In controlled conditions, snails were found to prefer rocks covered in algae to those covered with only diatoms over a 54 hour observation period, even when silt was present on the substrate (Suren 2005). This preference has also been observed in Piru Creek in southern California where most adults and juveniles were present on macrophytes (Bennett et al. 2014). Filamentous green algae is more common in the types of disturbed, developed watersheds that are high in nutrients and light penetrations where *P. antipodarum* is often found in both its invaded and native ranges (Suren 2005; ANS Task Force 2007). At Clayton (Mt. Diablo Creek), there was a large snail population but a weak relationship between snails and filamentous algae. However, it had the highest periphyton density. Perhaps at Clayton, the population relies on a less preferred substrate that can support its grazing pressure.

There are several benefits for small invertebrates to live on or in the matrix of large macrophytes. Mats of *Cladophora,* a common macrophyte algae in California, attenuate high flow conditions and alter other microhabitat conditions (Dudley et al. 1986; Power 1990; Dudley 1992). Snails also have the benefit of not getting tangled in filamentous algae like some of their competitors and their main predator in the invasive range, crayfish(Suren 2005; Bennett et al. 2014). Crayfish were present in all study creeks but in low numbers. This allows snails to exploit a microhabitat rich in food resources as filamentous algae has high surface area and tends to host more epiphytic diatoms than other substrates (Suren 2005). *P. antipodarum* is notably a voracious grazer, consuming up to 75% of gross primary productivity in its densest populations recorded at Polecat Creek, Wyoming (Hall et al. 2003). *P. antipodarum* effectively controls nitrogen cycling in Polecat Creek as it excretes two-thirds of the available nitrogen in the stream as well. The relationship between New Zealand mud snails and algae is likely mutually beneficial because snails obtain their preferred food source and excrete bio-available nutrients while clearing photosynthetic surfaces of epiphytes and promoting algal growth (Hall et al. 2003; Suren 2005; Hall et al. 2006; Moore et al. 2012; Bennett et al. 2014).

*Assessment of this modeling approach*

In this study, we did not see strong effects of some variables that we expected to be important. It was surprising not to see any signature of the importance of stream temperature due to its importance in regulating many physiological rates and its effects on growth rates in the lab and other field studies (Dybdahl and Kane 2005; McKenzie et al. 2013; Bennett et al. 2014). Based on my results from chapter 1, I expected temperature and its interactions with dissolved oxygen to limit movement required for foraging under conditions observed in this field study. However, the intensity and duration of those stresses in nature may not have reached the level of measurable lethal or sublethal effects. The effects of temperature may be included in the presence of filamentous algae or other variables. It is possible that there are no drivers of large effect that explain population density in *P. antipodarum* and instead many drivers of small effect with complex interactions between them. This species broad tolerance of variation in many abiotic and biotic factors has contributed to its success as a worldwide invader of fresh and brackish water habitats.

It is notoriously difficult to generate models with meaningful predictive power on ecological datasets because of the complexity of ecological systems and assumptions we must make in the analytical process (Loo et al. 2007; Roland and Matter 2016; Matter and Roland 2017; Tredennick et al. 2021). Other powerful ecological modeling tools, such as multivariate autoregressive models (MAR), could not be used on such a short time series (Hampton et al. 2013; Ruhí et al. 2015). Other methods that can handle small datasets, including the methods I used, generally benefit from larger datasets so that datasets can be divided for cross-validation or model training and testing (Tredennick et al. 2021). Even still, predictions gleaned from large data sets are not always robust. Roland and Matter (2016 & 2017) have used extreme weather and climate variables independently to predict population growth of alpine butterflies in Canada, but models using both predictors together did not increase predictive power. Even with these limitations, I was able to identify three important variables (calcium, conductivity and filamentous algae) for explaining *P. antipodarum* population size that may be limiting snail density in these study streams in some times of the year more than others. Given the seasonal pattern of the most stressful factors (e.g. winter rain influencing water chemistry and low algae cover in winter ), a multi-year dataset may be able to uncover even stronger evidence of the effects of these factors on *P. antipodarum* population density.

## Conclusion

This study investigated which abiotic and biotic factors act as environmental filters to the establishment of the invasive New Zealand mud snail, *Potamopyrgus antipodarum*, in three creeks in the San Francisco Bay Area. *P. antipodarum* is robust to variation in many ecological factors and none of the factors included in this study had a significant statistical relationship with population density. However, I found that calcium, conductivity and filamentous algae are the most important variables related to variation in population density. Low algae cover and low ion content are that may act as filters together or individually in these creeks. Future studies should use longer time series and locations in different regions to test the strength of the role of filamentous green algae on population density.

**Acknowledgments**

Funding for this project was granted by the Save Mount Diablo Mary Bowerman Science and Research Program and the UC Berkeley Department of Integrative Biology. Special thanks to Tyler McClellan for help with equipment design and data collection in the field and to Benjamin Liu for analyzing the snail photos and measuring thousands of individual snails. Animal work was permitted by CDFW permits S-182910001-18291-001.

**Table 1. Study locations of creeks containing invasive *Potamopyrgus antipodarum***. Environmental parameters were measured at two sites on each creek (one upstream and one downstream). Upstream sites are closer to headwaters and farther from the San Francisco Bay. Precipitation data was downloaded from the nearest weather station to each creek. Colors are used to represent sites on the same creek in the remaining figures.

| Creek | Upstream Site (Latitude N, longitude W) | Downstream Site (Latitude N, longitude W) | Distance (km) | Weather Station |
|---|---|---|---|---|
| San Mateo Creek | De Anza Park (37.562256, -122.32885) | Gateway Park (37.569648, -122.31787) | 4.16 | USW00023234 |
| Mt. Diablo Creek | Clayton Library (37.943958, -121.9374) | Brazil Quarry Park (37.961169, -121.96923) | 1.24 | USW00023254 |
| Refugio Creek | Ohlone Park (38.005754, -122.27385) | John Muir Parkway (38.016814, -122.27472) | 1.33 | USC00047414 |

**Table 2. Streambed composition and canopy cover at the study sites**

| | | | Streambed composition (%) | | | | Canopy |
|---|---|---|---|---|---|---|---|
| **Stream** | **Site** | **Date** | **Gravel** | **Mud** | **Plants** | **Rocks** | **(% cover)** |
| Mt. Diablo | Clayton | 19 July 2020 | 76.0 | 25.0 | 63.5 | 88.5 | 67.3 |
| San Mateo | DeAnza | 26 July 2020 | 92.2 | 0 | 66.7 | 82.2 | 63.8 |
| | Gateway | 26 July 2020 | 36.8 | 53.9 | 80.3 | 71.0 | 65.8 |
| Refugio | John Muir | 18 July 2020 | 0 | 100 | 55.8 | 0 | 8.1 |
| | Ohlone | 18 July 2020 | 42.9 | 81.0 | 81.0 | 47.6 | 51.9 |

**Table 3. Results of ANOVA on snail population density between creeks.** Bold type represents statistical significance, α=0.05

| **One-way ANOVA** | | | | | |
|---|---|---|---|---|---|
| | **df** | **Sum Sq** | **Mean Sq** | **F value** | **p-value** |
| Creek | 2 | 226164 | 113082 | 5.206 | **0.009** |
| Residuals | 51 | 1107792 | 21721 | | |
| **Tukey Post-hoc Test** | | | | | |
| | | **diff** | **lower** | **upper** | **adj. p** |
| Refugio-Mt. Diablo | | 34.61 | -83.98 | 153.20 | 0.76 |
| San Mateo-Mt. Diablo | | -116.66 | -235.26 | 1.93 | 0.05 |
| San Mateo-Refugio | | -151.28 | -269.87 | -32.69 | **0.009** |

**Table 4. Results of linear mixed model explaining population density**. **A)** model output with all data **B)** model output if outlier is excluded. Bold type represents statistical significance, $\alpha=0.05$

**A)**

| **Random effects** | | | | | |
|---|---|---|---|---|---|
| **Creek** | | | | | |
| Intercept SD | 75.56 | | | | |
| **Site in Creek** | | | | | |
| Intercept SD | 0.008 | | | | |
| Residual SD | 141.97 | | | | |
| **Fixed effects** | | | | | |
| | **Value** | **Std Error** | **df** | **t-value** | **p-value** |
| Intercept | 77.57 | 54.33 | 34 | 1.43 | 0.16 |
| Algae cover | 2.08 | 0.82 | 34 | 2.53 | **0.02** |

**B)**

| **Random effects** | | | | | |
|---|---|---|---|---|---|
| **Creek** | | | | | |
| Intercept SD | 113.84 | | | | |
| **Site in Creek** | | | | | |
| Intercept SD | 0.005 | | | | |
| Residual SD | 88.28 | | | | |
| **Fixed effects** | | | | | |
| | **Value** | **Std Error** | **DF** | **t-value** | **p-value** |
| Intercept | 113.79 | 69.02 | 33 | 1.65 | 0.11 |
| Algae cover | 0.35 | 0.57 | 33 | 0.62 | 0.54 |

**Table 5. Results of ANOVA on calcium concentration between streams.** Bold type represents statistical significance, α=0.05

| **One-way ANOVA** | | | | | |
|---|---|---|---|---|---|
| | **df** | **Sum Sq** | **Mean Sq** | **F value** | **p-value** |
| Creek | 2 | 3301500 | 1650750 | 796.3 | **<2e-16** |
| Residuals | 37 | 76706 | 2073 | | |
| **Tukey Post-hoc Test** | | | | | |
| | | **diff** | **lower** | **upper** | **adj. p** |
| Refugio-Mt. Diablo | | 521.5 | 473.36 | 569.64 | **0** |
| San Mateo-Mt. Diablo | | -91.44 | -139.58 | -43.31 | **<0.001** |
| San Mateo-Refugio | | -612.94 | -652.24 | -573.64 | **0** |

**Figures**

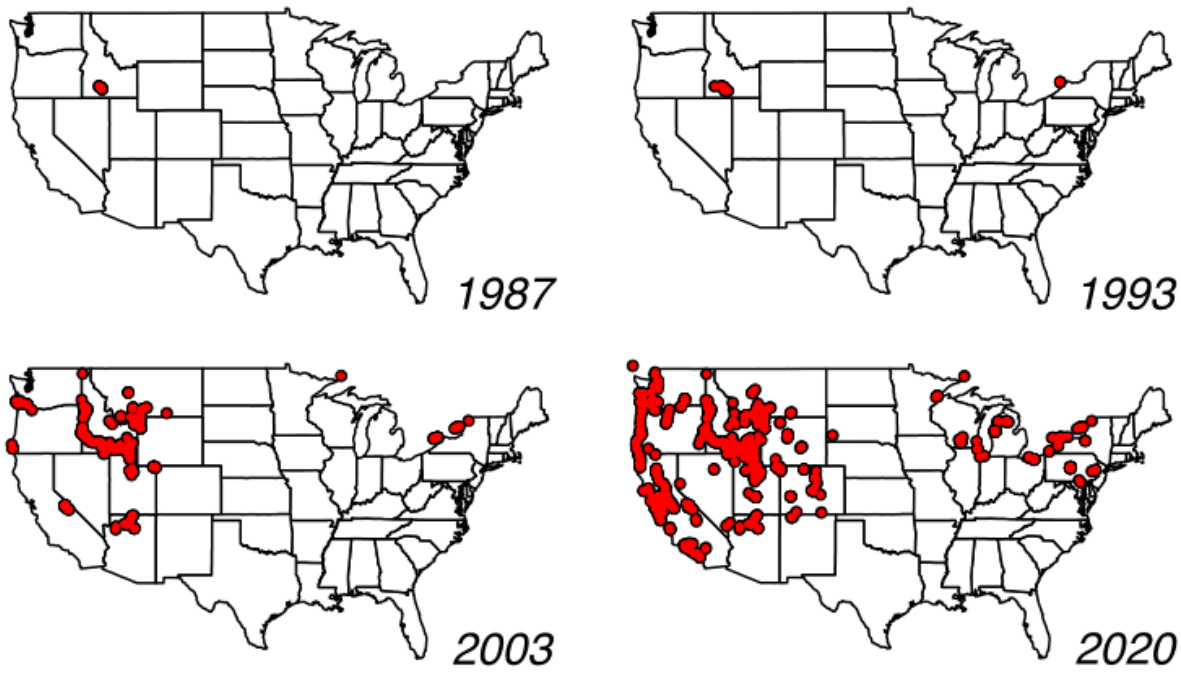


**Figure 1. Invasion timeline of *Potamopyrgus antipodarum* in the United States 1987 – 2020.** Siting reports accessed from USGS Nonindigenous Aquatic Species database[1].

[1] https://nas.er.usgs.gov/viewer/omap.aspx?SpeciesID=1008

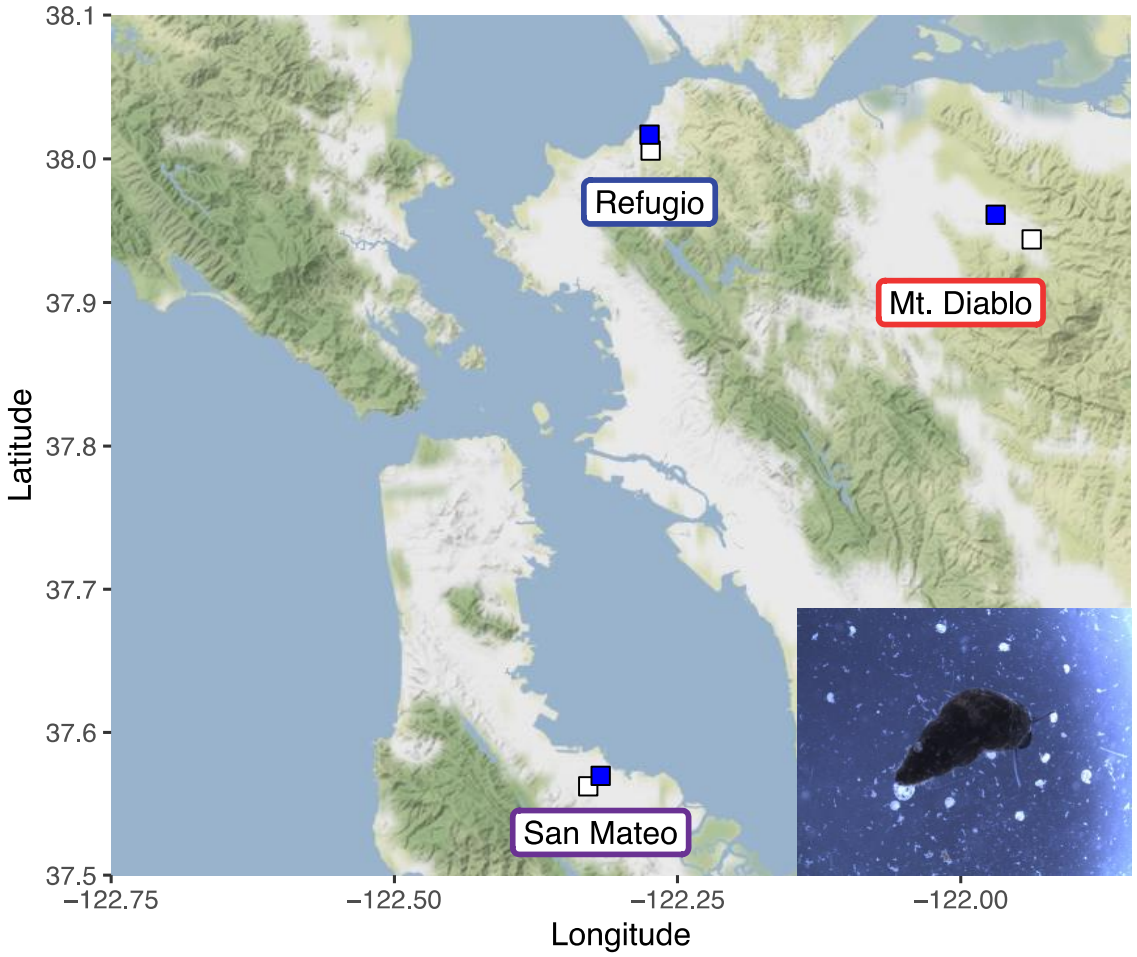


**Figure 2. Map of creek locations in the San Francisco Bay Area used in this study.** White points denote upstream locations and blue points denote downstream locations on the same creek. Upstream sites are closer to creek headwaters and farther from the San Francisco Bay Inset is a photo of a New Zealand mud snails *Potamopyrgus antipodarum:* large adult in the center surrounded by white neonate clones. Photo credit: Emily King

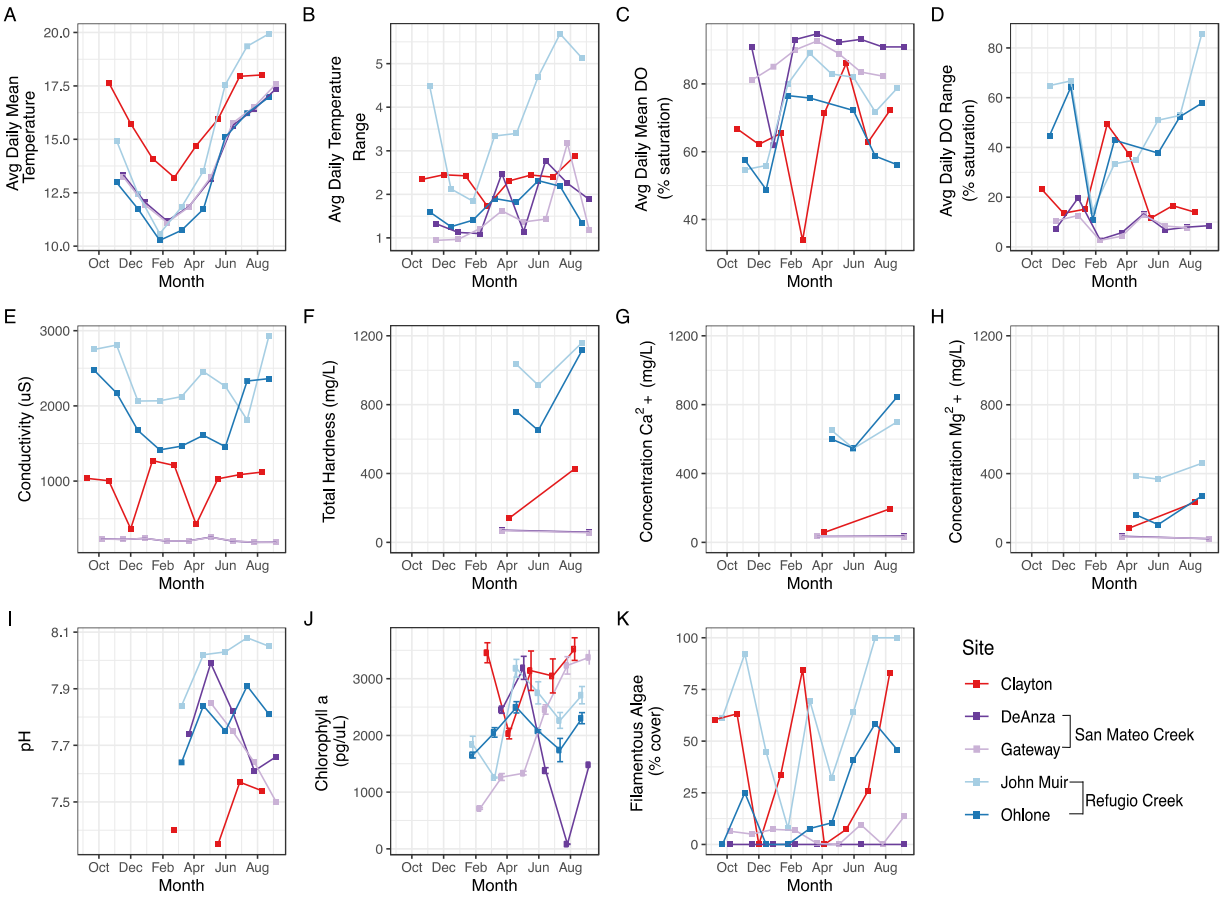


**Figure 3. Environmental variation within and between creeks (September 2019-September 2020).** Panels A-D are continuous recordings summarized into 6-week periods to match other low frequency data. **A)** Average daily mean temperature for each 6-week interval, **B)** Average daily temperature range for each 6-week interval, **C)** Average daily mean oxygen saturation for each 2-week interval, **D)** Average daily oxygen range for each 2-week interval, **E)** conductivity, **F)** total hardness, **G)** calcium concentration, **H)** magnesium concentration, **I)** pH, **J)** chlorophyll *a* concentration, **K)** percent cover of filamentous green algae.

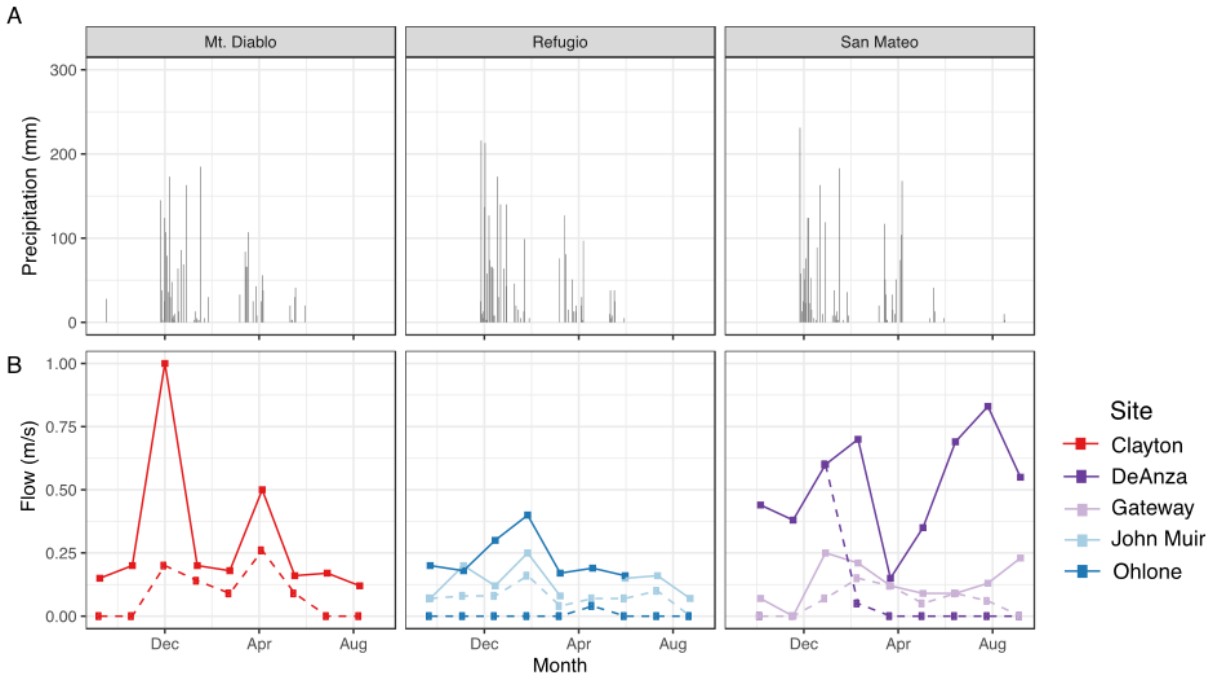


**Figure 4. Precipitation and streamflow throughout the study period (September 2019-September 2020). A)** Precipitation from the weather station nearest to the stream sites[2]. Data were accessed from the NOAA Climate Data Online tool[3] **B)** Average (dashed line) and maximum (solid line) streamflow at each site.

[2] Stations: Mt. Diablo Creek: USW00023254, Refugio Creek: USC00047414, San Mateo Creek: USW00023234

[3] https://www.ncdc.noaa.gov/cdo-web/

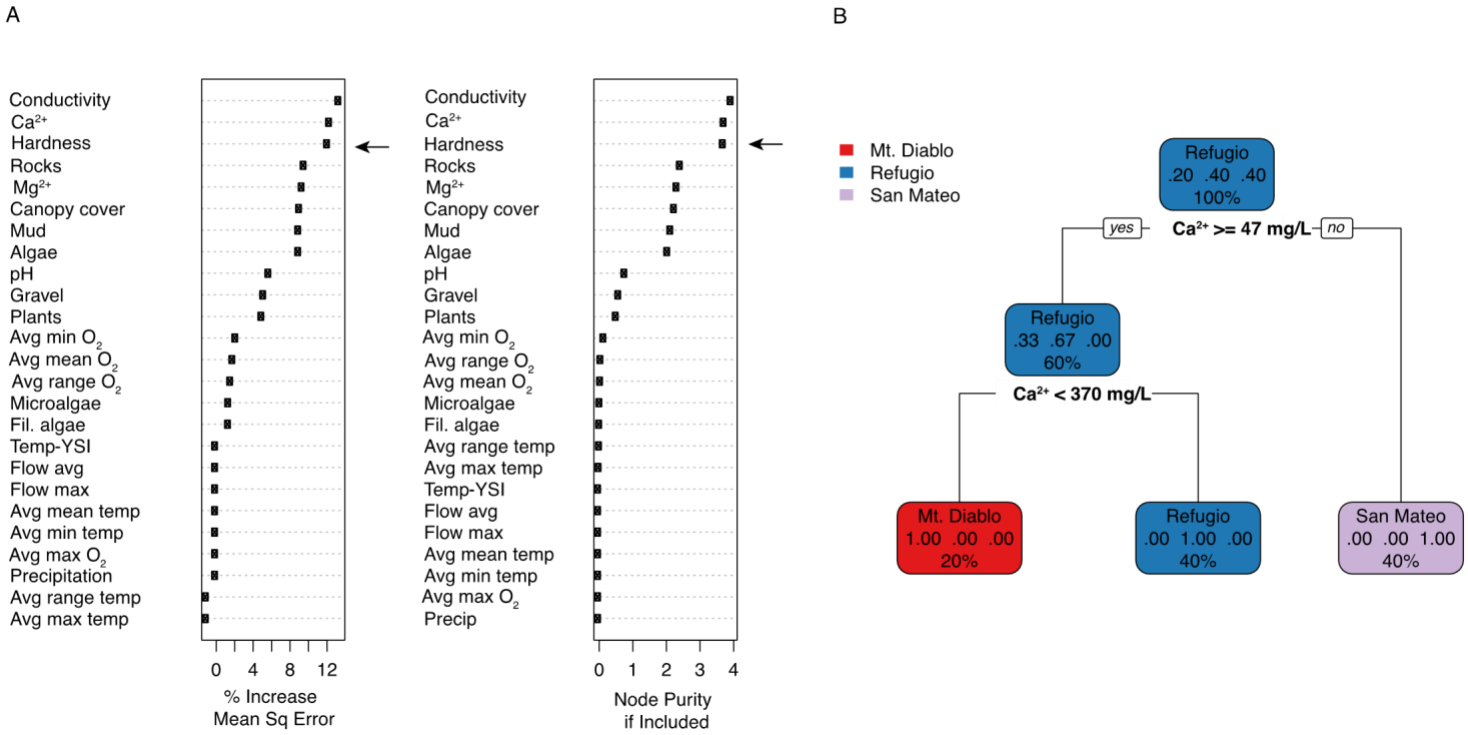


**Figure 5**. **Important variables of creek classification** determined sequentially by **A)** random forest modeling and **B)** recursive partitioning classification tree analysis. Arrows indicate cutoffs for inclusion in the next step. Percentage values in the classification tree represent how much data is handled at that node.

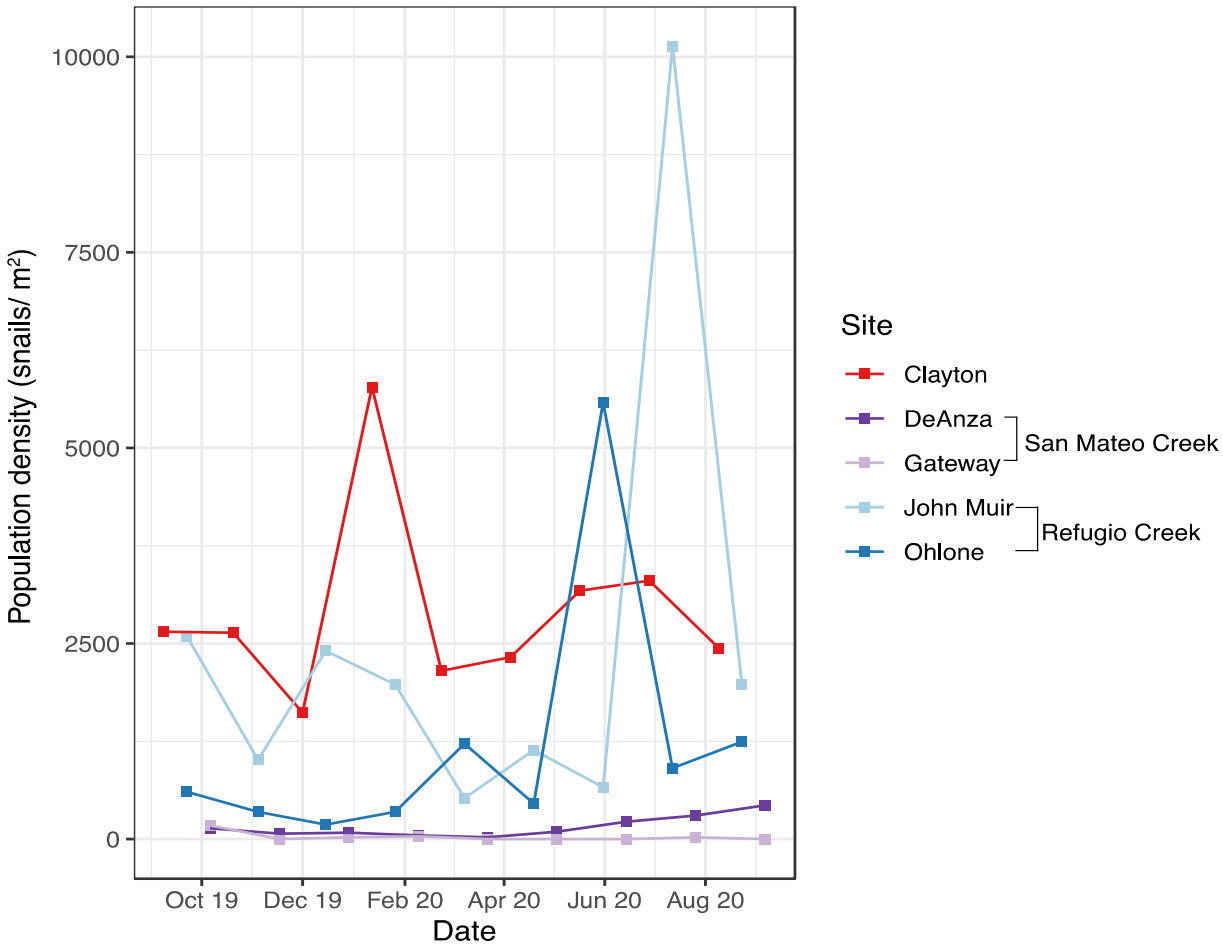


**Figure 6. Estimated *Potamopyrgus antipodarum* density every six weeks at each site from Sept 2019 - Sept 2020.** Each point represents the population estimate of snails calculated from one Hess sampler (0.086 $m^2$ ) at each timepoint. Different sites are indicated by point and line color. Sites on the same creek are different shades of the same color.

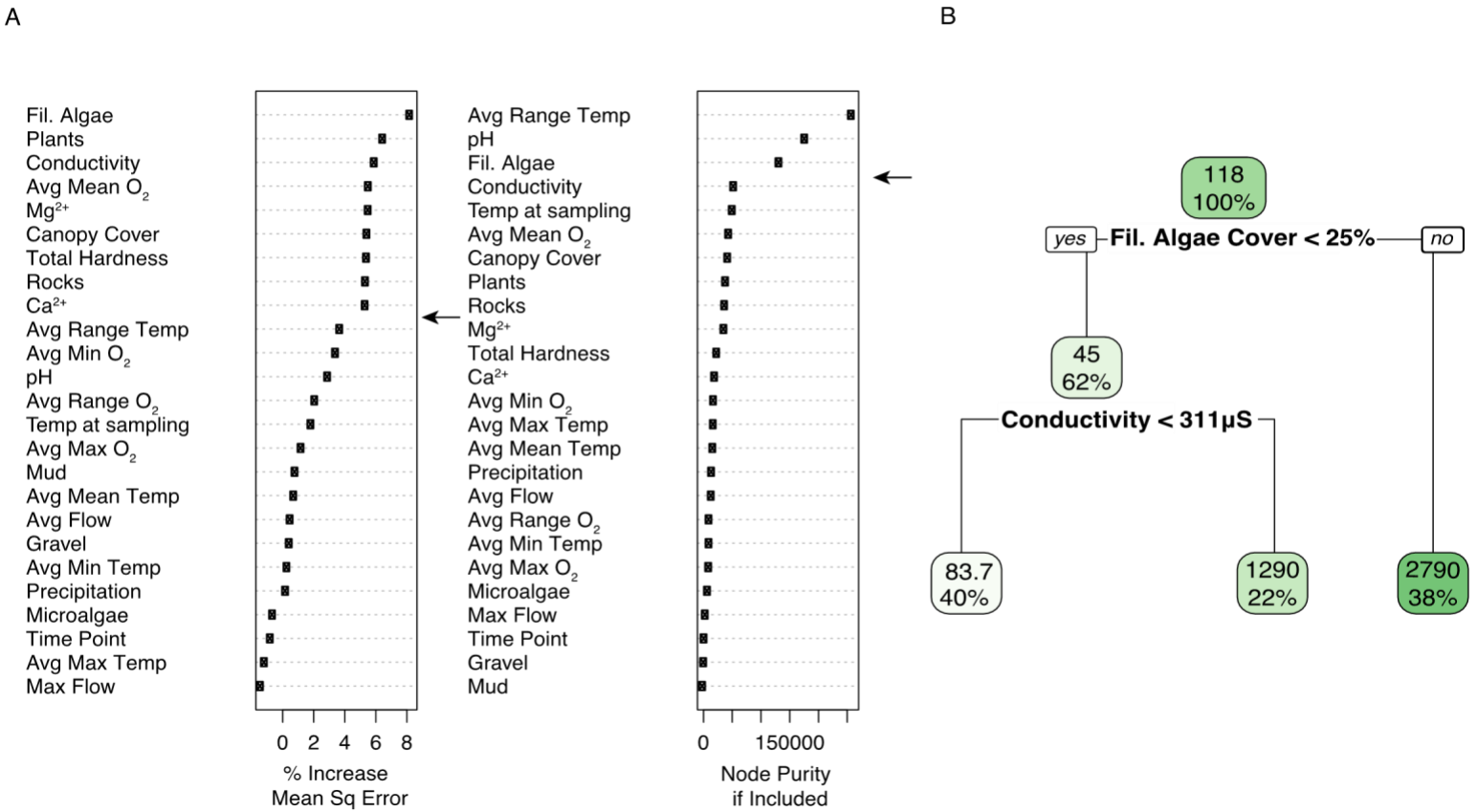


**Figure 7.** Important variables related to snail population density determined sequentially by **A)** random forest modeling and **B)** recursive partitioning regression tree analysis. Arrow indicate cutoffs for inclusion in the next step.

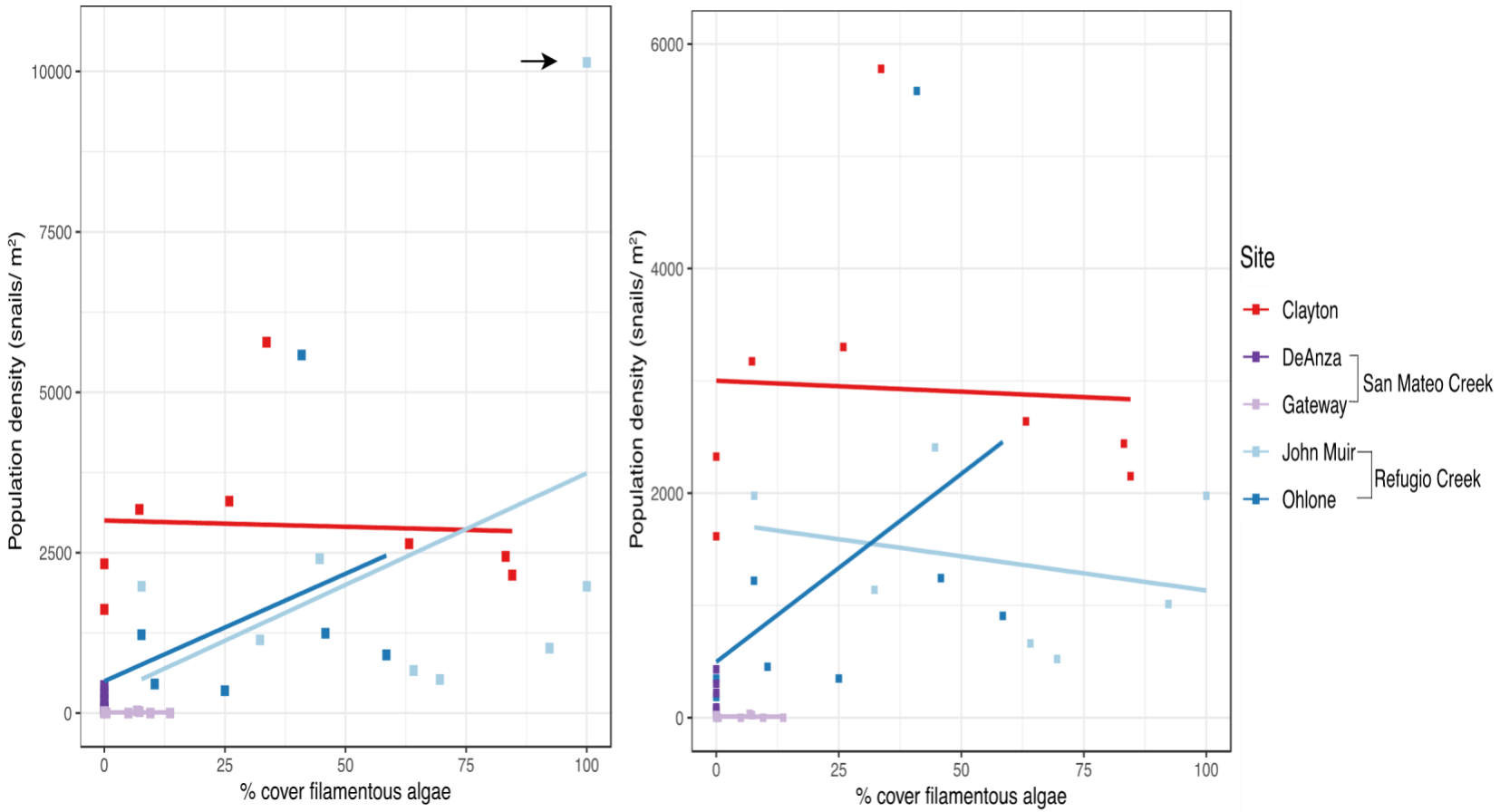


**Figure 8.** Relationship between percent cover of filamentous green algae and snail population density. **A)** All data **B)** Without the outlier strongly driving the patterns in A (with arrow). Colors represent the sites where these data were collected. Points represent the data. Lines are the linear model fit of the data for each site

**Supplementary Materials**

**Table S1.** Sampling dates

| Date | Creek | Site | Time Point |
|---|---|---|---|
| 9/8/19 | Mt. Diablo | Brazil Quarry | 0 |
| 9/8/19 | Mt. Diablo | Clayton | 0 |
| 9/22/19 | Refugio | John Muir | 0 |
| 9/22/19 | Refugio | Ohlone | 0 |
| 10/6/19 | San Mateo | DeAnza | 0 |
| 10/6/19 | San Mateo | Gateway | 0 |
| 10/20/19 | Mt. Diablo | Brazil Quarry | 1 |
| 10/20/19 | Mt. Diablo | Clayton | 1 |
| 11/4/19 | Refugio | John Muir | 1 |
| 11/4/19 | Refugio | Ohlone | 1 |
| 11/17/19 | San Mateo | DeAnza | 1 |
| 11/17/19 | San Mateo | Gateway | 1 |
| 12/1/19 | Mt. Diablo | Brazil Quarry | 2 |
| 12/1/19 | Mt. Diablo | Clayton | 2 |
| 12/15/19 | Refugio | John Muir | 2 |
| 12/15/19 | Refugio | Ohlone | 2 |
| 12/29/19 | San Mateo | DeAnza | 2 |
| 12/29/19 | San Mateo | Gateway | 2 |
| 1/12/20 | Mt. Diablo | Brazil Quarry | 3 |
| 1/12/20 | Mt. Diablo | Clayton | 3 |
| 1/26/20 | Refugio | John Muir | 3 |
| 1/26/20 | Refugio | Ohlone | 3 |
| 2/9/20 | San Mateo | DeAnza | 3 |

| | | | |
|---|---|---|---|
| 2/9/20 | San Mateo | Gateway | 3 |
| 2/23/20 | Mt. Diablo | Brazil Quarry | 4 |
| 2/23/20 | Mt. Diablo | Clayton | 4 |
| 3/8/20 | Refugio | John Muir | 4 |
| 3/8/20 | Refugio | Ohlone | 4 |
| 3/22/20 | San Mateo | DeAnza | 4 |
| 3/22/20 | San Mateo | Gateway | 4 |
| 4/5/20 | Mt. Diablo | Brazil Quarry | 5 |
| 4/5/20 | Mt. Diablo | Clayton | 5 |
| 4/19/20 | Refugio | John Muir | 5 |
| 4/19/20 | Refugio | Ohlone | 5 |
| 5/3/20 | San Mateo | DeAnza | 5 |
| 5/3/20 | San Mateo | Gateway | 5 |
| 5/17/20 | Mt. Diablo | Brazil Quarry | 6 |
| 5/17/20 | Mt. Diablo | Clayton | 6 |
| 5/31/20 | Refugio | John Muir | 6 |
| 5/31/20 | Refugio | Ohlone | 6 |
| 6/14/20 | San Mateo | DeAnza | 6 |
| 6/14/20 | San Mateo | Gateway | 6 |
| 6/28/20 | Mt. Diablo | Brazil Quarry | 7 |
| 6/28/20 | Mt. Diablo | Clayton | 7 |
| 7/12/20 | Refugio | John Muir | 7 |
| 7/12/20 | Refugio | Ohlone | 7 |
| 7/26/20 | San Mateo | DeAnza | 7 |
| 7/26/20 | San Mateo | Gateway | 7 |
| 8/9/20 | Mt. Diablo | Brazil Quarry | 8 |
| 8/9/20 | Mt. Diablo | Clayton | 8 |

| | | | |
|---|---|---|---|
| 8/23/20 | Refugio | John Muir | 8 |
| 8/23/20 | Refugio | Ohlone | 8 |
| 9/6/20 | San Mateo | DeAnza | 8 |
| 9/6/20 | San Mateo | Gateway | 8 |

**Table S2. Model selection table of fixed factors for models explaining snail population density.** The optimal model is in bold.

| | Intercept | Conductivity | Fil. Algae Cover | Cond * Algae | DF | logLik | AICc | Δ | Weight |
|---|---|---|---|---|---|---|---|---|---|
| **1** | **77.57249** | *NA* | **2.076025** | *NA* | **5** | **-250.742** | **513.2495** | **0** | **0.737515** |
| 2 | 232.2008 | -0.17224 | 3.309813 | *NA* | 6 | -250.772 | 516.0898 | 2.840281 | 0.178243 |
| 3 | 137.083 | *NA* | *NA* | *NA* | 4 | -254.263 | 517.6692 | 4.419705 | 0.080918 |
| 4 | 136.8423 | 0.000618 | *NA* | *NA* | 5 | -256.182 | 524.1278 | 10.87832 | 0.003203 |
| 5 | 197.1787 | -0.13742 | 4.166861 | -0.00055 | 7 | -256.588 | 530.6754 | 17.42593 | 0.000121 |

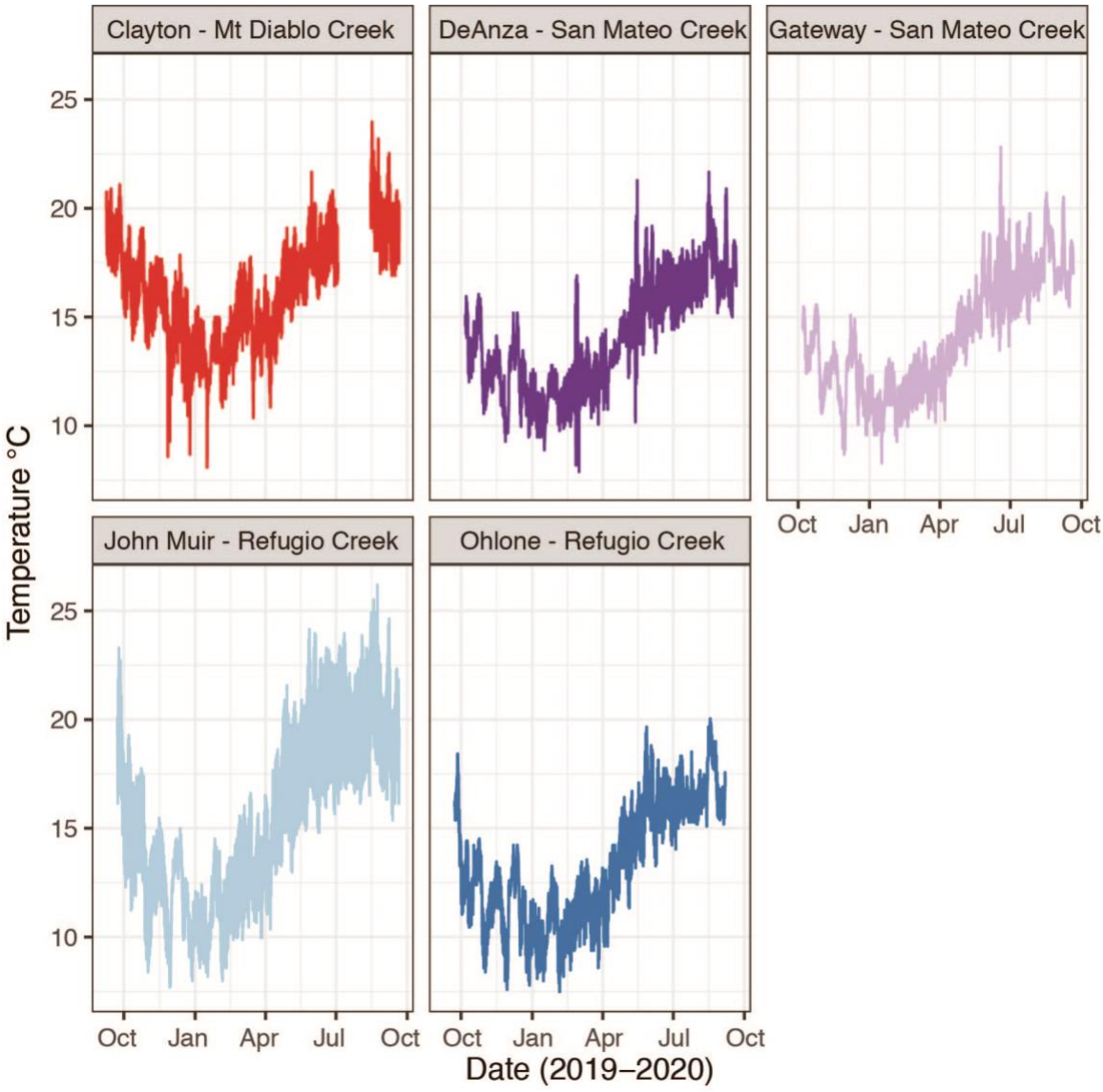


**Figure S1.** High resolution temperature data from each site containing New Zealand mud snails. Water temperature was recorded every 30 minutes between Sept 2019-Sept 2020.

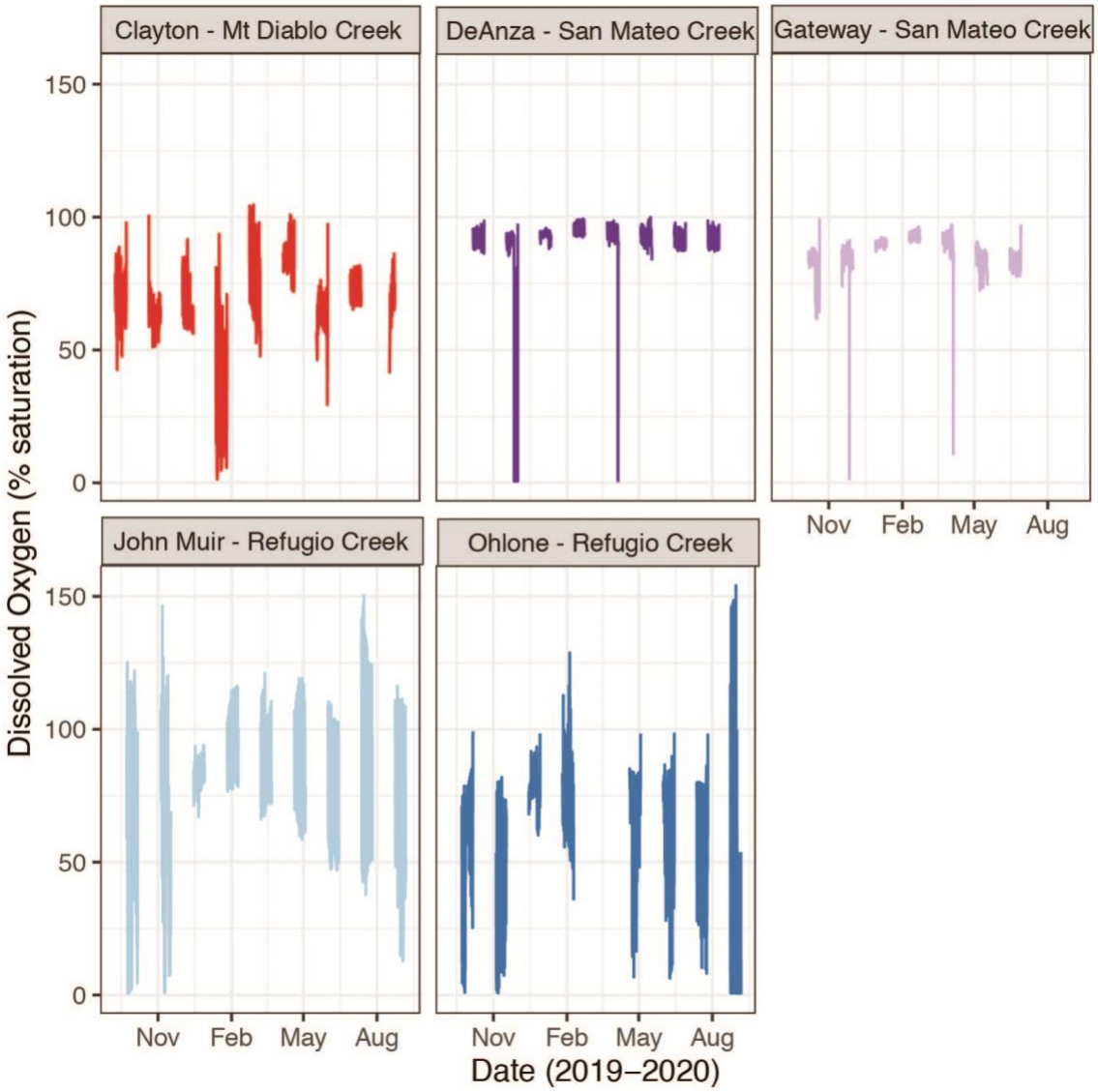


**Figure S2.** High resolution dissolved oxygen data from each site containing New Zealand mud snails. Dissolved oxygen was recorded every 30 minutes Sept 2019-Sept 2020.

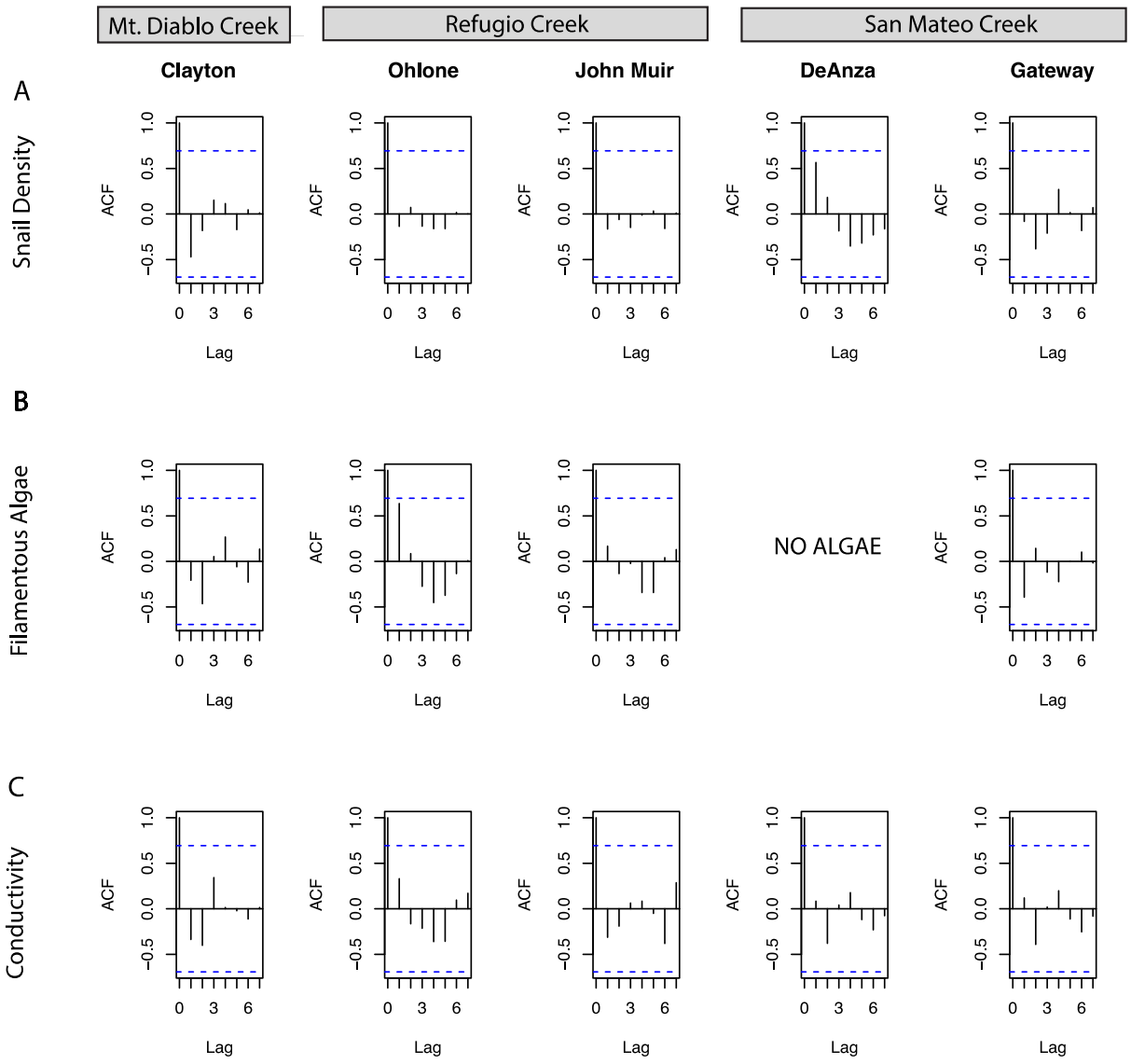


**Figure S3.** Autocorrelation plots (ACF) of variables in the model explaining population density through the study period. Dashed blue lines indicate threshold for significant autocorrelation. **A)** ACF plots of snail population density **B)** ACF of filamentous algae, **C)** ACF of conductivity

**Literature Cited**


Alonso A, Castro-Diez P. 2008. What explains the invading success of the aquatic mud snail *Potamopyrgus antipodarum* (Hydrobiidae, Mollusca)? In: Hydrobiologia. Vol. 614. p. 107–116.

Alonso Á, Castro-Díez P. 2012. The exotic aquatic mud snail *Potamopyrgus antipodarum* (Hydrobiidae, Mollusca): State of the art of a worldwide invasion. Aquat Sci 74:375–383. doi:10.1007/s00027-012-0254-7.

ANS Task Force. 2007. National management and control plan for the New Zealand mudsnail (*Potamopyrgus antipodarum*) prepared for the Aquatic Nuisance Species Task Force by the New Zealand mudsnail management and control plan working group.

Bankers L, Fields P, McElroy KE, Boore J, Logsdon JM, Neiman M. 2017. Genomic evidence for population-specific responses to coevolving parasites in a New Zealand freshwater snail. Mol Ecol:1–13. doi:10.1111/mec.14146.

Barton K. 2016. MuMIn: Multi-Model Inference.

Bennett DM, Dudley TL, Cooper SD, Sweet SS. 2014. Ecology of the invasive New Zealand mud snail, *Potamopyrgus antipodarum* (Hydrobiidae), in a Mediterranean-climate stream system. Hydrobiologia 746:375–399. doi:10.1007/s10750-014-2136-6.

Breiman L. 2001. Random forests. Mach Learn 45:5–32. doi:10.1201/9780429469275-8.

Cadotte MW, Tucker CM. 2017. Should environmental filtering be abandoned? Trends Ecol Evol 32:429–437. doi:10.1016/j.tree.2017.03.004.

California Departement of Water Resources (CA Dept Water Resources). 2020. Water Year 2020 Summary Information.

Canton SP, Chadwick JW. 1984. A new modified hess sampler. Progress Fish-Culturist 46:57–59.

Drown DM, Levri EP, Dybdahl MF. 2011. Invasive genotypes are opportunistic specialists not general purpose genotypes. Evol Appl 4:132–143.

Dudley TL. 1992. Beneficial effects of herbivores on stream macroalgae via epiphyte removal. Oikos 65:121–127.

Dudley TL, Cooper SD, Hemphill N. 1986. Effects of macroalgae on a stream invertebrate community. J North Am Benthol Soc 5:93–106.

Dybdahl MF, Drown DM. 2011. The absence of genotypic diversity in a successful parthenogenetic invader. Biol Invasions 13:1663–1672. doi:10.1007/s10530-010-9923-4.

Dybdahl MF, Kane SL. 2005. Adaptation vs. phenotypic plasticity in the success of a clonal invader. Ecology 86:1592–1601. doi:10.1890/04-0898.

Gunderson AR, Abegaz M, Ceja AY, Lam EK, Souther BF, Boyer K, King EE, You Mak KT, Tsukimura B, Stillman JH. 2019. Hot rocks and not-so-hot rocks on the seashore: patterns and body-size dependent consequences of microclimatic variation in intertidal zone boulder habitat. Integr Org Biol 1. doi:10.1093/iob/obz024.

Hall RO, Dybdahl MF, VanderLoop MC. 2006. Extremely high secondary production of introduced snails in rivers. Ecol Appl 16:1121–1131.

Hall RO, Tank JL, Dybdahl MF. 2003. Exotic snails dominate nitrogen and carbon cycling in a highly productive stream. Front Ecol Environ 1:407–411.

Hampton SE, Holmes EE, Scheef LP, Scheuerell MD, Katz SL, Pendleton DE, Ward EJ. 2013. Quantifying effects of abiotic and biotic drivers on community dynamics with multivariate autoregressive (MAR) models. Ecology 94:2663–2669.

Harrison XA, Donaldson L, Correa-Cano ME, Evans J, Fisher DN, Goodwin CED, Robinson BS, Hodgson DJ, Inger R. 2018. A brief introduction to mixed effects modelling and multi-model inference in ecology. PeerJ 2018:1–32. doi:10.7717/peerj.4794.

Herbst DB., Bogan MT., Lusardi RA. 2008. Low specific conductivity limits growth and survival of the New Zealand mud snail from the Upper Owens River, California. West North Am Nat 68:324–333.

Hess A. 1941. New limnological sampling equipment. Limnol Soc Am 6:1–5.

Hoy M, Boese BL, Taylor L, Reusser D, Rodriguez R. 2012. Salinity adaptation of the invasive New Zealand mud snail (*Potamopyrgus antipodarum*) in the Columbia River estuary (Pacific Northwest, USA): Physiological and molecular studies. Aquat Ecol 46:249–260. doi:10.1007/s10452-012-9396-x.

Hulme PE. 2009. Trade, transport and trouble: Managing invasive species pathways in an era of globalization. J Appl Ecol 46:10–18. doi:10.1111/j.1365-2664.2008.01600.x.

Jacobsen R, Forbes VE. 1997. Clonal variation in life-history traits and feeding rates in the gastropod, *Potamopyrgus antipodarum*: performance across a salinity gradient. Source Funct Ecol 11:260–267. doi:10.1046/j.1365-2435.1997.00082.x.

Kerans BL, Dybdahl MF, Gangloff MM, Jannot JE. 2005. *Potamopyrgus antipodarum*: distribution, density, and effects on native macroinvertebrate assemblages in the Greater Yellowstone Ecosystem. J North Am Benthol Soc 24:123–138.

Lennox R, Choi K, Harrison PM, Paterson JE, Peat TB, Ward TD, Cooke SJ. 2015. Improving science-based invasive species management with physiological knowledge, concepts, and tools. Biol Invasions 17:2213–2227. doi:10.1007/s10530-015-0884-5.

Liaw A, Wiener M. 2002. Classification and Regression by randomForest. R News 2:18–22.

Loo SE, Mac Nally R, Lake PS. 2007. Forecasting New Zealand mudsnail invasion range: Model comparisons using native and invaded ranges. Ecol Appl 17:181–189. doi:10.1890/1051-0761(2007)017[0181:FNZMIR]2.0.CO;2.

Mandalakis M, Stravinskaitė A, Lagaria A, Psarra S, Polymenakou P. 2017. Ultrasensitive and high-throughput analysis of chlorophyll *a* in marine phytoplankton extracts using a fluorescence microplate reader. Anal Bioanal Chem 409:4539–4549. doi:10.1007/s00216-017-0392-9.

Matter SF, Roland J. 2017. Climate and extreme weather independently affect population growth, but neither is a consistently good predictor. Ecosphere 8. doi:10.1002/ecs2.1816.

McKenzie VJ, Hall WE, Guralnick RP. 2013. New Zealand mudsnails (*Potamopyrgus antipodarum*) in Boulder Creek, Colorado: Environmental factors associated with fecundity of a parthenogenic invader. Can J Zool 91:30–36. doi:10.1139/cjz-2012-0183.

McMahon RF. 1983. Physiological ecology of freshwater pulmonates. In: Russell-Hunter WD, editor. Ecology. Academic Press. p. 360–430.

Moore JW, Herbst DB, Heady WN, Carlson SM. 2012. Stream community and ecosystem responses to the boom and bust of an invading snail. Biol Invasions 14:2435–2446. doi:10.1007/s10530-012-0240-y.

National Centers for Environmental Information (NCEI). 2021. Climate Data Online.

Paolucci EM, Thuesen E V. 2020. Effects of osmotic and thermal shock on the invasive aquatic mudsnail *Potamopyrgus antipodarum*: Mortality and physiology under stressful conditions. NeoBiota 54:1–22. doi:10.3897/neobiota.54.39465.

Pinheiro JC, Bates DM. 2000. Mixed-Effects Models in S and S-Plus.

Power ME. 1990. Benthic turfs vs floating mats of algae in river food webs. Oikos 58:67–79.

Rahel FJ. 2002. Homogenization of freshwater faunas. Annu Rev Ecol Syst 33:291–315. doi:10.1146/annurev.ecolsys.33.010802.150429.

Ribi G. 1986. Within-lake dispersal of the prosobranch snails, *Viviparus ater* and *Potamopyrgus jenkinsi*. Oecologia 69:60–63.

Roland J, Matter SF. 2016. Pivotal effect of early-winter temperatures and snowfall on population growth of alpine *Parnassius smintheus* butterflies. Ecol Monogr 86:412–428. doi:10.1002/ecm.1225.

Ruhí A, Holmes EE, Rinne JN, Sabo JL. 2015. Anomalous droughts, not invasion, decrease persistence of native fishes in a desert river. Glob Chang Biol 21:1482–1496. doi:10.1111/gcb.12780.

Schneider, C.A., Rasband, W.S., Eliceiri KW. 2012. NIH Image to ImageJ: 25 years of image analysis. Nat Methods 9:671–675.

Sepulveda AJ, Marczak LB. 2012. Active dispersal of an aquatic invader determined by resource and flow conditions. Biol Invasions 14:1201–1209. doi:10.1007/s10530-011-0149-x.

Shoup C. 1943. Distribution of fresh-water gastropods in relation to total alkalinity of streams. Nautilis 56:130–134.

Suren AM. 2005. Effects of deposited sediment on patch selection by two grazing stream invertebrates. Hydrobiologia 549:205–218. doi:10.1007/s10750-005-5323-7.

Team RC. 2018. R: A Language and Environment for Statistical Computing.

Therneau TM, Atkinson EJ. 2019. An introduction to recursive partitioning using the RPART routines.

Thorp JH, Rogers DC. 2011. Snails: Phylum Mollusca, Class Gastropoda. F Guid to Freshw Invertebr North Am:65–82. doi:10.1016/B978-0-12-381426-5.00009-0.

Tredennick AT, Hooker G, Ellner SP, Adler PB. 2021. A practical guide to selecting models for exploration, inference, and prediction in ecology. Ecology:1–44. doi:10.1002/ecy.3336.

U.S. Geological Survey. 2021. Nonindigenous Aquatic Species Database. :1–71.

Vinson MR, Baker MA. 2008. Poor growth of rainbow trout fed New Zealand mud snails *Potamopyrgus antipodarum*. North Am J Fish Manag 28:701–709. doi:10.1577/m06-039.1.

Winterbourn MJ. 1970. The New Zealand species of *Potamopyrgus* (Gastropoda: Hydrobiidae). Malacologia 10:283–321.

## Mild temperatures differentiate while extreme temperatures unify gene expression profiles among populations of *Dicosmoecus gilvipes* in California

### Introduction

Predicting the responses of aquatic ectothermic animals to changing temperature regimes is critical for managing biodiversity in the future. Temperature influences many vital aspects of physiology, development, and life history, and ultimately shapes biogeography (Sweeny et al. 1992; Gillooly et al. 2001; Seebacher et al. 2015). Animals can deal with changes in temperature at different time and biological scales. At the organismal level, animals can acclimate or adjust their physiology after long-term exposure to a thermal stimulus (days to weeks) (Bowler 2005; Angilletta 2009; Shah et al. 2017). Organisms from more variable environments are expected to have a greater capacity for acclimation than organisms in stable environments (Shah et al. 2017). Warm acclimated individuals are expected to have higher thermal tolerances than cold-acclimated individuals. In freshwater organisms specifically, this results in decreased thermal sensitivity of organismal traits to further warming for already warm acclimated populations (Seebacher et al. 2015). At the biochemical level, organisms can change the regulation of gene expression in response to thermal exposures. Specifically, expression of heat shock proteins and other molecular chaperones, macromolecules that quickly protect damaged or denaturing proteins, is a reliable indicator of rapid temperature changes (over hours) (Feder and Hoffman 1999; Dahlhoff 2004; Somero 2005; Somero 2010). However, the thermal history of the organism's environment causes interactions between the whole organism and biochemical scales.

Thermal history is made up of both average temperatures and thermal variation and can lead to sustained differences in physiological responses between environments or populations. Protein expression of aquatic stonefly species in Japan differs along stream temperature gradients that covary with latitude and elevation. Protein expression was more similar between species with shared thermal history than within a species across regions (Gamboa et al. 2017). Acclimation to different thermal histories can also cause warm-acclimated populations to induce heat shock protein expression at higher temperatures than cold-acclimated populations (Bowler 2005). What may appear as a muted response to a temperature change in one population may indicate a warmer thermal history. Thermal history (average temperature and variation) play a critical role in our ability to forecast future responses to temperature change in wild populations. However, it still represents a gap in our knowledge because it is often ignored in laboratory experiments.

Physiologists often acclimate animals to constant temperatures before an experiment and use "average" conditions as the experimental treatments (e.g., average summer temperature vs. average winter temperature) (Morash et al. 2018). In these highly controlled lab studies, we can focus on responses to a particular stimulus without certain complexity (e.g., individual variation, temperature variation), but this simplicity comes at the cost of biological realism. Stable laboratory conditions mask thermal history and rarely elicit responses similar to those measured under fluctuating conditions (Denny 2017; Morash et al. 2018; Marshall et al. 2021). One solution is to study animals in their natural, variable environments to understand how thermal history affects the response of different populations. To make the best conclusions about future changes in biogeography and population dynamics under future warming conditions, we need to make population-level inferences under realistic conditions (Pörtner and Knust 2007; Dong et al. 2015; Morash et al. 2018)

Caddisfly larvae are an integral element of California river ecosystems. *D. gilvipes* occur in various eco-regions of California, including mountain, valley, and coastal populations experiencing different thermal means and variabilities. Mountain streams freeze over then warm dramatically through the summer, while coastal streams stay within a much warmer, narrower temperature range. Future warming is likely to raise the maximum water temperatures in all eco-regions (Null et al. 2013). Temperature has clear effects on the physiology and life history of *D. gilvipes*. Larvae develop faster in stream regions with a higher number of degree days until they disappear in the most downstream regions (Hannaford 1998; Resh et al. 2011). There is low gene flow between populations due to a short-lived adult stage (~ 2 weeks) and short-range mating cues (Resh and Wood 1985; Peterson et al. 2017), thus separating populations genetically and by thermal environment. Therefore, *D. gilvipes* is a good model for understanding how temperature warming will impact wild, free-living aquatic animals with different thermal histories.

This study tests the hypotheses that wild populations of larval *D. gilvipes* will differ in baseline gene expression and responses to current and future warming scenarios due to differences in thermal history. Specifically, we expect that 1) populations from warm locations will have less thermally sensitive gene expression responses, 2) that the more extreme warming scenario will generate more extreme transcriptional responses, 3) that long and short summer acclimatization will generate different transcriptional responses, and that 4) gene co-expression will be similar between warming scenarios. To test these hypotheses, we assayed the expression of thermally sensitive mRNA transcripts in three populations of field acclimated *D. gilvipes* from three eco-regions at two dates through the summer.

## Methods

*Animal Collection and Thermal Exposure*

We collected larval *Dicosmoecus gilvipes* (Hagen, 1875) from three distinct populations at stream sites within the University of California Natural Reserve System. Larvae in the 5th (terminal) instar stage were collected by hand in the morning on the day of each experiment from Angelo Coast Range Reserve (39.7186°, -123.6528°), Sagehen Creek Reserve (39.4333°, -120.2407°), and Landels-Hill Big Creek Reserve (36.071298°, -121.599153°) (Figure 1a). Larval stage was determined by case-building materials (Resh et al. 2011; Holomuzki et al. 2013). Thermal stress experiments were performed streamside May-June of 2013 (Table 2). The experiment was run twice at the Angelo site (i.e., “Angelo early, “Angelo late”) just under one month apart to measure the effects of seasonal acclimatization on the same population. Stream temperatures for the 30 days preceding each experiment were obtained from stream sensor data collected by other researchers (Table 1, Figure 1b). These sites represent three temperature regions in California: mountain (Sagehen, elevation 1972m), valley (Angelo), and coastal (Big Creek).

Three to four individual caddisflies were held in continuously aerated 1L glass jars inside one of three insulated water coolers to maintain specific temperatures (Table 2). Cooler temperatures were manipulated to represent three temperature treatments: a cool control, gradual warming mimicking the daily increase in stream temperature, or a heat shock to 30°C. We will refer to the treatments as “cool control”, “daily warming”, and “heat shock”. The cool control treatment was held at the temperature of the stream at the time the caddisflies were collected in the morning (Table 2, Figure 1c) for the duration of the experiment, approximately 9 hours. The daily warming treatment matched the warming stream through the day by measuring the

temperature of the stream every two minutes with an Omega HH603A handheld thermometer. The temperature of the treatment water was manipulated manually by adding hot water or bags of ice into the outer chamber of the cooler to achieve a temperature matching the stream. Each site had a slightly different natural warming profile, but endpoint temperatures were between 15°-17°C (Table 2). The heat shock treatment water was warmed from the control temperature to 30°C at a rate of approximately 3°C/hour. The maximum temperature, 30°C, reflects the annual maximum temperature observed at the Angelo Coast Reserve plus a 4°C warming based on end-century climate change predictions (Hannaford 1998; IPCC 2019). After a one-hour exposure to the maximum temperature of the respective treatment, individuals were removed from their case, blotted dry, flash-frozen in liquid nitrogen, and stored at -80°C prior to RNA extraction.

*Selection of Biomarkers*

Target genes were chosen for NanoString analysis from among the most differentially expressed genes in a previous laboratory temperature exposure RNA-Seq experiment (Stillman, JH. unpublished data, Figure S1). Reference candidate genes were selected based on the lowest coefficient of variation in FPKM (fragments per kilobase of exon per million fragments mapped) values from the same RNA-Seq experiment with a range of expression levels and reasonable biological function (i.e., transcription apparatus, cytoskeleton). Thirty-one NanoString targets were selected, representing both those that increased and decreased with warming, to be normalized to the three reference genes described above (Table 3).

*RNA Preparation*

Head and thorax tissues were homogenized with stainless steel ball bearings (3mm, McMaster Carr) in Tri Reagent (Molecular Research Center, USA) using a TissueLyser II (Qiagen). RNA was isolated according to the manufacturer's recommended protocol, using bromochloropropane (BCP, Molecular Research Center, USA) for phase separation and isopropanol for RNA precipitation (Chomczyński and Sacchi 1987). RNA quality and quantity were measured with a Bioanalyzer (Agilent). Only samples with little to no degradation and adequate concentration were used in downstream steps.

DNA-free RNA was prepared by mixing 5µg of RNA, 5µl of 10x reaction buffer (Thermo Scientific, 100 mM Tris-HCl, 25 mM MgCl2, 1 mM CaCl2) and 5 U of DNase I enzyme (Thermo Scientific). RNase-free water was added to a final volume of 55µl. The DNase reaction proceeded at 37°C for 30 minutes and was stopped by adding 5 µl of 50 mM EDTA with heating at 65°C for 10 minutes. The DNA-free RNA was stored at -80°C.

*NanoString Expression and Data Quality Control*

Gene expression was measured using the nCounter System (NanoString Technologies) (Geiss et al. 2008). Some of the RNA extracted from each caddisfly sample was diluted with RNase-free water to a concentration of 20ng/µl in a final volume of 20µl. Samples were then sent to NanoString Technologies in Seattle, WA, USA for processing and gene expression quantification. This method allows for many genes to be analyzed at once without cDNA reverse transcription or amplification to reduce bias in counts of rare or abundant transcripts. The resulting expression data were background corrected by subtracting the mean plus two standard deviations of the negative controls. Transcripts with post-background correction expression values in the negative range were excluded. Expression levels of the remaining transcripts were

normalized to the geometric mean of the three reference genes for that individual and log-transformed.

*Data Analysis*

All analysis was completed in the R Computing Environment (v 3.5.1, Core Team 2018). Principal components analysis using the "pcaMethods" package in R (v1.72.0, Stacklies et al. 2007) was used to identify potential population-level differences in the entire suite of genes. The data were mean-centered and scaled using the Pareto scaling method prior to running the principal components analysis. The Pareto method scales the data with the square root of the standard deviation (Eriksson L, Johansson E, Kettaneh-Wold N 1999). We tested for statistical differences in PC scores between groups using a MANOVA with the Wilks λ test statistic. One analysis compared the first sampling date at all sites and the second analysis compared the two sampling dates from Angelo (early and late). The model structures were: PC1+PC2~Population*Treatment and PC1+PC2~Date*Treatment. We ran univariate ANOVAs on the significant components of the MANOVA to do Tukey's multiple pairwise comparisons (Table S1). We excluded one individual (from Sagehen control) from the PCA analysis because inspection of residuals suggested that it was a multivariate outlier and thus violated the assumptions of MANOVA (Figures S2, S3). The overall conclusions did not change when this outlier was excluded, and normality of residuals was improved (Figure S3).

To focus on the responses to the two warming scenarios, we analyzed the change in expression between the cool control and each of the warming treatments. For each transcript, the average expression level for that population under control conditions was subtracted from each individuals' warming response to give Δ expression, separately for daily warming and heat shock. The resulting positive values indicate increased expression under a warming treatment, while negative values indicate decreased expression relative to the control. This procedure was performed for the daily warming treatment and the heat shock treatment. Comparisons between sites within one warming treatment and between warming treatments were made using Kruskal-Wallis tests and Nemenyi post-hoc tests to handle non-parametric datasets.

Heatmaps were created with "heatmap3" (v1.1.9, Zhao et al. 2021). Dendrograms clustered rows of genes by similarity of Δ expression from the treatment control. The colors of the heat map cells represent the magnitude and direction of the change in expression, scaled and centered by row.

Gene co-expression matrices were created for each warming treatment using "corrplot" (v0.84, Wei and Simko 2016). Matrix data were Pearson's correlations of gene expression in each treatment and were ordered by gene function. The threshold for a significant correlation was $\alpha=0.05$. Populations were combined to provide a sufficient sample size for correlation analysis. Clusters of important genes were identified by visual inspection.

## Results

*Thermal history*

In the month preceding the first round of sampling, the stream temperature was very similar at Angelo (valley) and Big Creek (coastal) (Table 1, Figure 1b). Stream temperature at Sagehen, a montane site, is characterized by much lower minimum temperatures and a much larger daily temperature range. At Sagehen, there was also a sustained warming trend in the ten days before the experiment (Figure 1b). A few days before the experiment, maximum daily water

temperatures exceeded the temperature of the daily warming treatment for that population (Table 1, Table 2). The mean temperature preceding the Angelo "late" sampling was 2°C warmer with a wider range and higher maximum temperature relative to the Angelo "early" sampling. Fifteen days before the Angelo "late" sampling time, maximum temperatures were higher than any daily warming treatment and were only exceeded by the heat shock treatments (Table 1).

*Gene expression differentiates populations and treatments*

Population, treatment, and their interaction had significant effects on PCs 1 and 2 for the first sampling time from all populations (Figure 2A, Table 4). PC1 represented 28% of the variation in expression, while PC 2 represented 15% of the variation. Differences along PC1 were significantly positively correlated with 4 of 5 heat shock proteins in our study (Figure S4). PC1 was negatively correlated with *apoptosis inhibitor* and *circadian clock protein*. PC 2 was positively correlated with a suite of genes containing metabolic genes and molecular transporters, among genes of other functions. Broadly, all treatments in the same populations grouped together (Figure 2A). Angelo typically had low PC1 scores and high PC2 scores. Big Creek had significantly lower PC2 scores than the other populations (Table S1B). Sagehen had medium to high PC1 scores significantly different from the other populations (Table S1A). When the treatments are compared separately, they group by population in the control and daily warming treatments, but not in the heat shock treatment (Figure 2 B-D).

We compared the early and late sampling times from Angelo to understand if gene expression responses to warming change with seasonal acclimatization during summer warming. The two sampling dates and the treatments significantly differed along PC1, but there was no differentiation on PC2 (date: $p<0.001$, treatment: $p<0.01$) (Table 4B). The Angelo "late" samples generally had lower scores on PC1 compared to the Angelo "early" samples. The daily warming treatment did not differ from the control treatment, but all other treatments were distinct from each other (Table S1).

*Response to warming is site and treatment specific*

The magnitude of changes in gene expression relative to the control treatment was larger in the heat shock treatment than the daily warming treatment (Figure 3A) (Kruskal-Wallis test, $\chi^2= 6.3835$, $p<0.05$). At Sagehen, $\Delta$ expression in the daily warming treatment is more than two times higher than at Angelo (Kruskal-Wallis test, $p<0.05$, Table 5A). $\Delta$ expression in the heat shock treatment did not differ across populations (Kruskal-Wallis test, $p>0.05$)

Five genes were clustered together with the most similar $\Delta$ expression profiles (Figure 3b). Three genes in that cluster are molecular chaperones (*hsp10, hsp23, hsp90 activator*), and the others are related to metabolism (*ATPase inhibitor, carbonic anhydrase*). There are significant differences in $\Delta$ expression with the main effects of population, treatment, and their interaction (MANOVA, Table 5). Within that cluster, gene expression was generally up-regulated to a greater degree in response to heat shock than daily warming at Angelo and Big Creek, with little or no up-regulation of gene expression in response to daily warming (Figure 4). In contrast, Sagehen individuals up-regulated expression of these genes to similar levels in both warming treatments (Figure 4).

*Gene co-expression differs between warming treatments*

We constructed co-expression matrices to explore patterns of co-regulation among genes. There were a greater number of significant correlations in the daily warming treatment than the heat

shock treatment, 295 and 244, respectively (Figure 5, Table 6). Positive correlations in expression levels among genes were more prevalent under daily warming conditions than heat shock, while the number of negative correlations in expression levels was similar between treatments (Table 6). Correlations in the daily warming treatment were stronger on average than correlations in the heat shock treatment, both more positive and more negative (Table 6). In the daily warming treatment, there were 3 major clusters of strong positive correlations: 1) between molecular chaperones, 2) molecular chaperones and a mixed group of metabolic genes, transporters, and transcription/translation regulators, and 3) the group of metabolic genes, transporters and transcription/translation regulators with themselves. In the heat shock treatment, cluster 1was maintained (between molecular chaperones) while cluster 2 was reduced. In the daily warming treatment, there were 3 genes with strong negative correlations with many other genes: *protein henna*, *apoptosis inhibitor*, and *GST*. However, the sign of the correlations between protein henna and the molecular chaperones changed under heat shock conditions. *Protein henna* was positively correlated with molecular chaperones under heat shock conditions but negatively correlated with the same genes under daily warming.

## Discussion

Accurately predicting the future of ectotherms to warming requires studies that include populations with distinct thermal histories to understand variations in the physiological response to warming. In the current study, we tested the molecular physiology responses of three populations of *D. gilvipes* from different eco-regions (mountain, valley, coast) to different heat exposures. We hypothesized that distinct thermal histories could differentiate populations at baseline "control" levels of gene expression and gene expression changes in response to daily warming and heat shock. Population-specific responses were apparent under the control and daily warming conditions, while responses to heat shock were similar across populations. In addition, underlying gene expression patterns in the daily warming and heat shock treatments were different.

### *Mild temperatures differentiate populations, but extremes connect them*

Under control conditions, the three populations had distinct expression profiles. As temperature-sensitive biomarkers, heat shock proteins can signal current stress or the effects of thermal history (Feder and Hoffman 1999; Dahlhoff 2004; King and Macrae 2015). Given that these animals were not exposed to temperatures we expected to induce stress, differences in constitutive expression of thermally sensitive transcripts support our hypothesis that the populations experienced distinct thermal histories (Bowler 2005; King and Macrae 2015).

Thermal history likely also contributed to and magnified the gene expression responses in the daily warming treatment. There was a 5°C warming trend at the Sagehen site beginning 12 days before the experiment was performed, while the other sites stayed within 2.5°C. This rapid warming may have already induced a warming response that was magnified during an otherwise mild temperature increase that resulted in molecular chaperone expression under daily warming conditions that was greater than or equal to the expression of those genes under heat shock (Figures 3 and 4). This difference between the response to daily warming at Sagehen and the other sites may also be related to differences in the thermal sensitivity of gene expression. The average$\Delta$ expression at Sagehen was two times that of other populations after a similar increase in temperature. Big Creek and Angelo are generally warmer than Sagehen throughout the year.

This supports our hypothesis that warm-adapted populations would be less thermally sensitive and exhibit a more muted expression response to warming. Similarly, the common killifish, *Fundulus heteroclitus*, from warm-acclimated populations showed a muted response in the expression of several hsp70 isoforms in response to high temperatures when compared with cold-adapted populations (Fangue et al. 2006). Muted responses in other physiological traits have also been measured in response to warmer thermal histories (Seebacher et al. 2015; Tanner et al. 2019).

Under heat shock conditions, there were no differences between the populations. Potentially, 30°C is approaching a sub-lethal thermal limit and the response to such temperatures is canalized evolutionarily. The CTmax for several North American aquatic insects, including caddisflies, is near 30°C (Houghton et al. 2014; Houghton and Shoup 2014; Hotaling et al. 2020). Hotaling et al. (2020) also found no transcriptomic grouping by population in high altitude stoneflies exposed to their CTmax. This evidence does not support our hypothesis that we would see a muted thermal response in populations that are already warmer since all populations responded similarly. This contrasts with the differences in thermal sensitivity we saw in the daily stream warming treatment. Extreme warming (rate and maximum temperature achieved) may trigger a consistent species-level response that supersedes differences in thermal history.

*Populations specific responses may mask the effects of seasonal acclimatization*

We repeated our experiment at Angelo one month later in the summer to assess the effect of a warmer thermal history on the same population's gene expression response. The late samples had lower expression of molecular chaperones than the early samples, especially in the control and daily warming treatments (Figure 2, Figure S4). This may be evidence of the effect of thermal history on thermal sensitivity, an effect of developmental stage of the individual caddisflies, or some combination of the two. Several individuals observed in the creek on the experiment day were older but were not included in the experiment. The month between the two trials at Angelo represents a large number of the degree-heating days for emergence. By late June, most caddisflies near our study site on the Eel River will have entered prepupal diapause (Hannaford 1998; Resh et al. 2011). Similar gene expression effects have been measured in walleye maintained in warming regions of Lake Manitoba for a short or long portion of the summer (Jeffrey et al. 2020). Fish held in the lake until later in the summer had increased expression of molecular chaperones. Though the directionality was reversed in our experiment, it is clear that seasonal acclimation can change gene expression patterns.

The main difference between the early and late experiments is that the later timepoint had lower values on PC1, which were driven by expression of *apoptosis inhibitor* and *circadian clock protein* (Figure 2, Figure S4). This circadian-clock protein, named *daywake* in *Drosophila melanogaster*, was primarily expressed in individuals from Angelo. Only one individual from elsewhere, Sagehen, expressed this gene. In *D. melanogaster*, *daywake* acts as a behavioral thermometer that promotes daytime sleep under warm conditions to avoid heat damage (Yang and Edery 2019). Higher expression of *daywake* in the later Angelo samples would indicate warmer days, which matches the actual thermal history at the site. However, we would expect to see this gene expressed more widely at Sagehen after the warming trend. Surprisingly, the late Angelo samples were more similar to the earlier Angelo samples and even further differentiated than the other groups from the Sagehen samples in every treatment (Figure 2). This indicates

some combination of population-specific and temperature-specific responses occurring under natural conditions.

*Differences between mild and extreme warming are greatest in a subset of genes*

The differences we expected to see between the daily warming treatment and the heat shock treatment were only apparent relative to control expression (Figure 3, Figure 4). Even then, the differences were gene- and population-specific. Consistently, the heat shock proteins were more strongly induced in the heat shock treatment at all sites except Sagehen. A large body of research supports our findings that heat shock protein expression increases with higher temperature exposure (Feder and Hoffman 1999; King and Macrae 2015; Somero 2020).

Co-expression patterns between genes also changed between warming treatments suggesting that it's important to focus on the relationships between genes in addition to individual genes. Under daily warming conditions, protein henna, an amino acid metabolism gene, was negatively correlated with molecular chaperones, suggesting that the importance of protein protection superseded energy production. However, the correlation changed sign under the heat shock conditions. This may indicate that our heat shock treatment was so stressful that energy production and protein homeostasis both needed to increase simultaneously. Similarly, Dong and Zhang (2016) also found that molecular chaperones, specifically *hsp70,* were only positively correlated with metabolic genes under extreme heat conditions. Some other changes in co-expression between treatments signaled that some macromolecules were not further protected under extreme heat. Under daily warming conditions, *trehalose transporter* was positively correlated with many genes but negatively correlated with them under heat shock. Trehalose has multiple protective roles during heat stress, such as stabilizing membranes and preventing further unfolding of proteins (Ebner et al. 2019; Somero 2020). Its decrease in relation to other molecular chaperones at very high temperatures may highlight a change in exactly which molecules are being protected (Ebner et al. 2019).

*Importance of individual and environmental variation*

We studied wild-caught and naturally acclimatized individuals, thus incorporating ecologically relevant impacts of thermal history. In addition, we used a warming treatment that mirrored natural increases in water temperature throughout the day. Maintenance of population-specific thermal history allowed us to measure the baseline expression levels of each population more accurately than a laboratory study could. For example, we can contrast the effects of the warming trend that occurred before sampling at Sagehen with stable temperatures before early sampling at Angelo and Big Creek.

However, ecological realism comes at the cost of control and standardization; and in our study, undetected differences in developmental stage, body condition, or sex may have influenced gene expression patterns. We collected individuals in the final larval instar, indicated by case-building materials in this species (Hannaford 1998; Holomuzki et al. 2013), but we do not know the individual's age or proximity to pupation. Warming is known to increase developmental rate and has even been seen to drive pupation and emergence during thermal stress experiments in stoneflies (Hannaford 1998; Hotaling et al. 2020). Though the differences in developmental state were likely products of degree heating days at each site, we must consider that the warming treatment itself may have had an effect.

Studies of ecologically relevant stress must also consider the timing, intensity, duration, and frequency of the stress. Our study matches the ecological timing of stress to the later larval

period and used a relevant duration and two relevant warming intensities (current and future), but for only one cycle. In nature, both warming and cooling on a diel cycle contribute to population acclimatization. Under future warming scenarios, caddisflies may experience warming to 30°C repeatedly with carryover effects each day that influence gene expression and phenotypes that may take longer to appear. These carryover effects may be detrimental such as reduced growth and faster development, resulting in small individuals that are phenologically mismatched, or positive effects such as rapid heat hardening that prepare and protect them from the effects of future thermal stress (Bowler 2005; Bergmann et al. 2010; Verberk and Calosi 2012; King and Macrae 2015; Hotaling et al. 2020; Bernhardt et al. 2020). Field-acclimatized gene expression in response to warming over one day is a critical snapshot of the processes that underlie the whole organism response. Still, it is only part of the story that will help us understand the future of the species. Aquatic invertebrates in California face a warmer future due to climate change induced droughts and surface water warming (Null et al. 2013; Swain et al. 2014; Diffenbaugh et al. 2015). Using physiology to understand the effects of warming may help us understand which populations are likely to persist or not.

**Conclusion**

The present study investigated the field-acclimatized transcriptional response to two warming regimes in the three populations of the larval caddisfly *Dicosmoecus gilvipes* from three eco-regions. We found that gene expression of populations from different eco-regions differ in cool control and mild warming scenarios, but not under extreme warming. Populations from warmer eco-regions showed evidence of decreased thermal sensitivity under mild warming conditions. Co-expression between genes should be considered to understand the interactions between molecular processes affected by warming. Our results highlight the importance and limitations of measuring the stress response of wild-caught organisms in their natural environment.

**Acknowledgments**

Carl Hendrickson and Joseph Gapuz conducted the field collections and thermal exposures. Scott Fay and Cecilia Tran conducted the RNA and NanoString preparation. Special thanks to Dave Rundio (NOAA Fisheries, Santa Cruz) for Big Creek stream temperature data.

This work was supported by the Gordon and Betty Moore Foundation and the Berkeley Initiative for Global Change.

**Table 1. Stream temperatures in the field for 30 days before collection (°C).**

| Site | Avg. Daily Temp | Avg. Daily Max | Avg. Daily Min | Avg. Daily Range | Absolute Max | Absolute Min | Source | Date Range |
|---|---|---|---|---|---|---|---|---|
| Angelo | 12.8 | 14.0 | 11.7 | 2.4 | 15.6 | 10.1 | Berkeley Sensor Database[1] | 4/29/13 – 5/29/13 |
| Big Creek | 13.8 | 15.0 | 12.8 | 2.2 | 16.4 | 10.9 | NOAA Fisheries, Santa Cruz[2] | 5/10/13-6/9/13 |
| Sagehen | 9.19 | 13.9 | 6.1 | 7.9 | 18.5 | 3.2 | USGS NWIC[3] | 5/12/13 – 6/11/13 |
| Angelo | 14.9 | 17.0 | 13.6 | 3.4 | 21.2 | 10.1 | Berkeley Sensor Database[1] | 5/24/13 – 6/22/13 |

1:http://sensor.berkeley.edu/cgi/sensor_query2?view=check_password&Access=4&username=Guest+User&MC_Name=Angelo+Reserve&VariableCode=Water+Temp+C&ONEVAR=1

2: Personal communication with Dave Rundio, 3: https://waterdata.usgs.gov/ca/nwis/uv/?site_no=10343500&PARAmeter_cd=00065,00060

**Table 2.** Experimental temperatures treatments (°C) and number of individuals analyzed in parentheses

| Site | Experiment Date | Control | Daily Warming | Heat Shock |
|---|---|---|---|---|
| Angelo early | May 29, 2013 | 12° (3) | 12°-15° (3) | 12°-30° (4) |
| Sagehen | June 9, 2013 | 13° (4) | 13°-17° (4) | 13°-30° (3) |
| Big Creek | June 11, 2013 | 14° (4) | 14°-16° (4) | 14°-30° (3) |
| Angelo late | June 22, 2013 | 14° (4) | 14°-17° (4) | 14°-30° (2) |

**Table 3.** NanoString target and reference genes

| **Target Transcripts** | | | | | |
|---|---|---|---|---|---|
| **Abbreviation** | **Full Transcript Name** | **ContigID** | **UniProtID** | **Function** | **Expected Heat Δ** |
| alpha-amylase | Alpha-amylase A | comp57363_c0_seq1 | P08144 | carbohydrate metabolism | down |
| apoptosis inhibitor | Apoptosis inhibitor | comp58747_c0_seq1 | P41436 | apoptosis inhibition | down |
| aquaporin | Aquaporin AQPAe.a | comp64170_c1_seq1 | Q9NHW7 | transporter activity | down |
| ATPase inhibitor | ATPase inhibitor mai-2 | comp60498_c0_seq1 | A8XZB0 | negative regulation of ATPase activity | up |
| carbonic anhydrase | Carbonic anhydrase 2 | comp61667_c0_seq1 | Q8UWA5 | carbonate dehydratase activity | up |
| carbonyl reductase | Carbonyl reductase [NADPH] | comp61657_c0_seq4 | Q28960 | metabolic process | down |
| chymotrypsin | Chymotrypsin-1 | comp55087_c0_seq1 | Q27289 | digestion | down |
| circadian clock | Circadian clock-controlled protein | comp57418_c0_seq3 | O76879 | circadian rhythm | down |
| copper chaperone | Copper chaperone for superoxide dismutase | comp58560_c3_seq5 | Q9JK72 | metal ion transport, superoxide radical removal | up |
| GST | Glutathione S-transferase | comp58392_c0_seq1 | P46437 | Transferase, antioxidant | down |

| | | | | | |
|---|---|---|---|---|---|
| hsp10 | 10 kDa heat shock protein, mitochondrial | comp63721_c5_seq 1 | Q5DC69 | protein folding | up |
| hsp23 | Heat shock protein 23 | comp54992_c0_seq 1 | P02516 | protein folding | up |
| hsp70 | Heat shock protein 70 B2 | comp64140_c1_seq 7 | P41827 | stress response | up |
| hsp70-3 | Heat shock 70 kDa protein cognate 3 | comp58617_c2_seq 1 | P29844 | protein folding | up |
| hsp70-5 | Heat shock 70 kDa protein cognate 5 | comp63373_c1_seq 4 | P29845 | protein folding | up |
| hsp90 activator | Activator of 90 kDa heat shock protein ATPase homolog 1 | comp63956_c0_seq 2 | O95433 | co-chaperone of hsp90 | up |
| MAPK-activator | Arf-GAP with dual PH domain-containing protein 1 | comp62480_c4_seq 2 | O75689 | regulation of GTPase activity | up |
| mito enolase | Mitochondrial enolase superfamily member 1 | comp58198_c0_seq 2 | Q7L5Y1 | amino acid and carbohydrate catabolism | down |
| mobility group | Mobility group protein 1A | comp38073_c0_seq 1 | P40622 | DNA binding | down |
| PGM | Phosphoglucomutase | comp63948_c2_seq 1 | Q7KHA1 | glucose metabolic process | down |
| phenoloxidase 2 | Phenoloxidase subunit 2 | comp61132_c0_seq 1 | Q27452 | melanin biosynthesis, defense response | down |
| phenoloxidase A3 | Phenoloxidase subunit A3 | comp56149_c0_seq 1 | Q9V521 | melanin biosynthesis, defense response | down |

| | | | | | |
|---|---|---|---|---|---|
| procollagen | Procollagen-lysine,2-oxoglutarate 5-dioxygenase 1 | comp61977_c0_seq1 | P24802 | collagen formation | down |
| protein henna | Protein henna EC | comp64492_c0_seq6 | P17276 | amino acid metabolism | up |
| protein ubiquination | E3 ubiquitin-protein ligase RNF139 | comp63534_c0_seq2 | Q8WU17 | protein ubiquination regulation | up |
| RNA-binding | RNA-binding protein Rsf1 | comp55145_c0_seq1 | Q24491 | gene expression regulation | down |
| TAM41 | Mitochondrial translocator assembly and maintenance protein 41 homolog | comp60449_c0_seq4 | Q8INF2 | cardiolipin biosynthesis | up |
| TRAP-beta | Translocon-associated protein subunit beta | comp31633_c0_seq1 | P23438 | co-translational protein targeting to membrane | down |
| trehalose transporter | Facilitated trehalose transporter Tret1 | comp63446_c0_seq1 | A9ZSY3 | sugar transport | down |
| xanthine dehydro | Xanthine dehydrogenase | comp64423_c0_seq2 | P08793 | xanthine catabolic process | up |
| zonadhesin | Zonadhesin Flag | comp62844_c0_seq3 | O88799 | cell adhesion | down |
| **Reference Transcripts** | | | | | |
| elongation 1B | Elongation factor 1-beta | comp51037_c0_seq1 | P29522 | Protein biosynthesis | down |
| troponin | Troponin I | comp62634_c1_seq14 | P36188 | Actin binding | down |
| unknown ref | NA | comp60946_c5_seq1 | NA | NA | up |

**Table 4.** Effect of population and date on principal component scores of temperature-sensitive transcripts in *Dicosmoecus gilvipes.* Results of MANOVA tests to determine the **A)** effects of population on the early experiments and **B)** the effect of the additional warming between the two Angelo dates. Significant results are bolded

**A)**

| | **df** | **Wilks λ** | **F** | **num df** | **den df** | **p** |
|---|---|---|---|---|---|---|
| Population | 2 | 0.18238 | 14.0869 | 4 | 42 | **2.27e-07** |
| Treatment | 2 | 0.57752 | 3.3168 | 4 | 42 | **0.019** |
| Population*Treatment | 4 | 0.33791 | 3.7815 | 8 | 42 | **0.002** |
| Residuals | 22 | | | | | |

**B)**

| | **df** | **Wilks λ** | **F** | **num df** | **den df** | **p** |
|---|---|---|---|---|---|---|
| Date | 1 | 0.34354 | 12.4207 | 2 | 13 | **0.001** |
| Treatment | 2 | 0.28410 | 5.6949 | 4 | 26 | **0.002** |
| Date*Treatment | 2 | 0.77925 | 0.8634 | 4 | 26 | 0.499 |
| Residuals | 14 | | | | | |

**Table 5.** Effect of population and treatment on gene expression responses to warming **A)** Results of Kruskal-Wallis test to determine population differences for absolute Δ expression of genes in the daily warming treatment and the Nemenyi post-hoc test **B)** Results of MANOVA to determine the effects of population and treatment on the expression of genes grouped together in Figs. 3 & 4

**A)**

| **Kruskal-Wallis test** | | | |
|---|---|---|---|
| | $\chi^2$= 60.317 | df: 3 | **p<0.001** |
| **Post-hoc comparisons using Nemenyi test** | | | |
| | Angelo early | Angelo late | Big Creek |
| Angelo late | 0.9988 | - | - |
| Big Creek | 0.0727 | **0.0330** | **-** |
| Sagehen | **3.8e-07** | **4.0e-10** | **0.0064** |

**B)**

| | **df** | **Wilks λ** | **F** | **num df** | **den df** | **p** |
|---|---|---|---|---|---|---|
| Population | 3 | 0.15806 | 2.6503 | 15 | 41.81 | **0.007** |
| Treatment | 1 | 0.09988 | 27.0362 | 5 | 15 | **<0.001** |
| Population*Treatment | 3 | 0.15948 | 2.6327 | 15 | 41.81 | **0.007** |
| Residuals | 19 | | | | | |

**Table 6**. Significant gene correlations in each warming treatment

| Treatment | Mean positive | SE positive | N positive | Mean negative | SE negative | N negative | Total significant |
|---|---|---|---|---|---|---|---|
| Daily Warming | 0.552 | 0.013 | 198 | -0.349 | 0.018 | 97 | 295 |
| Heat Shock | 0.390 | 0.020 | 152 | -0.254 | 0.020 | 92 | 244 |

**Figures**

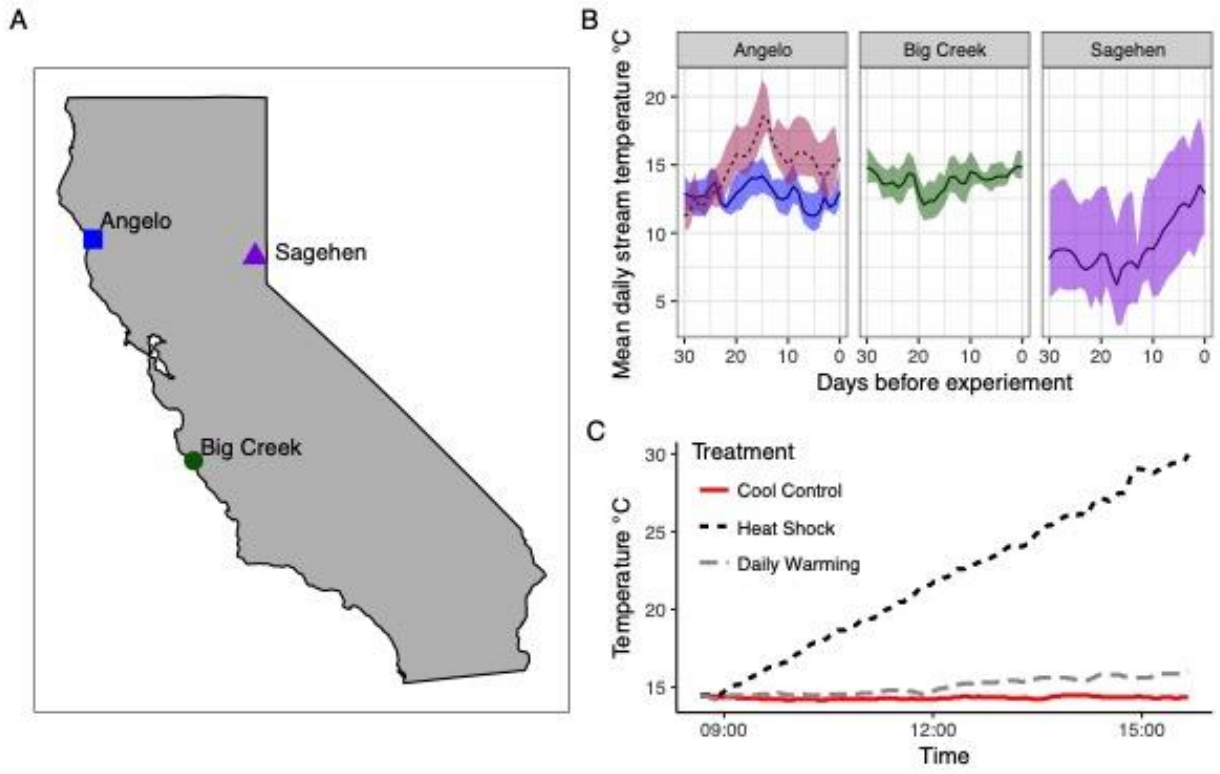


**Figure 1.** Thermal histories and experimental exposures of larval Dicosmoecus gilvipes caddisflies **A)** Three California populations used in this study and **B)** stream temperatures at each of these sites in the 30 days before the experiment. The data represent the following dates from each site: Angelo (4/29/13 – 5/29/13 and 5/24/13 – 6/22/13) in blue and pink, respectively, Big Creek (5/10/13-6/9/13) in green, and Sagehen(5/12/13 – 6/11/13) in violet. The solid line represents the mean daily stream temperature. The shaded area around the line indicates the daily temperature range **C)** Example of experimental temperature treatments from Big Creek (6/9/13). Colors and line types represent the warming treatment.

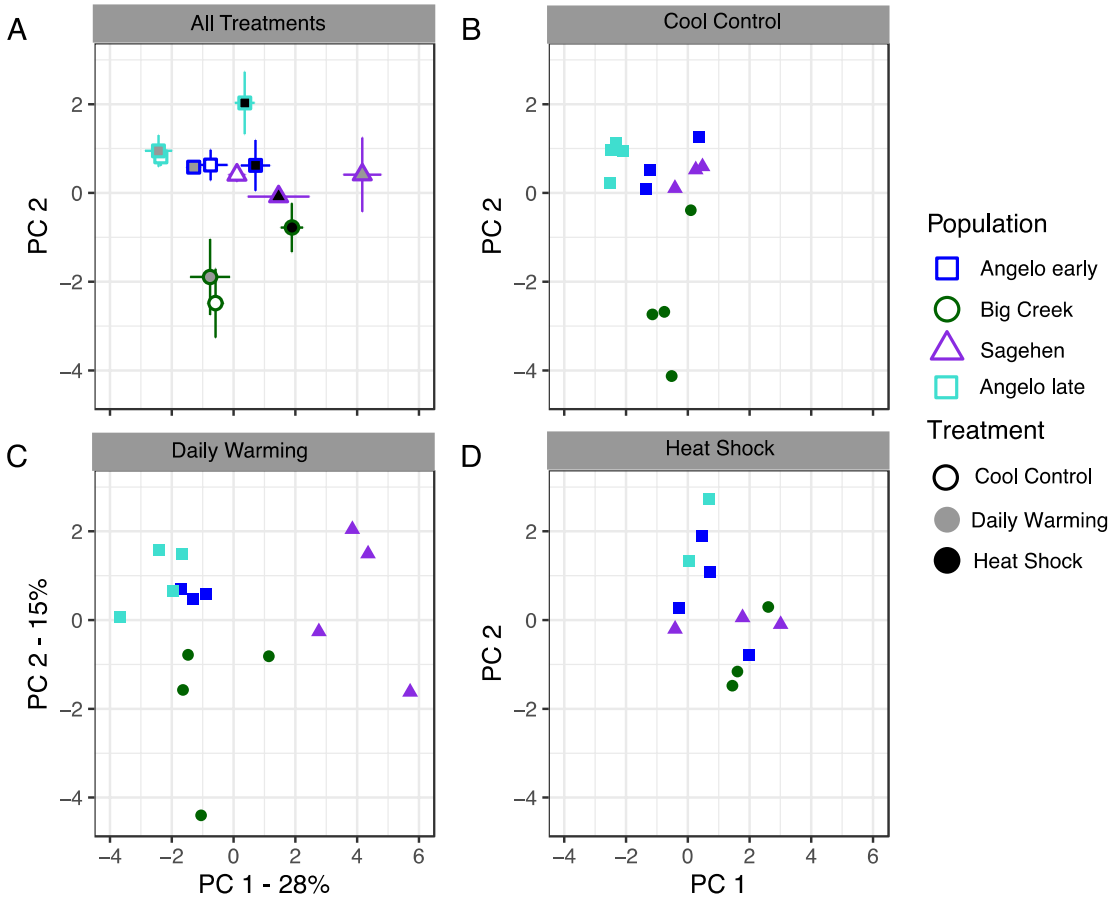


**Figure 2.** Gene expression analysis of *Dicosmoecus gilvipes* caddisflies exposed to three different temperature treatments. PC 1 represents 28% of the variation, while PC 2 represents 15% of the variation. **A)** Mean PC scores for all population and treatment combinations. Points represent means with standard error bars along both axes. Point outlines represent population of origin, fill color represents the treatment **B) -D)** Individuals plotted by their scores on PC1 and PC2 in the **B)** cool control treatment, **C)** daily stream warming treatment, and **D)** heat shock treatment. This analysis removed one outlier point from Sagehen control.

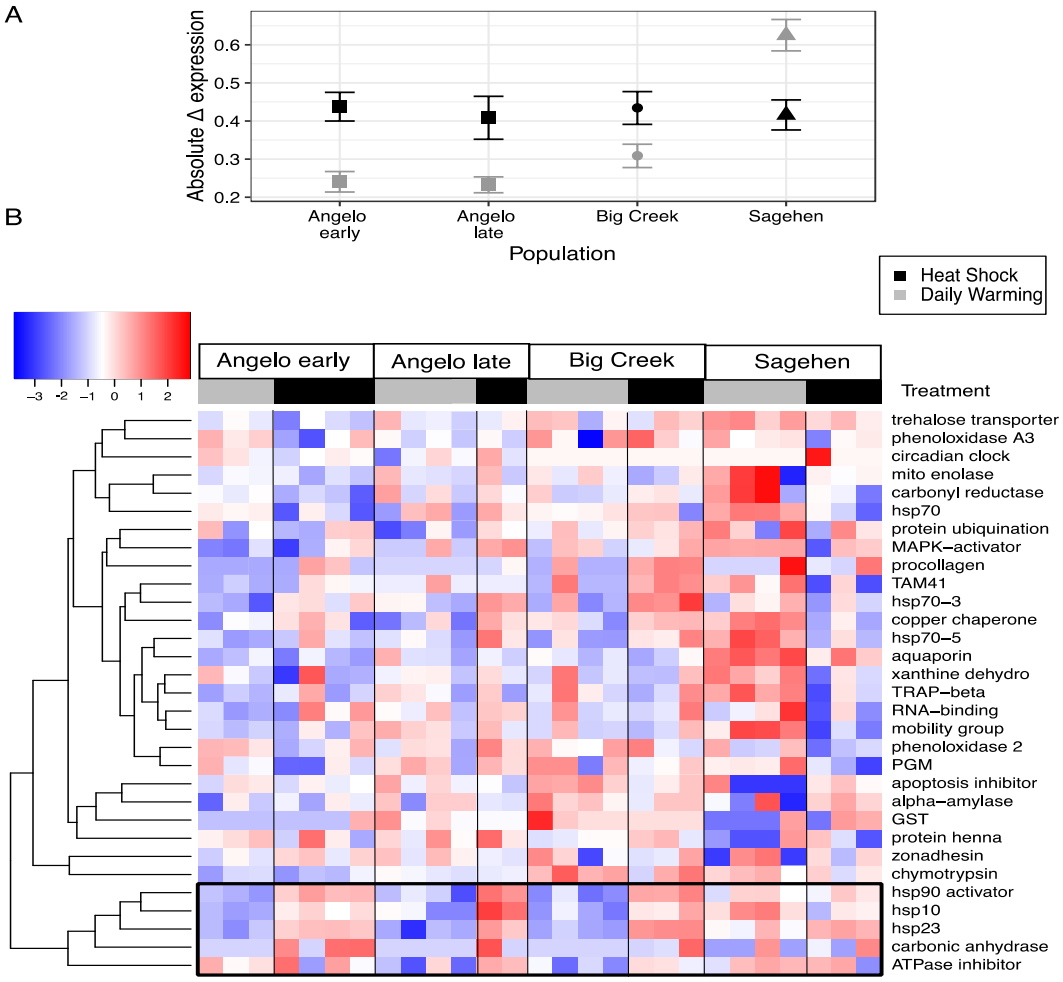


**Figure 3.** Change in expression between cool control and warming treatments for *Dicosmoecus gilvipes* from 3 California streams **A)** Mean ± standard error of the absolute change in expression (Δ expression) from the control at each site and treatment. Gray points represent the daily stream warming treatment, and black points represent the heat shock treatment. **B)** Heatmap of difference in gene transcript abundance relative to the cool control treatment. Genes are arranged in rows and grouped by similarity of induction value (dendrogram). Each column is an individual caddisfly, labeled by its warming treatment. Black and grey bars correspond to the daily warming treatment and heat shock, respectively. The colors of the heat map cells represent the magnitude and direction of the change in expression, scaled and centered by row. The black box highlights a cluster of genes with similar expression patterns (See Fig 4).

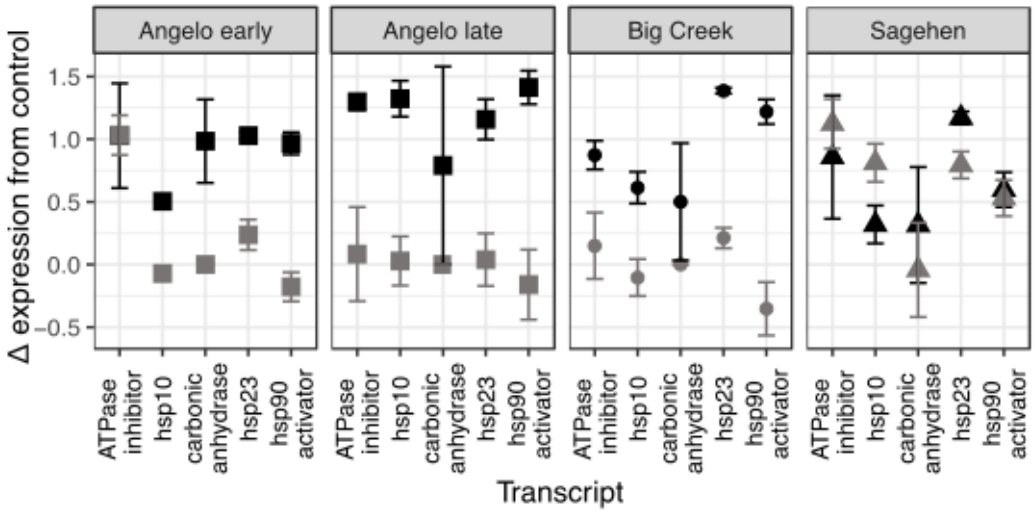


**Figure 4.** Change in expression relative to the control treatment for the five genes clustered in the box in B) for each site. The daily warming treatment is represented in gray, and the heat shock treatment is represented in black.

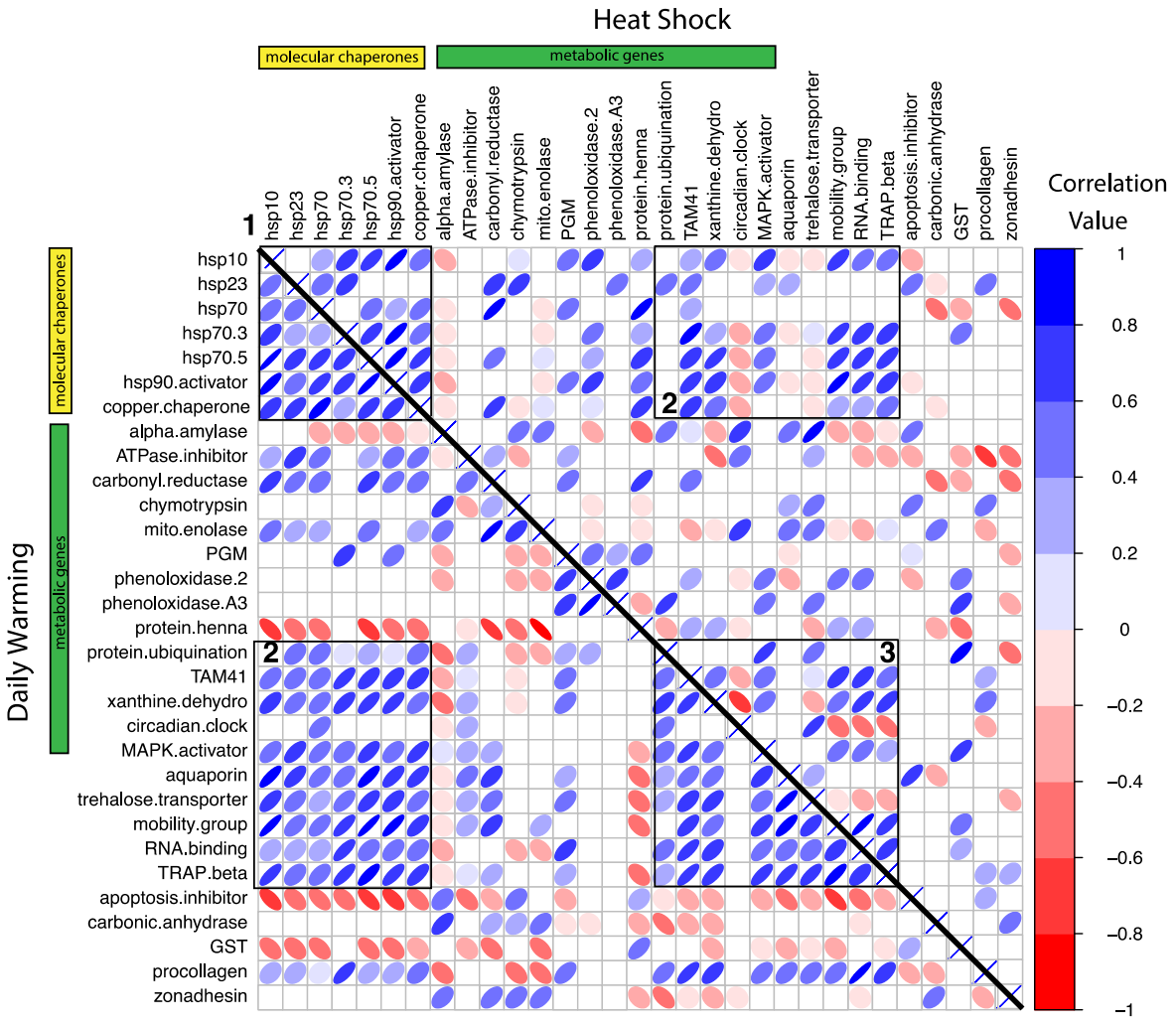


**Figure 5.** Correlation matrices of gene expression change ordered by functional category for the daily warming treatment on the lower triangle and the heat shock treatment on the upper triangle. The yellow bar indicates molecular chaperones. The green bar indicates metabolic genes. The remaining genes have various functions (see Table 3). Each row/column is one gene-by-gene comparison. The color and width of the ellipse indicate the correlation strength and direction. Blank cells represent non-significant correlations. Numbered boxes denote clusters of strong positive correlations described in the text.

## Supplementary Figures

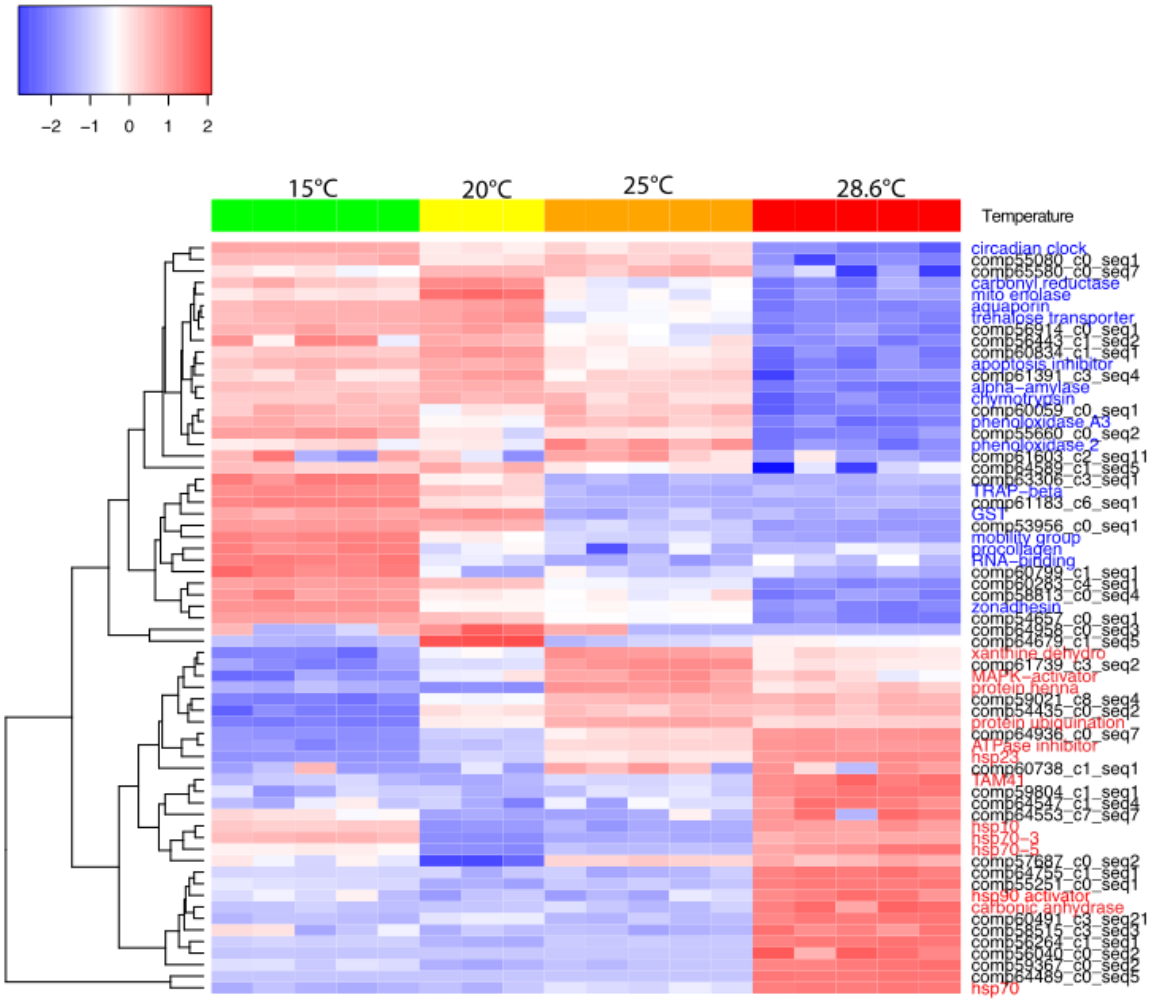


**Figure S1.** RNA-Seq results (unpublished) of genes used in the current study. The text colors indicate if we expected an increase (red) or decrease (blue) in transcripts in the current study. These RNA-Seq data were from a lab acclimation study where *D. gilvipes* were common-garden acclimated to 11°C for a few weeks and then exposed to 15°, 20°, 25°, or 28.6°C for 24 hours. The RNA-Seq samples represent independently made pools of RNA from n=8 individuals (i.e., technical replicates).

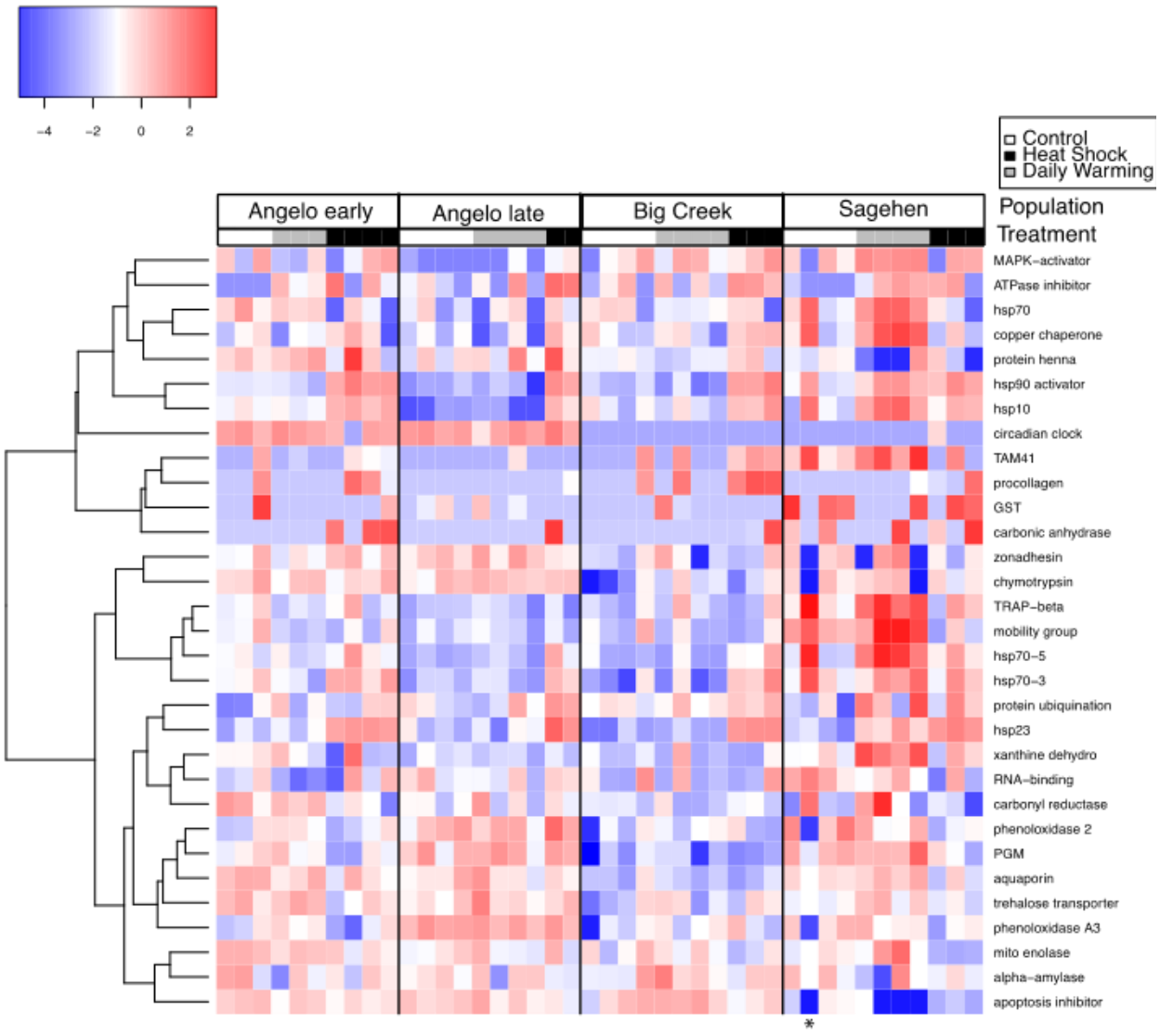


**Figure S2.** Heatmap of all genes and treatments, without any induction calculations. Genes are arranged in rows and grouped by similarity of expression value (dendrogram). Each column is an individual caddisfly, labeled by its warming treatment. White bars represent individuals in the cool control treatment. Black and grey bars correspond to the daily warming treatment and heat shock, respectively. The colors of the heat map cells represent the magnitude and direction of the change in expression, scaled and centered by row. Asterisk represents the individual left out of the PCA analysis.

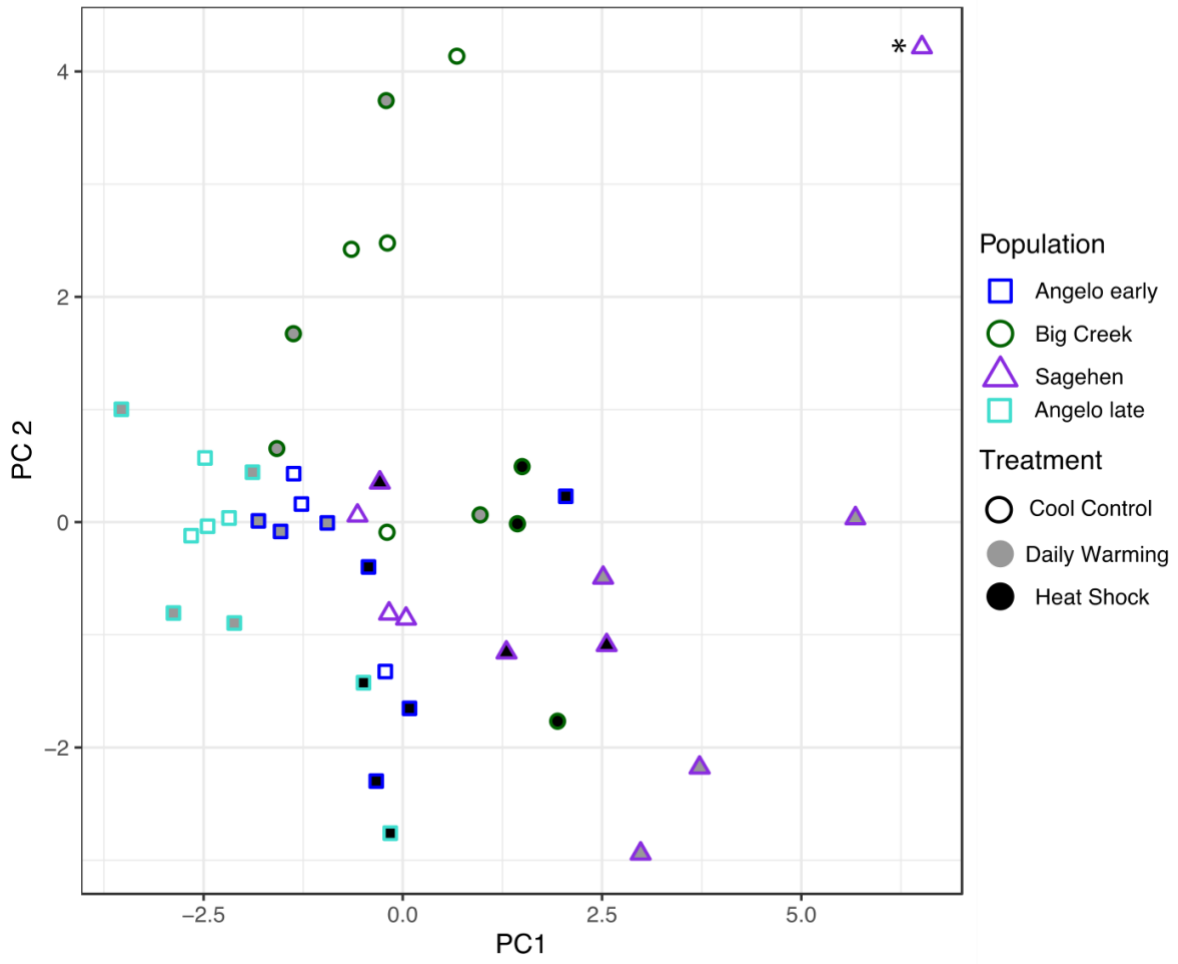


**Figure S3.** Population and treatment differentiation along principal components 1 and 2. This figure and analysis are identical to Fig 2, except that it includes one outlier point from Sagehen control, represented by the asterisk. Data represent PC scores for all population and treatment combinations. Symbol shape represents population of origin, fill color represents the treatment.

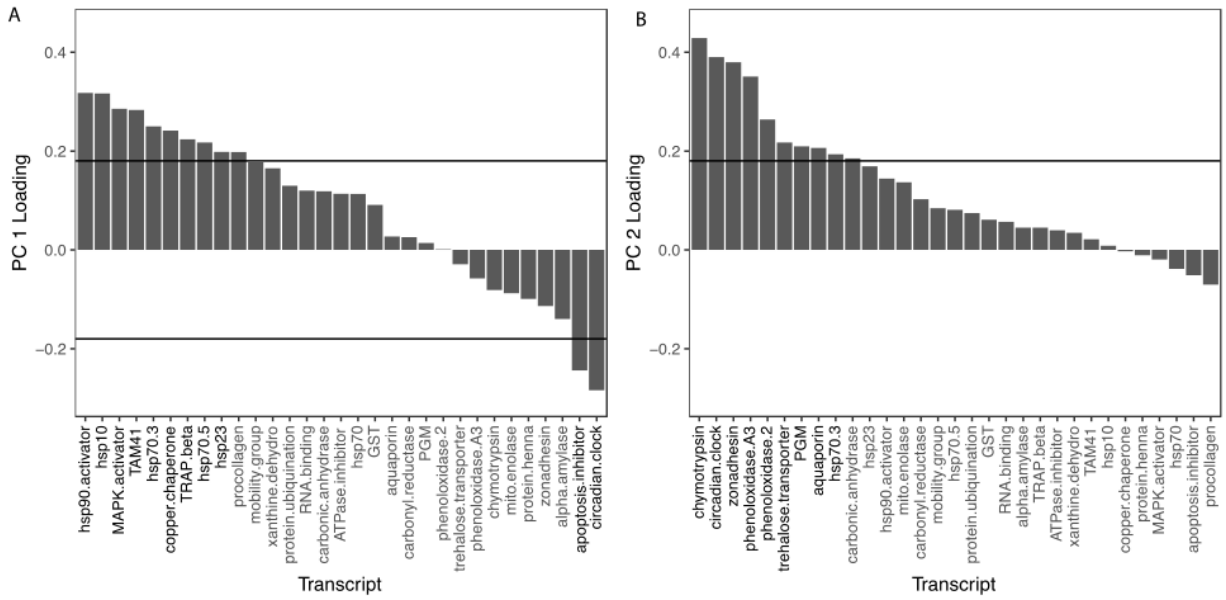


**Figure S4.** Principal component loadings for **A)** PC 1 **B)** PC 2. Horizontal lines indicate significance level. Transcripts with significant loadings are in black. All others are in gray.

**Supplementary Materials**

**Table S1 .** Tukey multiple comparison tests. Significance codes for adjusted p-values: 0=***, 0.001=**, 0.01=*, 0.05=., 0.1=NS **A)** Population differentiation PC1 **B)** Population differentiation PC2 **C)** Angelo dates PC1

A)

| | *P adj* |
|---|---|
| ***Population*** | |
| BigCreek-Angelo | NS |
| Sagehen-Angelo | *** |
| Sagehen-BigCreek | *** |
| ***Treatment*** | |
| HS-control | * |
| stream-control | * |
| stream-HS | NS |
| ***Population*Treatment*** | |
| Sagehen:stream - Angelo:stream | *** |
| Sagehen:stream - BigCreek:stream | *** |
| Sagehen:stream - BigCreek:control | *** |
| Sagehen:stream - Angelo:control | *** |
| Sagehen:stream - Sagehen:control | *** |
| Sagehen:stream - Angelo:HS | ** |
| Angelo:stream - BigCreek:HS | ** |
| Sagehen:stream - Sagehen:HS | ** |
| BigCreek:stream - BigCreek:HS | ** |
| Angelo:stream - Sagehen:HS | . |
| BigCreek:HS - BigCreek:control | . |
| BigCreek:HS - Angelo:control | . |
| Sagehen:stream - BigCreek:HS | NS |
| BigCreek:stream - Sagehen:HS | NS |

| | |
|---|---|
| Sagehen:HS - Angelo:control | NS |
| Sagehen:HS - BigCreek:control | NS |
| Angelo:stream - Angelo:HS | NS |
| BigCreek:HS - Sagehen:control | NS |
| BigCreek:stream - Angelo:HS | NS |
| Angelo:HS - Angelo:control | NS |
| Angelo:HS - BigCreek:control | NS |
| Angelo:stream - Sagehen:control | NS |
| Sagehen:HS - Sagehen:control | NS |
| BigCreek:HS - Angelo:HS | NS |
| BigCreek:stream - Sagehen:control | NS |
| Sagehen:control - Angelo:control | NS |
| Sagehen:HS - Angelo:HS | NS |
| Angelo:stream - BigCreek:control | NS |
| Sagehen:control - BigCreek:control | NS |
| Angelo:HS - Sagehen:control | NS |
| BigCreek:stream - Angelo:stream | NS |
| Angelo:stream - Angelo:control | NS |
| Sagehen:HS - BigCreek:HS | NS |
| BigCreek:stream - BigCreek:control | NS |
| BigCreek:control - Angelo:control | NS |
| BigCreek:stream - Angelo:control | NS |
| Sagehen:control - Angelo:control | NS |

| | |
|---|---|
| Sagehen:HS - Angelo:HS | NS |

| | |
|---|---|
| Angelo:stream - BigCreek:control | NS |

B)

| | *P adj* |
|---|---|
| ***Population*** | |
| BigCreek - Angelo | *** |
| Sagehen - Angelo | NS |
| Sagehen - BigCreek | *** |
| ***Treatment*** | |
| HS-control | NS |
| stream-control | NS |
| stream-HS | NS |
| ***Population*Treatment*** | |
| Angelo:HS - BigCreek:control | * |
| Sagehen:stream - BigCreek:control | * |
| BigCreek:control - Angelo:control | * |
| Sagehen:control - BigCreek:control | . |
| BigCreek:stream - Angelo:HS | NS |
| BigCreek:stream - Angelo:control | NS |
| Sagehen:stream - BigCreek:stream | NS |
| BigCreek:stream - Angelo:stream | NS |
| Sagehen:HS - BigCreek:control | NS |
| BigCreek:stream - Sagehen:control | NS |
| BigCreek:stream - Sagehen:HS | NS |

| | |
|---|---|
| BigCreek:HS - BigCreek:control | NS |
| BigCreek:HS - Angelo:HS | NS |
| BigCreek:HS - Angelo:control | NS |
| Angelo:stream - BigCreek:HS | NS |
| Sagehen:stream - BigCreek:HS | NS |
| BigCreek:HS - Sagehen:control | NS |
| BigCreek:stream - BigCreek:HS | NS |
| Sagehen:HS - Angelo:HS | NS |
| Sagehen:HS - Angelo:control | NS |
| Sagehen:HS - BigCreek:HS | NS |
| BigCreek:stream - BigCreek:control | NS |
| Angelo:stream - Sagehen:HS | NS |
| Sagehen:stream - Sagehen:HS | NS |
| Sagehen:HS - Sagehen:control | NS |
| Sagehen:stream - Angelo:HS | NS |
| Sagehen:stream - Angelo:control | NS |
| Angelo:HS - Sagehen:control | NS |
| Sagehen:control - Angelo:control | NS |
| Sagehen:stream - Angelo:stream | NS |
| Angelo:HS - Angelo:control | NS |
| Angelo:stream - Angelo:control | NS |
| Angelo:stream - Sagehen:control | NS |
| Sagehen:stream - Sagehen:control | NS |

| | |
|---|---|
| Angelo:stream - Angelo:HS | NS |

C)

| | *P adj* |
|---|---|
| ***Date*** | |
| early-late | *** |
| ***Treatment*** | |
| HS-control | *** |
| stream-control | NS |
| stream-HS | *** |
| ***Date*Treatment*** | |
| late:stream - early:HS | *** |
| early:HS - late:control | *** |
| late:stream - late:HS | ** |
| late:HS - late:control | ** |
| early:stream - early:HS | * |
| late:stream - early:control | . |
| *late:control - early:control* | . |
| early:HS - early:control | NS |
| early:stream - late:HS | NS |
| *late:stream - early:stream* | NS |
| early:stream - late:control | NS |
| late:HS - early:control | NS |
| early:stream - early:control | NS |
| *late:HS - early:HS* | NS |
| late:stream - late:control | NS |
| late:stream - early:control | NS |

**Literature Cited**


Angilletta MJ. 2009. Thermal Adaptation. New York: Oxford University Press.

Bergmann N, Winters G, Rauch G, Eizaguirre C, Gu J, Nelle P, Fricke B, Reusch TBH. 2010. Population-specificity of heat stress gene induction in northern and southern eelgrass *Zostera marina* populations under simulated global warming. Mol Ecol. 19:2870–2883.

Bernhardt J, O'Connor M, Sunday J, Gonzalez A. 2020. Life in fluctuating environments.

Bowler K. 2005. Acclimation, heat shock and hardening. J Therm Biol. 30:125–130.

Chomczyński P, Sacchi N. 1987. Single-step method of RNA isolation by acid guanidinium thiocyanate-phenol-chloroform extraction. Anal Biochem. 162:156–159.

Dahlhoff EP. 2004. Biochemical Indicators of Stress and Metabolism: Applications for Marine Ecological Studies. Annu Rev Physiol. 66:183–207.

Denny M. 2017. The fallacy of the average: on the ubiquity, utility and continuing novelty of Jensen's inequality. J Exp Biol. 220:139–146.

Diffenbaugh NS, Swain DL, Touma D. 2015. Anthropogenic warming has increased drought risk in California. Proc Natl Acad Sci. 112:3931–3936.

Dong Y wei, Zhang S. 2016. Ecological relevance of energy metabolism: transcriptional responses in energy sensing and expenditure to thermal and osmotic stresses in an intertidal limpet. Funct Ecol. 30:1539–1548.

Dong YW, Han GD, Ganmanee M, Wang J. 2015. Latitudinal variability of physiological responses to heat stress of the intertidal limpet *Cellana toreuma* along the Asian coast. Mar Ecol Prog Ser. 529:107–119.

Ebner JN, Ritz D, von Fumetti S. 2019. Comparative proteomics of stenotopic caddisfly *Crunoecia irrorata* identifies acclimation strategies to warming. Mol Ecol. 28:4453–4469.

Eriksson L, Johansson E, Kettaneh-Wold N WS. 1999. Introduction to multi- and megavariate data analysis using projection methods (PCA & PLS). Umetrics.

Fangue NA, Hofmeister M, Schulte PM. 2006. Intraspecific variation in thermal tolerance and heat shock protein gene expression in common killifish, *Fundulus heteroclitus*. J Exp Biol. 209:2859–2872.

Feder ME, Hoffman GE. 1999. Heat-shock proteins, molecular chaperones, and the stress response: evolutionary and ecological physiology. Annu Rev Physiol. 61:243–282.

Gamboa M, Tsuchiya MC, Matsumoto S, Iwata H, Watanabe K. 2017. Differences in protein expression among five species of stream stonefly (Plecoptera) along a latitudinal gradient in Japan. Arch Insect Biochem Physiol. 96:1–16.

Gillooly JF, Brown JH, West GB, Savage VM, Charnov EL. 2001. Effects of size and temperature on metabolic rate. Science. 293:2248–2251.

Hannaford M. 1998. Development and Comparison of Biological Indicators of Habitat Disturbance for Streams and Wetlands.

Holomuzki JR, Furey PC, Lowe RL, Power ME. 2013. Microdistributional variability of larval caddisflies in Mediterranean-climate streams in Northern California. West North Am Nat. 73:261–269.

Hotaling S, Shah AA, McGowan KL, Tronstad LM, Giersch JJ, Finn DS, Woods HA, Dillon ME, Kelley JL. 2020. Mountain stoneflies may tolerate warming streams: Evidence from organismal physiology and gene expression. Glob Chang Biol. 00:1–15.

Houghton DC, Logan AC, Pytel AJ. 2014. Validation of CTmax protocols using cased and uncased *Pycnopsyche guttifer* (Trichoptera: Limnephilidae) larvae. Gt Lakes Entomol. 47:1–8.

Houghton DC, Shoup L. 2014. Seasonal changes in the critical thermal maxima of four species of aquatic insects (Ephemeroptera, Trichoptera). Environ Entomol. 43:1059–1066.

IPCC. 2019. Climate Change and Land: an IPCC special report on climate change, desertification, land degradation, sustainable land management, food security, and greenhouse gas fluxes in terrestrial ecosystems.

Jeffrey JD, Carlson H, Wrubleski D, Enders EC, Treberg JR, Jeffries KM. 2020. Applying a gene-suite approach to examine the physiological status of wild-caught walleye (*Sander vitreus*). Conserv Physiol. 8:1–12.

King AM, Macrae TH. 2015. Insect heat shock proteins during stress and diapause. Annu Rev Entomol. 60:59–75.

Marshall KE, Anderson KM, Brown NEM, Dytnerski JK, Flynn KL, Bernhardt JR, Konecny CA, Gurney-Smith H, Harley CDG. 2021. Whole-organism responses to constant temperatures do not predict responses to variable temperatures in the ecosystem engineer *Mytilus trossulus*. Proc R Soc B Biol Sci. 288:rspb.2020.2968.

Morash AJ, Neufeld C, MacCormack TJ, Currie S. 2018. The importance of incorporating natural thermal variation when evaluating physiological performance in wild species. J Exp Biol. 221:jeb164673.

Null SE, Viers JH, Deas ML, Tanaka SK, Mount JF. 2013. Stream temperature sensitivity to climate warming in California's Sierra Nevada: Impacts to coldwater habitat. Clim Change. 116:149–170.

Peterson MG, O'Grady PM, Resh VH. 2017. Phylogeographic comparison of five large-bodied aquatic insect species across the western USA. Freshw Sci. 36:823–837.

Pörtner HO, Knust R. 2007. Climate change affects marine fishes through the oxygen limitation of thermal tolerance. Science. 315:95–97.

Resh VH, Hannaford M, Jackson JK, Lamberti G a, Mendez PK. 2011. The biology of the limnephilid caddisfly *Dicosmoecus gilvipes* (Hagen) in Northern California and Oregon (USA) streams. Zoosymposia. 5:413–419.

Resh VH, Wood JR. 1985. Site of sex pheromone production in three species of Trichoptera. Aquat Insects. 7:65–71.

Seebacher F, White CR, Franklin CE. 2015. Physiological plasticity increases resilience of ectothermic animals to climate change. Nat Clim Chang. 5:61–66.

Shah AA, Chris Funk W, Ghalambor CK. 2017. Thermal acclimation ability varies in temperate and tropical aquatic insects from different elevations. Integr Comp Biol. 57:977–987.

Somero GN. 2005. Linking biogeography to physiology: evolutionary and acclimatory adjustments of thermal limits. Front Zool. 2:1–9.

Somero GN. 2010. The physiology of climate change: how potentials for acclimatization and

genetic adaptation will determine “winners” and “losers.” J Exp Biol. 213:912–920.

Somero GN. 2020. The cellular stress response and temperature: function, regulation, and evolution. J Exp Zool Part A Ecol Integr Physiol.:1–19.

Stacklies W, Redestig H, Scholz M, Walther D, Selbig J. 2007. pcaMethods - A bioconductor package providing PCA methods for incomplete data. Bioinformatics. 23:1164–1167.

Swain DL, Tsiang M, Haugen M, Singh D, Charland A, Rajaratnam B, Diffenbaugh NS. 2014. The extraordinary California drought of 2013/2014: character, context, and the role of climate change. Bull Amer Meteor Soc. 95:S3–S7.

Sweeny BW, Jackson JK, Newbold JD, Fun DH. 1992. Climate change and the life histories and biogeography of aquatic insects in eastern North America. In: Firth P, Fisher SG, editors. Global Climate Change and Freshwater Ecosystems. New York: Springer-Verlag. p. 143–176.

Tanner RL, Faye LE, Stillman JH. 2019. Temperature and salinity sensitivity of respiration, grazing, and defecation rates in the estuarine eelgrass sea hare, *Phyllaplysia taylori*. Mar Biol. 166:1–12.

Team RC. 2018. R: A Language and Environment for Statistical Computing.

Verberk WCEP, Calosi P. 2012. Oxygen limits heat tolerance and drives heat hardening in the aquatic nymphs of the gill breathing damselfly *Calopteryx virgo* (Linnaeus, 1758). J Therm Biol. 37:224–229.

Wei T, Simko V. 2016. corrplot: Visualization of a Correlation Matrix.

Yang Y, Edery I. 2019. Daywake, an anti-siesta gene linked to a splicing-based thermostat from an adjoining clock gene. Curr Biol. 29:1728-1734.e4.

Zhao S, Yin L, Guo Y, Sheng Q, Shyr Y. 2021. heatmap3.